Fraunhofer
ITWM

H. Lang

Comparison of quaternionic and rotation-free null space formalisms for multibody dynamics

Berichte des Fraunhofer ITWM, Nr. 180 (2010)

ISSN 1434-9973

Bericht 180 (2010)

Die Veröffentlichungen in der Berichtsreihe des Fraunhofer ITWM können bezogen werden über:

Fraunhofer-Institut für Techno- und
Wirtschaftsmathematik ITWM
Fraunhofer-Platz 1

67663 Kaiserslautern
Germany

Telefon: +49(0)631/3160 0-0
Telefax: +49(0)631/3160 0-1099
E-Mail: info@itwm.fraunhofer.de
Internet: www.itwm.fraunhofer.de

Vorwort

Das Tätigkeitsfeld des Fraunhofer-Instituts für Techno- und Wirtschaftsmathematik ITWM umfasst anwendungsnahe Grundlagenforschung, angewandte Forschung sowie Beratung und kundenspezifische Lösungen auf allen Gebieten, die für Techno- und Wirtschaftsmathematik bedeutsam sind.

In der Reihe »Berichte des Fraunhofer ITWM« soll die Arbeit des Instituts kontinuierlich einer interessierten Öffentlichkeit in Industrie, Wirtschaft und Wissenschaft vorgestellt werden. Durch die enge Verzahnung mit dem Fachbereich Mathematik der Universität Kaiserslautern sowie durch zahlreiche Kooperationen mit internationalen Institutionen und Hochschulen in den Bereichen Ausbildung und Forschung ist ein großes Potenzial für Forschungsberichte vorhanden. In die Berichtreihe werden sowohl hervorragende Diplom- und Projektarbeiten und Dissertationen als auch Forschungsberichte der Institutsmitarbeiter und Institutsgäste zu aktuellen Fragen der Techno- und Wirtschaftsmathematik aufgenommen.

Darüber hinaus bietet die Reihe ein Forum für die Berichterstattung über die zahlreichen Kooperationsprojekte des Instituts mit Partnern aus Industrie und Wirtschaft.

Berichterstattung heißt hier Dokumentation des Transfers aktueller Ergebnisse aus mathematischer Forschungs- und Entwicklungsarbeit in industrielle Anwendungen und Softwareprodukte – und umgekehrt, denn Probleme der Praxis generieren neue interessante mathematische Fragestellungen.

Prof. Dr. Dieter Prätzel-Wolters
Institutsleiter

Kaiserslautern, im Juni 2001

Comparison of quaternionic and rotation-free null space formalisms for multibody dynamics

Holger Lang[♮]

[♮] Fraunhofer Institute for Industrial Mathematics
Fraunhofer Platz 1, 67663 Kaiserslautern, Germany
holger.lang@itwm.fraunhofer.de,

Abstract

In this article, we summarise the rotation-free and quaternionic parametrisation of a rigid body. We derive and explain the close interrelations between both parametrisations. The internal constraints due to the redundancies in the parametrisations, which lead to DAEs, are handled with the null space technique. We treat both single rigid bodies and general multibody systems with joints, which lead to external joint constraints. Several numerical examples compare both formalisms to the index reduced versions of the corresponding standard formulations.

Keywords. Parametrisation of rotations, Differential-algebraic equations, Multibody dynamics, Constrained mechanical systems, Lagrangian mechanics.

MSC Classification: 65L80, 70E15, 70E55, 70E17.

Contents

1 Introduction

Recently, both rotation-free [6, 7, 8] and quaternionic parametrisation of rotations [9, 10, 19, 20, 21, 24, 26, 32, 34, 38] found new attraction. The reason is that *there exists no* singularity-free parametrisation of the three-dimensional rotation group $SO(3)$ with three variables [41]. In contrast to the rotation-free parametrisation method, which uses nine variables, the quaternionic parametrisation uses only four and is thus minimal among all singularity-free possibilities [5]. However, the presence of redundant variables leads to internal constraints, resulting in DAEs in any case, not ODEs. One of several instruments [4, 27] to overcome these redundancies partially is the null space method [6, 7, 8, 12, 25], keeping all the redundant variables for rigid bodies (nine resp. four) on position level, but using a minimal number of variables (three) on velocity level. In this article, we compare both parametrisations for rigid bodies, both in index-0 absolute coordinate and null space coordinate formulation.

There are close interconnections between both parametrisations and both formulations. It is the aim of this paper to clarify these relations and to compare the respective methods. As a result, a procedure is developed that allows a systematic construction of quaternionic null space matrices for multibody systems including joints. From the analytical point of view all those methods are clearly equivalent. But numerically, these methods differ significantly, which is illustrated by three elementary examples.
As we will see, the null space formulations are superior to the absolute index-0 formulations. One reason for that is that the constraints are satisfied exactly on *velocity* level, not on *acceleration* level. Further, the quaternionic parametrisation is superior to the rotation-free parametrisation due to its smaller number of primary unknowns. Concerning accuracy and numerical task, the quaternionic null space method turns out to be competitive to the mostly preferred three-dimensional minimal parametrisation with Euler angles — and, in contrast — is free of singularities.
Any parametrisation of $SO(3)$ does have their pros and cons. One has to make compromises in any case. So as a pro for a higher dimensional — i. e. more than three — parametrisation of $SO(3)$, gimbal locking can be avoided, which is clearly the decisive pro. A con is that such a parametrisation inevitably leads to internal kinematic constraints and DAEs — even if there are no joints in the multibody model: In rotation-free parametrisation, each director must be kept on unit length, and the directors must be kept pairwise orthogonal. This leads to *six internal constraints*. In quaternionic parametrisation, the quaternion must be of unit norm, leading to just *one internal constraint*. A beautiful advantage of the rotation-free method is that mechanical joints can be incorporated very easily [7].

The topics and the structure of this article

In Section 2, we summarise the idea of null space coordinates in general, for classical Lagrangian mechanical systems with holonomic constraints.
In Sections 3 resp. 4, we summarise the rotation-free resp. quaternionic parametrisation for single rigid bodies, where we as well expose appropriate null space matrices [7, 25] for the respective cases. We do so, since we want the paper to be self-contained and since, for the rotation-free case in Section 3, we choose slightly different null space matrices than the ones presented in [7] for several reasons to be explained. It will turn out in Section 4 that — for the quaternionic parametrisation — a well-known formulation is obtained, which can be found already in the literature [12, 30, 34] before. However, its derivation from the viewpoint of the systematic and general null space methodology is new.
The close interconnection between the rotation-free and quaternionic descriptions — each both in standard absolute and null space coordinate formulations — is analysed in Section 5. Here, the key tool is the Moore-Penrose pseudoinverse of the differential of the classical Euler map, for which we give an explicit analytical expression in closed form. It provides the basis to obtain suitable quaternionic null space matrices for multibody systems that are built up with internal and external joint constraints in rotation-free form. Especially, all the standard joints ('lower kinematic pairs') in [7] can be transformed into quaternionic description.
Section 6 is concerned about the projection technique in order to stabilise the drift-off effect for all our four formulations of single rigid bodies, i. e. {rotation-free, quaternionic} × {absolute, null space}. Here, especially for the rotation-free descriptions, we propose an explicit projection method, which in turn is based on quaternions and the algorithm of Spurrier and Klumpp [24, 37, 38].
Section 7 exposes three elementary comparative examples, computed with standard time integration methods such as DoPri5 (Ode45 in Matlab), Radau5 or Dassl/Daspk (Ode15s in Matlab). Here, typical differences — in view of numerical accuracy and performance — between the formulations become illustrative. Where possible, we additionally compare the results to the classical parametrisation with Euler angles.

Let us remark as well, what we *not* discuss in this article. In contrast to [6, 7, 8], we do not deal with the discrete mechanics approach, but treat the time t continuously. This is, we consider, what is called the *continuous null space* method in [7]. Especially, time integration is not performed by variational integrators, but with classical standard solution techniques such as Runge-Kutta or BDF methods. We do so, since these solvers — due to their high accuracy and robustness — are well-established in nowadays multibody dynamics packages such as VirtualLab, Adams or SimPack. Our aim is not to have invariants — e. g. the total energy or the linear/angular momentum — exactly conserved. If the reader is interested in such conserving methods for quaternionic rigid bodies, we refer to [9]. Likewise, we do not apply the local reparametrisation technique in [7].

2 The null space technique in multibody dynamics

We consider a **general Lagrangian mechanical system**, described by a set of $N_q \geq 1$ generalised coordinates $q \in \mathbb{R}^{N_q}$, subjected to $N_\lambda \geq 0$ holonomic constraints of the form $g(q,t) = 0 \in \mathbb{R}^{N_\lambda}$. With the generalised velocities $v = \dot{q} \in \mathbb{R}^{N_q}$, the Lagrange multipliers $\lambda \in \mathbb{R}^{N_\lambda}$, the mass matrix $\mathcal{M}(q) \in \mathbb{R}^{N_q \times N_q}$, the potential energy $V = V(q,t)$, the kinetic energy $T = T(q,v,t) = \frac{1}{2} v^\top \mathcal{M}(q) v$, the Lagrangian function $L = L(q,v,t) = T(q,v,t) - V(q,t) - g(q,t)^\top \lambda$ and prescribed exterior forces $\phi(q,v,t) \in \mathbb{R}^{N_q}$, the variational principle $\delta \int_0^T L \,\mathrm{d}t + \int_0^T \phi\, \delta q \,\mathrm{d}t$ yields the well-known classical Euler-Lagrange equations [2, 19, 30] of the first kind,

$$\left\{ \begin{array}{rcl} \dot{q} & = & v \\ \mathcal{M}(q)\dot{v} & = & \psi(q,v,t) - \mathcal{G}(q,t)^\top \lambda \\ 0 & = & g(q,t) \end{array} \right. . \tag{1}$$

with the generalised forces

$$\psi(q,v,t) = \phi(q,v,t) - \nabla_q V(q,t)^\top + \frac{1}{2} \nabla_q \big(v^\top \mathcal{M}(q) v \big)^\top - \nabla_q (\mathcal{M}(q)v) v \in \mathbb{R}^{N_q}. \tag{2}$$

We assume the Grübler condition that the rank $\operatorname{rk} \mathcal{G}(q,t)^\top = N_\lambda$ of the constraint gradient $\mathcal{G}(q,t) = \nabla_q g(q,t) \in \mathbb{R}^{N_\lambda \times N_q}$ is maximal, excluding singular — especially redundant — constraints. We further assume the mass matrix to be positive semi-definite and symmetric. Under these assumptions, (1) is known to be a system of differential algebraic equations of *index 3*, see [2, 19]. It is also well known that the numerical solution an index-3 system involves difficulties such as poor convergence of Newton's method in the corrector iterations [2, 12, 13, 19, 27]. Thus, we reduce the index twice, where we differentiate the algebraic constraint equation with respect to time. We receive the *index-2*

$$\left\{ \begin{array}{rcl} \dot{q} & = & v \\ \mathcal{M}(q)\dot{v} & = & \psi(q,v,t) - \mathcal{G}(q,t)^\top \lambda \\ 0 & = & G(q,t)v + g^{\mathrm{I}}(q,t) \end{array} \right. \tag{3}$$

and the *index-1* system

$$\left(\begin{array}{ccc} \mathcal{I} & 0 & 0 \\ 0 & \mathcal{M}(q) & \mathcal{G}(q,t)^\top \\ 0 & \mathcal{G}(q,t) & 0 \end{array} \right) \left(\begin{array}{c} \dot{q} \\ \dot{v} \\ \lambda \end{array} \right) = \left(\begin{array}{c} v \\ \psi(q,v,t) \\ -g^{\mathrm{II}}(q,v,t) \end{array} \right) . \tag{4}$$

In these two lower index systems, all the right-hand-side terms that emerge from time differentiation of $g(q,t)$ are collected in the functions

$$g^{\mathrm{I}}(q,t) = \frac{\partial g}{\partial t}(q,t), \qquad g^{\mathrm{II}}(q,v,t) = \frac{\partial^2 g}{\partial q^2}(q,t)[v,v] + 2\frac{\partial \mathcal{G}}{\partial t}(q,t)v + \frac{\partial^2 g}{\partial t^2}(q,t). \tag{5}$$

With these functions, the constraints on the level of position, velocity and acceleration are written $g = 0$, $\dot{g} = \mathcal{G}\dot{q} + g^{\mathrm{I}} = 0$ and $\ddot{g} = \mathcal{G}\ddot{q} + g^{\mathrm{II}} = 0$, respectively. Solving (4) for $(\dot{q}, \dot{v}, \lambda)$, where we

formally write

$$\boxed{\begin{pmatrix} \dot{q} \\ \dot{v} \\ \lambda \end{pmatrix} = \begin{pmatrix} \mathcal{I} & 0 & 0 \\ 0 & \mathcal{M}(q) & \mathcal{G}(q,t)^\top \\ 0 & \mathcal{G}(q,t) & 0 \end{pmatrix}^{-1} \begin{pmatrix} v \\ \psi(q,v,t) \\ -g^{\mathrm{II}}(q,v,t) \end{pmatrix},} \tag{6}$$

and discarding the equations for the Lagrange multipliers λ, we receive an ODE $(\dot{q}, \dot{v}) = \Psi(q, v, t)$ for the $2N_q$ unknowns (q, v). We refer to $(6_{1,2})$ as the *index-0 subsystem*, corresponding to (1). It can be solved numerically by any standard method for ODEs, where the λ's are obtained in a postprocessing from (6_3).
The presence of the d'Alembert's constraint forces $\mathcal{G}(q,t)^\top \lambda$ usually cause the above systems to be bad or even ill conditioned. In that case, the constraints — and its partial derivatives — must be scaled in an appropriate fashion [3].

We summarise the elegant idea of **null space coordinates** [4, 6, 7, 8, 12, 27]. It is some kind of *compromise* between absolute — redundant — and minimal coordinate formulations. On position level, we keep the coordinates $q \in \mathbb{R}^{N_q}$ — not minimal —, but on velocity level, instead of $v \in \mathbb{R}^{N_q}$, a minimal number of unknown velocities $\nu \in \mathbb{R}^{N_{\mathrm{DOF}}}$ is chosen.

$$N_{\mathrm{DOF}} = \dim_q\{q \in \mathbb{R}^{N_q} : g(q,t) = 0\} = \dim_q \operatorname{null} \mathcal{G}(q,t) = N_q - N_\lambda \geq 0$$

is the number of mechanical degrees of freedom of the system, that is, the dimension of the constraint manifold. The minimal unknowns $\nu = (\nu_1, \ldots, \nu_{N_{\mathrm{DOF}}})$ are the coefficients of the tangential part of the velocity v in the expansion w. r. t. an appropriate basis of the current tangential space at q. They are usually called 'independent quasi-velocities', 'generalised speeds' or 'kinematic characteristics', see [7, 27]. Note that in contrast to the current constraint manifold $\{q \in \mathbb{R}^{N_q} : g(q,t) = 0\}$ at t, the current tangential space $\operatorname{null} \mathcal{G}(q,t) = \{\xi \in \mathbb{R}^{N_q} : G(q,t)\xi = 0\}$ at (q,t) is a *linear* space. The constellation for holonomic, scleronomic constraints is depicted in Figure 1. Starting with the Lagrangian system (1), we expand the tangential component of v with respect to a basis

$$\mathcal{T}(q,t) = \left(\; \tau^1(q,t) \; \middle| \; \ldots \; \middle| \; \tau^{N_{\mathrm{DOF}}}(q,t) \; \right) \in \mathbb{R}^{N_q \times N_{\mathrm{DOF}}} \tag{7}$$

of the current tangential space,

$$v = \dot{q} = \sum_{n=1}^{N_{\mathrm{DOF}}} \nu_n \tau^n(q,t) - \mathcal{G}(q,t)^\top \big(\mathcal{G}(q,t)\mathcal{G}(q,t)^\top\big)^{-1} \frac{\partial g}{\partial t}(q,t) = \mathcal{T}(q,t)\nu - r(q,t). \tag{8}$$

Here

$$r(q,t) = \mathcal{G}(q,t)^\natural \frac{\partial g}{\partial t}(q,t), \qquad \mathcal{G}(q,t)^\natural = \mathcal{G}(q,t)^\top \big(\mathcal{G}(q,t)\mathcal{G}(q,t)^\top\big)^{-1},$$

and $\mathcal{G}(q,t)^\natural$ is the Moore-Penrose pseudoinverse [39] of $\mathcal{G}(q,t)$. The inverse of $\mathcal{G}(q,t)\mathcal{G}(q,t)^\top$ exists because of $\operatorname{null} \mathcal{G}(q,t)\mathcal{G}(q,t)^\top = \operatorname{null} \mathcal{G}(q,t)^\top = \{0\}$. Now, since

$$\operatorname{null} \mathcal{G}(q,t) = \operatorname{im} \mathcal{T}(q,t) \tag{9}$$

by construction, $\mathcal{T}(q,t)$ is called a 'null space matrix' for $\mathcal{G}(q,t)$, and the constraint on the *level of velocity* is satisfied exactly,

$$\dot{g} = \mathcal{G}\dot{q} + \frac{\partial g}{\partial t} = \mathcal{G}\left(\mathcal{T}\nu - \mathcal{G}^\top \big(\mathcal{G}\mathcal{G}^\top\big)^{-1} \frac{\partial g}{\partial t}\right) + \frac{\partial g}{\partial t} \equiv 0. \tag{10}$$

Especially, we have $\operatorname{rk} \mathcal{T}(q,t) = N_{\mathrm{DOF}}$, this is, the rank of $\mathcal{T}(q,t)$ is maximal. The constraint forces $\mathcal{G}(q,t)^\top \lambda$ are eliminated, if we multiply the dynamical equations (1_2) with $\mathcal{T}(q,t)^\top$ from

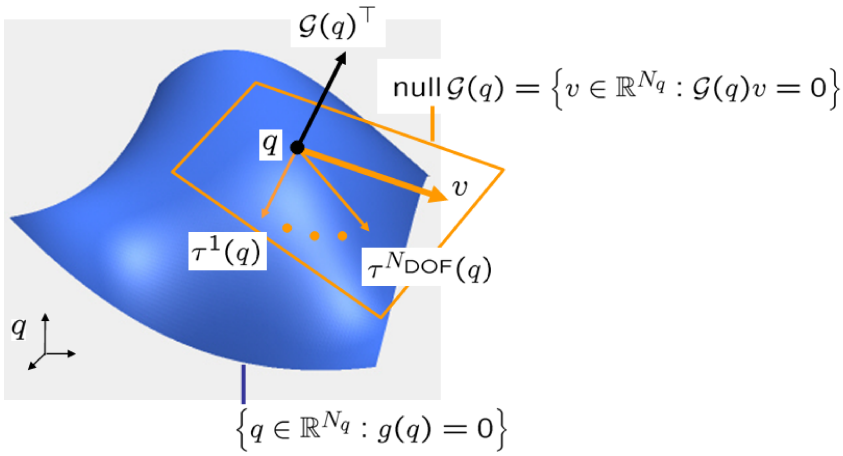

Figure 1: *Constraint manifold* $\{q \in \mathbb{R}^{N_q} : g(q) = 0 \in \mathbb{R}^{N_\lambda}\}$ *and tangential space* $\operatorname{null}\mathcal{G}(q) = \{v \in \mathbb{R}^{N_q} : \mathcal{G}(q)v = 0 \in \mathbb{R}^{N_\lambda}\}$ *at* q *for holonomic, scleronomic constraints* $g(q) = 0$.

the left. We receive the null space coordinate formulation

$$\left\{\begin{array}{rcl} \dot{q} &=& \mathcal{T}(q,t)\nu - r(q,t) \\ \mathcal{T}(q,t)^\top \mathcal{M}(q)\mathcal{T}(q,t)\dot{\nu} &=& \mathcal{T}(q,t)^\top \Big(\psi(q,\dot{q},t) + \mathcal{M}(q)\big(\dot{r}(q,\dot{q},t) - \dot{\mathcal{T}}(q,\dot{q},t)\nu\big)\Big) \\ 0 &=& g(q,t) \end{array}\right. . \tag{11}$$

(11_1) consists of N_q equations — as for absolute coordinates. (11_2) has N_{DOF} equations — as for minimal/relative coordinates. This is exactly the number N_{DOF} of degrees of freedom that are present in the physical model. In addition, we have N_λ equations in (11_3). Consequently, for $N_\lambda \geq 1$, system (11) is overdetermined. System $(11_{1,2})$ yields an ODE $(\dot{q}, \dot{\nu}) = \Psi(q, \nu, t)$ of dimension $N_q + N_{\mathrm{DOF}}$ for the unknown (q, ν) with the solution invariant (11_3), see [12, 14].

System formulation (11) in null space coordinates has the following *not insignificant advantages* compared to the absolute coordinate index-3, -2, -1 resp. -0 formulations (1), (3), (4) resp. $(6_{1,2})$.

(i) The constraint is satisfied exactly on the level of velocity.

(ii) The constraint forces $\mathcal{G}(q,t)^\top \lambda$ are eliminated exactly.

(iii) The number of unknowns and equations is reduced from $2N_q + N_\lambda$ for (q, v, λ) to $N_q + N_{\mathrm{DOF}} = 2N_q - N_\lambda$ for (q, ν). This is minimal on the level of velocity.

(iv) The reduced mass matrix $\mathcal{T}(q,t)^\top \mathcal{M}(q)\mathcal{T}(q,t)$ is of minimal possible size $N_{\mathrm{DOF}} \times N_{\mathrm{DOF}}$ and thus smaller than $\mathcal{M}(q)$ itself, which is $N_q \times N_q$.

(v) The condition of the system, which is usually bad/ill by the presence of the constraint forces $\mathcal{G}(q,t)^\top \lambda$, is improved [7, 36].

The null space coordinate method is equivalent to the solution of the index-2 version (3) in ODE form [12]. If one is interested in the Lagrange multipliers λ, they can be obtained from (q, ν) in a convenient postprocessing [27]. If an appropriate null space matrix $\mathcal{T}(q,t)$ is not available analytically, it can be computed numerically during time integration of (11), see [27] and the references cited therein. Throughout this paper, we prefer the letters $\mathcal{T}$ to denote null space matrices and τ^n to denote their columns, because the vectors τ^n span the current *t*angential space.

Remark 2.1 (Inversion of the mass-constraint matrix) For *explicit* solvers, which can only handle systems of the form

$$\mathcal{I}\dot{u} = f(t,u) \qquad \text{with identity 'mass' } \mathcal{I} \quad (\text{e. g. DoPri5, DoP853, Odex}), \tag{12}$$

system (4) must be solved for $(\dot{q}, \dot{v}, \lambda)$, so that one can choose $u = (q, v)$ in (12), e. g. by Gaussian LU factorisation [15]. In that sense, (6) should be understood. In order to avoid this decomposition step, one is restricted to solvers that may handle linearly implicit systems

$$\mathcal{A}\dot{u} = f(t,u) \qquad \text{with constant 'mass' } \mathcal{A} \quad (\text{e. g. Radau5, Seulex}) \tag{13}$$

or

$$\mathcal{A}(t,u)\dot{u} = f(t,u) \qquad \text{with state dependent 'mass' } \mathcal{A}(t,u) \quad (\text{e. g. Dassl/Daspk}). \tag{14}$$

Solvers for (14) do not eliminate the Lagrange multipliers λ in (4). They solve the full index-1 problem with $u = (q, v, \lambda)$. For solvers that may handle linearly implicit systems (13), the accelerations $w = \dot{v}$ must be introduced as additional primary unknowns. One has to solve an augmented index-1 problem with $u = (q, v, w, \lambda)$ with appropriate rescaling in the local error estimator [17, 19]. Clearly, these remarks do apply similarly, if we want to solve $(11_{1,2})$. □

3 Rotation-free parametrisation of a rigid body

In this section, we shortly summarise the so-called 'rotation-free' parametrisation for a single rigid body — or $SO(3)$ —, including an appropriate choice for a null space matrix [6, 7, 8] to eliminate the internal constraints. By 'single' we mean that the body may be connected to force elements, but not to joints. The idea of rotation-free parametrisation is to keep the nine components d^n_m of a frame $R = (d^1 \,|\, d^2 \,|\, d^3) = (d^n_m)_{n,m=1,2,3}$ in

$$SO(3) = \{R \in \mathbb{R}^{3\times 3} : \, RR^\top = R^\top R = \mathcal{I}, \det R = 1\}$$

as the primary unknowns and to enforce orthonormality with six internal constraints. This is highly redundant, but the governing equations remain very simple.

Let $(e^1 \,|\, e^2 \,|\, e^3)$ denote the global absolute coordinate system, i. e. the standard basis of the absolute Euclidean space $\mathbb{R}^3$. The orientation of a **rigid body** is completely determined by a proper orthonormal, body fixed coordinate system $R = (d^1 \,|\, d^2 \,|\, d^3) : [0,T] \to SO(3)$ at the center of mass. We assume that its directors $d^1 = Re^1$, $d^2 = Re^2$, $d^3 = Re^3$ coincide with the principal axes of inertia, so that the moment of inertia tensor becomes diagonal. The situation for the special case of a symmetric gyro top is depicted in Figure 2. The components Ω_n of the *spatial angular velocity vector* $\omega = \Omega_1 d^1 + \Omega_2 d^2 + \Omega_3 d^3 = \omega_1 e^1 + \omega_2 e^2 + \omega_3 e^3$ w. r. t. the body fixed coordinate system $R = (d^1 \,|\, d^2 \,|\, d^3)$ are given by $\Omega \simeq \mathcal{E}(\Omega) = R^\top \dot{R}$, where

$$\mathcal{E} : \mathbb{R}^3 \to so(3), \qquad u \mapsto \mathcal{E}(u) = \begin{pmatrix} 0 & -u_3 & +u_2 \\ +u_3 & 0 & -u_1 \\ -u_2 & +u_1 & 0 \end{pmatrix}, \qquad \mathcal{E}(u)w = u \times w \quad \text{for } w \in \mathbb{R}^3$$

identifies skew tensors in $so(3) = \{U \in \mathbb{R}^{3\times 3} : U + U^\top = 0\}$ with their corresponding axial vectors in $\mathbb{R}^3$, see [7, 26, 34]. We write $u \simeq \mathcal{E}(u)$ for $u \in \mathbb{R}^3$ in shorthand. We refer to $\Omega = \Omega_1 e^1 + \Omega_2 e^2 + \Omega_3 e^3 = R^{-1}\omega$ as the *material angular velocity vector*. Likewise, the components ω_n of ω w. r. t. $(e^1 \,|\, e^2 \,|\, e^3)$ are obtained from the relation $\omega \simeq \mathcal{E}(\omega) = \dot{R}R^\top$. From $\mathcal{E}(\Omega) = R^\top \dot{R}$ and the skew symmetry of $\mathcal{E}(\Omega)$ we find the three components Ω_n of Ω to be

$$\Omega_1 = \langle d^3, \dot{d^2}\rangle = -\langle d^2, \dot{d^3}\rangle, \qquad \Omega_2 = \langle d^1, \dot{d^3}\rangle = -\langle d^3, \dot{d^1}\rangle, \qquad \Omega_3 = \langle d^2, \dot{d^1}\rangle = -\langle d^1, \dot{d^2}\rangle, \tag{15}$$

where $\langle u, w\rangle = \sum_n u_n w_n$ denotes the standard inner (scalar) product for u, $w \in \mathbb{R}^N$. In contrast to the numbers ω_n, the numbers Ω_n are *objective* — or *frame indifferent*. This is, the Ω_n remain

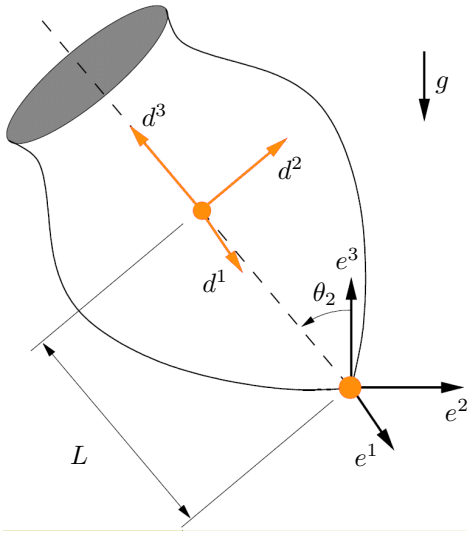

Figure 2: *Heavy symmetric gyro top.* ($I_1, I_2 \gg I_3 > 0$.)

unchanged by superimposed rotations [25, 26]. The rotatory kinetic energy T of the body can be expressed as

$$T = \frac{1}{2}\big(I_1\Omega_1^2 + I_2\Omega_2^2 + I_3\Omega_3^2\big) = \frac{1}{2}\Omega^\top \mathfrak{I}\Omega, \qquad \mathfrak{I} = \begin{pmatrix} I_1 & & \\ & I_2 & \\ & & I_3 \end{pmatrix}. \tag{16}$$

where I_1, I_2, $I_3 > 0$ denote the principal moments of inertia, i. e. the moments of inertia of the rigid body with respect to the principal axes d^1, d^2, d^3.

Let us introduce the **rotation-free** parametrisation for our rigid body. Noting that $2T = E_1(\Omega_2^2 + \Omega_3^2) + E_2(\Omega_3^2 + \Omega_1^2) + E_3(\Omega_1^2 + \Omega_2^2)$, the rotatory energy of the rigid body can equivalently be rewritten as

$$T = \frac{1}{2}\big(E_1\|\dot{d}^1\|^2 + E_2\|\dot{d}^2\|^2 + E_3\|\dot{d}^3\|^2\big) = \frac{1}{2}\dot{d}^\top M_d \dot{d} \tag{17}$$

in terms of the director velocities $\dot{d}^1$, $\dot{d}^2$, $\dot{d}^3$ and the rotation-free mass matrix

$$M_d = \begin{pmatrix} E_1\mathcal{I} & & \\ & E_2\mathcal{I} & \\ & & E_3\mathcal{I} \end{pmatrix} \in \mathbb{R}^{9\times 9}.$$

Here

$$E_1 = \frac{1}{2}(I_2 + I_3 - I_1), \qquad E_2 = \frac{1}{2}(I_3 + I_1 - I_2), \qquad E_3 = \frac{1}{2}(I_1 + I_2 - I_3) \tag{18}$$

denote the principal values of the Euler tensor of the rigid body [7] and $\|w\|^2 = \sum w_n^2$ is the standard Euclidean norm for $w \in \mathbb{R}^N$. We now parametrise $R = R(d) = (d^1 \,|\, d^2 \,|\, d^3) = (d^n_m)$ *directly* with the nine components

$$d = \big(\; d^1_1 \;\; d^1_2 \;\; d^1_3 \;\big|\; d^2_1 \;\; d^2_2 \;\; d^2_3 \;\big|\; d^3_1 \;\; d^3_2 \;\; d^3_3 \;\big)^\top = \big(\; (d^1)^\top \;\big|\; (d^2)^\top \;\big|\; (d^3)^\top \;\big)^\top : [0,T] \to \mathbb{R}^9,$$

of the directors d^1, d^2, $d^3 : [0,T] \to \mathbb{R}^3$ themselves. (So, at first glance, the terminology 'rotation-free' may be slightly misleading.) Then, three constraints of unity and three constraints of pairwise

orthogonality, in total

$$g_d(d) = \begin{pmatrix} \big((d_1^1)^2 + (d_1^2)^2 + (d_1^3)^2 - 1\big)/2 \\ \big((d_2^1)^2 + (d_2^2)^2 + (d_2^3)^2 - 1\big)/2 \\ \big((d_3^1)^2 + (d_3^2)^2 + (d_3^3)^2 - 1\big)/2 \\ \hline d_1^1 d_2^1 + d_1^2 d_2^2 + d_1^3 d_2^3 \\ d_3^1 d_1^1 + d_3^2 d_1^2 + d_3^3 d_1^3 \\ d_2^1 d_3^1 + d_2^2 d_3^2 + d_2^3 d_3^3 \end{pmatrix} = \begin{pmatrix} \big(\|d_1\|^2 - 1\big)/2 \\ \big(\|d_2\|^2 - 1\big)/2 \\ \big(\|d_3\|^2 - 1\big)/2 \\ \hline \langle d_1, d_2 \rangle \\ \langle d_3, d_1 \rangle \\ \langle d_2, d_3 \rangle \end{pmatrix} \in \mathbb{R}^6, \tag{19}$$

are required, so that R stays in $SO(3)$. This corresponds to the trivial embedding of the manifold $SO(3)$ as a submanifold in $\mathbb{R}^9$, and we write $d \sim R = R(d)$ in shorthand. In (19), we express the conditions of orthonormality w. r. t. the *rows* d_1, d_2, d_3 of R, which is the dual basis of d^1, d^2, d^3, satisfying $\langle d^n, d_m \rangle = \langle d_m, d^n \rangle = \delta_m^n$ with the Kronecker delta δ_m^n. The constraint gradient for (19) is

$$G_d(d) = \nabla_d g_d(d) = \left(\begin{array}{ccc|ccc|ccc} d_1^1 & & & d_1^2 & & & d_1^3 & & \\ & d_2^1 & & & d_2^2 & & & d_2^3 & \\ & & d_3^1 & & & d_3^2 & & & d_3^3 \\ \hline d_2^1 & d_1^1 & & d_2^2 & d_1^2 & & d_2^3 & d_1^3 & \\ d_3^1 & & d_1^1 & d_3^2 & & d_1^2 & d_3^3 & & d_1^3 \\ & d_3^1 & d_2^1 & & d_3^2 & d_2^2 & & d_3^3 & d_2^3 \end{array}\right) \in \mathbb{R}^{6\times 9}. \tag{20}$$

with $\operatorname{rk} G_d(d) = 6$ for $d \neq 0$. Letting $q = d$, $v = v_d$, $\lambda = \lambda_d$ in (1), with the kinetic energy T from (17) we arrive at the following index-3 system for a single rigid body,

$$\left\{\begin{array}{rcl} \dot{d} & = & v_d \\ M_d \dot{v}_d & = & \psi^d - G_d(d)^\top \lambda_d \\ 0 & = & g_d(d) \end{array}\right. , \tag{21}$$

where

$$\psi^d = \phi^d - \nabla_d V(d,t)^\top, \tag{22}$$

$N_q = 9$, $N_\lambda = 6$ and $N_{\mathrm{DOF}} = 3$. Here $\phi^d \in \mathbb{R}^9$ denote rotation-free exterior moments, and the scalar potential energy function V is expressed as a function of d. The corresponding index-1 system is

$$\boxed{\begin{pmatrix} \dot{d} \\ \dot{v}_d \\ \lambda_d \end{pmatrix} = \begin{pmatrix} \mathcal{I} & 0 & 0 \\ 0 & M_d & G_d(d)^\top \\ 0 & G_d(d) & 0 \end{pmatrix}^{-1} \begin{pmatrix} v_d \\ \psi^d \\ -g^{\mathrm{II}}(d, v_d) \end{pmatrix}} \tag{23}$$

with the constraint acceleration vector

$$g^{\mathrm{II}}(d, v_d) = \frac{\partial^2 g}{\partial d^2}[v_d, v_d] = \left(\begin{array}{ccc|ccc} \|\dot{d}_1\|^2 & \|\dot{d}_2\|^2 & \|\dot{d}_3\|^2 & 2\langle \dot{d}_1, \dot{d}_2 \rangle & 2\langle \dot{d}_3, \dot{d}_1 \rangle & 2\langle \dot{d}_2, \dot{d}_3 \rangle \end{array}\right)^\top.$$

According to our knowledge, there exists no explicit and cheap algebraic, closed-form expression to solve system (23) for $(\dot{d}, \dot{v}_d, \lambda_d)$. Consequently, in actual computations, we use the standard LU decomposition method to perform that step.

In order to apply the general **null space methodology** of the preceding section, we choose the following expansion for the rotation-free absolute velocity

$$v_d = \dot{d} = \sum_{n=1}^{3} \nu_n \tau_d^n(d) = T_d(d)\nu = \left(\begin{array}{c|c|c} \tau_d^1(d) & \tau_d^2(d) & \tau_d^3(d) \end{array}\right)$$

in (8) with $N_{\mathrm{DOF}} = 3$ and

$$T_d(d) = \left(\begin{array}{c|cc} & -d_1^3 & d_1^2 \\ & -d_2^3 & d_2^2 \\ & -d_3^3 & d_3^2 \\ \hline d_1^3 & & -d_1^1 \\ d_2^3 & & -d_2^1 \\ d_3^3 & & -d_3^1 \\ \hline -d_1^2 & d_1^1 & \\ -d_2^2 & d_2^1 & \\ -d_3^2 & d_3^1 & \end{array}\right) = \left(\begin{array}{c|c|c} & -d^3 & d^2 \\ \hline d^3 & & -d^1 \\ \hline -d^2 & d^1 & \end{array}\right) \in \mathbb{R}^{9\times 3}. \tag{24}$$

If we 'overload' the symbol $\mathcal{E}$ for that case, this matrix can conveniently be written $T_d(d) = \mathcal{E}(d)$ in shorthand. It is straightforwardly verified that $\operatorname{im} T_d(d) = \operatorname{null} G_d(d)$, especially that $\operatorname{rk} T_d(d) = \dim \operatorname{null} G_d(d) = 3 = N_{\mathrm{DOF}}$. We receive the following null space form for the rotation-free parametrisation of a rigid body.

Lemma 3.1 (Rotation-free null space formulation for rigid bodies) *The null space formalism, applied to the index-3 system (21) with expansion (24), yields $\nu = \Omega$ and the following special form of (11),*

$$\boxed{\left\{\begin{array}{rcl} \dot{d} & = & T_d(d)\Omega \\ \mathfrak{I}\dot{\Omega} & = & \mu - \Omega \times \mathfrak{I}\Omega, \quad \mu = T_d(d)^\top \psi^d \\ 0 & = & g_d(d) \end{array}\right.,} \tag{25}$$

where $\mathfrak{I}$ as in (16) and ψ^d as in (22).

Proof: With the aid of (18) is is seen that $T_d(d)^\top M_d T_d(d) = \mathfrak{I}$. Due to (15), we find $\nu = \Omega$. It is straightforwardly computed that

$$T_d^\top M_d \dot{T}_d \Omega = \begin{pmatrix} (E_3 - E_2)\Omega_3\Omega_2 \\ (E_1 - E_3)\Omega_1\Omega_3 \\ (E_2 - E_1)\Omega_2\Omega_1 \end{pmatrix} = \Omega \times \mathfrak{I}\Omega,$$

which follows from the inverse relationships $I_1 = E_2 + E_3$, $I_2 = E_3 + E_1$, $I_3 = E_1 + E_2$ of (18). As the system is scleronomic, it follows that $r = \dot{r} \equiv 0$ in (11). ■

It is worth mentioning that (25_2) consist the well-known Newton-Euler equations for the material angular velocity of a rigid body. The vector $\mu = \mu_1 e^1 + \mu_2 e^2 + \mu_3 e^3 = R(d)^{-1}(\mu_1 d^1 + \mu_2 d^2 + \mu_3 d^3)$ contains the components μ_n of the applied moments with respect to the body fixed coordinate system $(d^1 \,|\, d^2 \,|\, d^3)$.

Again, let us look at the general null space benefits (i), ..., (v) from Section 2 and let us give some additional remarks for our special case here.

(ii) The six internal constraint forces $G_d(d)^\top \lambda_d$, which are eliminated by the proposed null space technique, are somewhat artificial. They do not have any physical meaning and — consequently — are of no interest.

(iii) The number of unknowns is minimal on the level of velocity, still redundant on the level of position. But the parametrisation is still singularity-free — compared to *any* three-dimensional — e. g. 'vectorial' [5] or Euler/Cardan angle [10] — parametrisation of $SO(3)$, which necessarily *must* have singularities [41].

(iv) The reduced 3×3 mass matrix $T_d(d)^\top M_d T_d(d) = \mathfrak{I}$ is as well diagonal and state-independent, similarly to M_d itself.

	null space quaternionic $(42_{1,2})$	null space rotation-free $(25_{1,2})$	absolute quaternionic $(40_{1,2})$	absolute rotation-free $(23_{1,2})$	Euler angles $(66_{1,2})$
unknowns	p, Ω **7**	d, Ω **12**	p, $\dot{p}$ (λ_p) **8** $(+1)$	d, $\dot{d}$ (λ_d) **18** $(+6)$	θ, Ω **6**
$+$	5	0	17	16	2
$-$	7	12	4	1	5
$*$	18	24	24	10	14
$/$	6	3	3	0	5
^{2}	0	0	4	9	0
sin	0	0	0	0	2
cos	0	0	0	0	2
LU decomp.	0	0	0	15×15	0

Table 1: *Operation counts for the right-hand sides of* $(\dot{q}, \dot{v}) = \Psi(q, v, t)$ *(absolute coordinates, index-0) resp.* $(\dot{q}, \dot{\Omega}) = \Psi(q, \Omega, t)$ *(null space coordinates) in ODE form.*

(v) The problem of probable bad condition in the systems (21) or (23) is resolved completely. This is, because the Skeel condition of the diagonal matrix $\mathfrak{I}$ equals one.

In addition, we have the following benefit, which is lucky here.

(vi) The right-hand side of (25) in ODE form is cheaper than the right-hand side of (23) in ODE form, see Table 1. The same holds as well for the right-hand side Jacobian.

All these benefits lead to an improvement of automatic stepsize selection for all the time integrators that we have tested. These are ODE15S, ODE45, ODE23 from the MATLAB ODE suite [35], DOPRI5, DOP853, ODEX, RADAU5, DASSL/DASPK and SEULEX [17, 18, 19, 28, 29]. The reason is that the error estimator in a solver does not have to control as many redundant unknowns. (And, usually, errors in the velocities are more crucial and lead to more time step rejections than errors in the positions.) In fact, these benefits lead to improved accuracy — especially improved energetic behaviour —, as we shall see in our numerical test problems in Section 7.

4 Quaternionic parametrisation of a rigid body

In contrast to the rotation-free method, the **quaternionic parametrisation of rotations** is much older. Euler knew them already before Hamilton found his quaternion algebra $\mathbb{H}$, see [11, 16, 22]. This is why quaternions are frequently referred to as 'Euler parameters'. Unit quaternions in the subgroup

$$\mathbb{S}^3 = \{p \in \mathbb{H} : \|p\|^2 = 1\} \subset \mathbb{H},$$

the three-dimensional unit sphere, are an appropriate way to describe — non-commutative spatial — rotations in $SO(3)$. This is analogous to unit complex numbers in the subgroup $\mathbb{S}^1 = \{z \in \mathbb{C} : \|z\|^2 = 1\} \subset \mathbb{C}$, the complex unit circle, which describe — commutative plane — rotations in $SO(2) = \{R \in \mathbb{R}^{2\times 2} : RR^\top = R^\top R = \mathcal{I}, \det R = 1\}$. With a general quaternion

$$p = p_0 + p_1 i + p_2 j + p_3 k = p_0 + \hat{p} = \Re(p) + \Im(p) = (p_0 \mid p_1, p_2, p_3)^\top : [0, T] \to \mathbb{H}$$

a radially stretched frame $R = (d^1 \,|\, d^2 \,|\, d^3) = \mathcal{R} \circ p : [0, T] \xrightarrow{p} \mathbb{H} \xrightarrow{\mathcal{R}} \mathbb{R}\,SO(3)$ is obtained by composition with the Euler map

$$\mathcal{R} : \mathbb{H} \to \mathbb{R}SO(3), \quad p \mapsto \big(2p_0^2 - \|p\|^2\big)\mathcal{I} + 2\hat{p} \otimes \hat{p} + 2p_0\mathcal{E}(\hat{p}), \tag{26}$$

where $u \otimes w = uw^\top$ denotes the standard dyadic product for u, $w \in \mathbb{R}^N$. In components, the three directors are

$$d^1 = \varphi^1(p) = \begin{pmatrix} p_0^2 + p_1^2 - p_2^2 - p_3^2 \\ 2(p_1p_2 + p_0p_3) \\ 2(p_1p_3 - p_0p_2) \end{pmatrix}, \qquad d^2 = \varphi^2(p) = \begin{pmatrix} 2(p_1p_2 - p_0p_3) \\ p_0^2 - p_1^2 + p_2^2 - p_3^2 \\ 2(p_2p_3 + p_0p_1) \end{pmatrix}, \tag{27}$$

and

$$d^3 = \varphi^3(p) = \begin{pmatrix} 2(p_1p_3 + p_0p_2) \\ 2(p_2p_3 - p_0p_1) \\ p_0^2 - p_1^2 - p_2^2 + p_3^2 \end{pmatrix}. \tag{28}$$

Homogeneity $\mathcal{R}(\eta p) = \eta^2\mathcal{R}(p)$ holds for each quaternion $p \in \mathbb{H}$ and scalar $\eta \in \mathbb{R}$. This property makes $\mathcal{R}$ sensitive with respect to radial stretching of p. Especially, $\mathcal{R}$ maps the unit sphere $\mathbb{S}^3$ into $SO(3)$, that is, unit quaternions yield pure rotations that are not stretched. It holds $\mathcal{R}(-p) = \mathcal{R}(p)$, which implies that p and its antipode $-p$ describe the same rotation. It is well known that for each stretched rotation R in $\mathbb{R}SO(3)$ there exist exactly two quaternions $\pm p$ — necessarily antipodes — that produce $R = \mathcal{R}(\pm p)$. Via $\mathcal{R}$, the unit sphere $\mathbb{S}^3$ covers $SO(3)$ exactly two times, the correspondence $\mathcal{R} : \mathbb{S}^3/\{\pm 1\} \to SO(3)$ is one-to-one and onto [11, 16, 22]. This is, the quaternionic unit sphere $\mathbb{S}^3$ modulo antipodals is exactly $SO(3)$. Stretched rotation of a vector $w \in \Im(\mathbb{H}) = \mathbb{R}^3$ is expressed via quaternions as

$$\mathcal{R}(p)w = pw\bar{p} \ \text{(forward)} \qquad \text{and} \qquad \mathcal{R}(p)^\top w = \bar{p}wp \ \text{(backward)} \tag{29}$$

for $p \in \mathbb{H}$. Especially $d^n(p) = pe^n\bar{p} = \mathcal{R}(p)e^n$ for each of the spatially fixed global Euclidean base vectors $(e^1 \,|\, e^2 \,|\, e^3)$ of $\Im(\mathbb{H}) = \mathbb{R}^3$, which are classically denoted by the letters $e^1 = i$, $e^2 = j$ and $e^3 = k$. For a quaternion $p \in \mathbb{S}^3 \setminus \{\pm 1\}$, we can write $p = \cos(\alpha/2) + \sin(\alpha/2)\pi$ with a unique purely imaginary unit quaternion $\pi \in \Im(\mathbb{H}) \cap \mathbb{S}^3$ and a unique angle $0 < \alpha < 2\pi$. So in Euclidean space, $\mathcal{R}(p)w = \cos(\alpha)w + \sin(\alpha)\pi \times w + (1 - \cos(\alpha))\langle \pi, w\rangle\pi$ for $w \in \Im(\mathbb{H}) = \mathbb{R}^3$ is exactly the rotation of w about the axis $\mathbb{R}\pi$ with the angle α, see [16, 11]. Recall that the quaternion product is defined by

$$\begin{array}{rcl} pq & = & p_0q_0 - \langle \hat{p}, \hat{q}\rangle + p_0\hat{q} + q_0\hat{p} + \hat{p} \times \hat{q} \\ & = & \mathcal{Q}(p)q \end{array}, \qquad \mathcal{Q}(p) = \left(\begin{array}{c||ccc} p_0 & -p_1 & -p_2 & -p_3 \\ \hline p_1 & p_0 & -p_3 & p_2 \\ p_2 & p_3 & p_0 & -p_1 \\ p_3 & -p_2 & p_1 & p_0 \end{array}\right) \tag{30}$$

for $p, q \in \mathbb{H}$, where $\langle \cdot, \cdot \rangle$ is the inner (scalar) product in $\mathbb{H}$ and $\cdot \times \cdot$ the outer (cross) product in $\mathbb{R}^3$. It is convenient and common use to identify $\Im(\mathbb{H}) = \mathbb{R}^3$, this means, ordinary Euclidean vectors are treated as quaternions with vanishing real parts. Especially, $\langle p, q\rangle = \sum_{n=0}^3 p_nq_n$ for p, $q \in \mathbb{H}$ and $\langle p, q\rangle = \sum_{n=1}^3 p_nq_n$ for p, $q \in \Im(\mathbb{H})$. We use the symbols $p_0 = \Re(p)$ resp. $\hat{p} = \Im(p) = (p_1, p_2, p_3)^\top$ to denote the real resp. the imaginary (= vector) part and $\bar{p} = p_0 - \hat{p}$ to denote the conjugate of a quaternion $p \in \mathbb{H}$. Note that $\bar{p} = \|p\|^2p^{-1}$, where p^{-1} stands for the multiplicative inverse of p. In components, (30) is

$$\begin{array}{rcl} pq & = & p_0q_0 - (p_1q_1 + p_2q_2 + p_3q_3) \\ & & +(p_0q_1 + p_1q_0 + p_2q_3 - p_3q_2)i + (p_0q_2 + p_2q_0 + p_3q_1 - p_1q_3)j + (p_0q_3 + p_3q_0 + p_1q_2 - p_2q_1)k. \end{array}$$

For more details on the Hamilton quaternion division algebra (= skew field), we refer to [11, 16, 22]. The situation is depicted in the commutative diagram in Figure 3. For further details concerning the Lie group/algebra structures and their interconnections, see [9, 32, 40]. Note that from differential geometry it is known that the quaternion unit sphere $\mathbb{S}^3$ is completely isotropic — or 'fair' —, in the sense that no special direction is preferred. This makes $\mathbb{S}^3$ highly attractive for the interpolation of rotations [31].

The result of the following Lemma, which relates unit quaternions to the angular velocity of a moving frame — e. g. a rigid body —, is of utmost importance. Of course, it is well known [5] — and most probably due to Euler. However, we give a very short and compact proof for the reader's convenience.

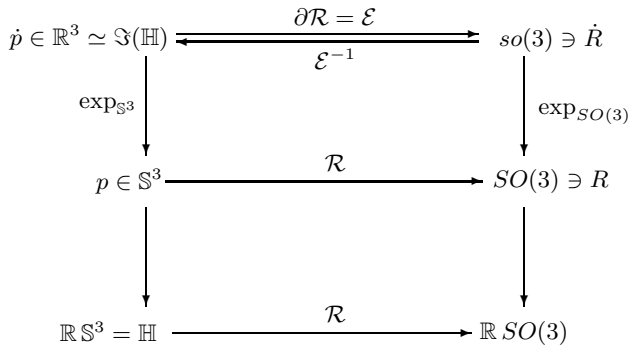

Figure 3: *Mappings between the involved manifolds — and their tangential spaces.*

Lemma 4.1 (Differential equations for Ω and ω) *For the angular velocity in terms of unit quaternions p and proper orthonormal frames R, we have the following equivalences.*

1. *The differential equations $\Omega = 2\bar p\dot p$ in $\mathbb{S}^3$ and $\Omega \simeq \mathcal{E}(\Omega) = R^\top\dot R$ in $SO(3)$ for the material angular velocity vector Ω are equivalent.*
2. *The differential equations $\omega = 2\dot p\bar p$ in $\mathbb{S}^3$ and $\omega \simeq \mathcal{E}(\omega) = \dot R R^\top$ in $SO(3)$ for the spatial angular velocity vector ω are equivalent.*

Proof: We prove the first assertion. For an arbitrary, but fixed, vector $w \in \Im(\mathbb{H})$, we compute with (30) and the fact that $\bar w = -w$ for $\hat w = w$,

$$\begin{aligned}\mathcal{E}(2\bar p\dot p)w = 2\bar p\dot p\times w \;&=\; 2\Im\big(\bar p\dot p\times w - \langle \bar p\dot p, w\rangle\big) \;=\; 2\Im(\bar p\dot p w) \;=\; \bar p\dot p w - \overline{\bar p\dot p w} \;=\; \bar p\dot p w + \overline{\bar p\dot p\bar w}\\ &= \bar p\dot p w + w\dot{\bar p}p \;=\; \bar p(\dot p w\bar p + pw\dot{\bar p})p \;=\; \bar p\frac{\mathrm{d}}{\mathrm{d}t}(pw\bar p)p \;=\; \bar p\frac{\mathrm{d}}{\mathrm{d}t}(Rw)p \;=\; \bar p(\dot R w)p \;=\; R^\top\dot R w.\end{aligned}$$

due to (29). Now, if $R^\top\dot R = \mathcal{E}(\Omega)$, it follows that $\Omega = 2\bar p\dot p$, as w can be chosen arbitrarily. The second assertion can be proven similarly. ■

The reader should note that $\Omega_0 = \Re(\Omega) = \Re(\bar p\dot p) = \langle p, \dot p\rangle = 0$ directly follows from the condition $\|p\|^2 = 1$ through time differentiation.

Let us return to our **rigid body**. A short computation with $\Omega = 2\bar p\dot p$ and the p-dependent quaternion mass matrix

$$M_p(p) = 4\mathcal{Q}(p)I\mathcal{Q}(p)^\top \in \mathbb{R}^{4\times 4}, \tag{31}$$

shows that the rotatory kinetic energy of the body can be rewritten as $2T = I_0\Omega_0^2 + I_1\Omega_1^2 + I_2\Omega_2^2 + I_3\Omega_3^2$, or

$$T = \frac{1}{2}\dot p^\top M_p(p)\dot p, \qquad I = \left(\begin{array}{c|ccc} I_0 & & & \\ \hline & I_1 & & \\ & & I_2 & \\ & & & I_3 \end{array}\right). \tag{32}$$

Here $I_0 \geq 0$ denotes any arbitrary — since fictive — non-negative zeroth 'radial moment of inertia'. The choice of I_0 does not play any role, since $\Omega_0 = \Re(\Omega) = \langle p, \dot p\rangle = 0$. Some authors set I_0 to a positive number, so that $M_p(p)$ becomes positive definite, e. g. $I_0 = \frac{1}{2}(I_1 + I_2 + I_3) = \frac{1}{2}\operatorname{trace}(I)$ in [9]. Throughout this article, we set $I_0 = 0$, so that $M_p(p)$ is cheaper to evaluate in numerical computations. $M_p(p)$ satisfies the symmetry property $M_p(-p) = M_p(p)$, which is a consequence of the fact that both p and $-p$ describe the same rotation $\mathcal{R}(p) = \mathcal{R}(-p)$. Kernel resp. image of $M_p(p)$ are given by $\operatorname{null} M_p(p) = \mathbb{R}p$ resp. $\operatorname{im} M_p(p) = \{p\}^\perp$. This is, $M_p(p)$ is positive *semi*-definite with its one singular dimension in radial direction. Consequently, we have $\operatorname{rk} M_p(p) = 3$. Interestingly and useful later, the columns of the quaternion matrix $\mathcal{Q}(p)$ in (30)

are the eigenvectors of $M_p(p)$ to the eigenvalues 0, $4I_1$, $4I_2$ and $4I_3$. The mass skew derivative in (2) admits the closed-form expression $\frac{1}{2}\nabla_p\big(\dot{p}^\top M_p(p)\dot{p}\big)^\top - \nabla_p\big(M_p(p)\dot{p}\big)\dot{p} = 8\mathcal{Q}(\dot{p})I\mathcal{Q}(\dot{p})^\top p$, so that the generalised quaternionic forces in (2) become

$$\psi^p = \phi^p - \nabla_p V(p,t)^\top + 8\mathcal{Q}(\dot{p})I\mathcal{Q}(\dot{p})^\top p, \tag{33}$$

if we express the potential energy V as a function of p. Letting $q = p$, $v = v_p$, $\lambda = \lambda_p$ in (1) with the kinetic energy T from (32), together with the spherical internal constraint

$$g_p(p) = \frac{1}{2}\big(\|p\|^2 - 1\big), \tag{34}$$

we receive the quaternionic index-3 description for the rigid body,

$$\left\{\begin{array}{rcl} \dot{p} & = & v_p \\ M_p(p)\dot{v}_p & = & \psi^p - \lambda_p p \\ 0 & = & \frac{1}{2}\big(\|p\|^2 - 1\big) \end{array}\right. \tag{35}$$

where

$$G_p(p) = \nabla_p g_p(p) = p^\top = \left(\begin{array}{c|ccc} p_0 & p_1 & p_2 & p_3 \end{array}\right) \in \mathbb{R}^{1\times 4}. \tag{36}$$

is of rank $\operatorname{rk} G_p(p) = 1$ for $p \neq 0$. The constraints on position, velocity and acceleration level are written $2g_p = \|p\|^2 - 1 = 0$, $\dot{g}_p = \langle p, \dot{p}\rangle = 0$, $\ddot{g}_p = \langle p, \ddot{p}\rangle + \|\dot{p}\|^2 = 0$, respectively. With the constraint acceleration $g^{\mathrm{II}}(p, v_p, t) = \|v_p\|^2$, we receive the index-1 system

$$\left\{\begin{array}{rcl} \dot{p} & = & v_p \\ M_p(p)\dot{v}_p & = & \psi^p - \lambda_p p \\ \langle p, \dot{v}_p\rangle & = & -\|v_p\|^2 \end{array}\right. . \tag{37}$$

Here $N_q = 4$, $N_\lambda = 1$ and $N_{\mathrm{DOF}} = 3$. The $\psi^p \in \mathbb{H}$ are sometimes called 'quaternionic moments' [34]. The rotatory quaternionic mass-constraint matrix in (37) and has the form

$$\left(\begin{array}{c|c} M_p(p) & G_p(p)^\top \\ \hline G_p(p) & 0 \end{array}\right) = \left(\begin{array}{c|c} M_p(p) & p \\ \hline p^\top & 0 \end{array}\right) \in \mathbb{R}^{5\times 5}. \tag{38}$$

The inverse of (38) exists, iff $p \neq 0$, and has the same form as (38), where $M_p(p)$ is replaced by the tangential inverse quaternion mass

$$M_p^\sharp(p) = \frac{1}{4\|p\|^4}\mathcal{Q}(p)I^\sharp\mathcal{Q}(p)^\top, \qquad I^\sharp = \left(\begin{array}{c|ccc} 0 & & & \\ \hline & I_1^{-1} & & \\ & & I_2^{-1} & \\ & & & I_3^{-1} \end{array}\right).$$

This is

$$\left(\begin{array}{c|c} M_p(p) & G_p(p)^\top \\ \hline G_p(p) & 0 \end{array}\right)^{-1} = \left(\begin{array}{c|c} M_p^\sharp(p) & G_p(p)^\top \\ \hline G_p(p) & 0 \end{array}\right). \tag{39}$$

$M_p^\sharp(p)$ satisfies the property $M_p(p)M_p^\sharp(p) = M_p^\sharp(p)M_p(p) = \mathcal{I} - p\otimes p$ for $p \in \mathbb{S}^3$, which justifies the nomenclature 'tangential inverse', since $M_p^\sharp(p)M_p(p)\pi = M_p(p)M_p^\sharp(p)\pi = \pi - (p\otimes p)\pi = \pi - \langle p, \pi\rangle p$ for $p \in \mathbb{S}^3$ and $\pi \in \mathbb{H}$. Left-multiplication of (37) with (39) gives

$$\boxed{\left\{\begin{array}{rcl} \dot{p} & = & v_p \\ \dot{v}_p & = & M_p^\sharp(p)\psi^p - \|v_p\|^2 p \\ \lambda_p & = & \langle p, \psi^p\rangle \end{array}\right. .} \tag{40}$$

It follows that only the tangential component $M_p^\sharp(p)\psi^p$ of ψ^p is physically relevant. The radial part of the acceleration, which is needed to keep the quaternion on its spherical orbit, is equal to $-\|v_p\|^2 p$.

Note that on $\mathbb{S}^3$, the structures of (38) and its inverse (39) are completely identical. Thus, the numerical complexities of (37) and its inverted version (40) are the same. Further details concerning these topics are carried out in [9, 26, 34].

Let us apply the general **null space framework** of Section 2. The tangential space $\operatorname{null} G_p(p) = \{p\}^\perp = \{\pi \in \mathbb{H} : \langle p, \pi\rangle = 0\}$ of $\mathbb{S}^3$ at p has dimension $N_{\mathrm{DOF}} = 3$. An adequate expansion for the tangential quaternionic absolute velocity

$$v_p = \dot{p} = \sum_{n=1}^{3} \nu_n \tau_p^n(p)$$

in (8) is

$$v_p = T_p(p)\nu = \left(\begin{array}{c|c|c} \tau_p^1(p) & \tau_p^2(p) & \tau_p^3(p) \end{array}\right)\nu, \qquad T_p(p) = \frac{1}{2}\left(\begin{array}{c|c|c} -p_1 & -p_2 & -p_3 \\ \hline p_0 & -p_3 & p_2 \\ p_3 & p_0 & -p_1 \\ -p_2 & p_1 & p_0 \end{array}\right) \in \mathbb{R}^{4\times 3}. \quad (41)$$

The matrix $T_p(p)$ consists of the last three columns of $\mathcal{Q}(p)$ in (30). Its rank is equal to 3 and satisfies $\operatorname{im} T_p(p) = \operatorname{null} G_p(p)$, as required. Then we receive the following quaternionic null space formulation for a rigid body.

Lemma 4.2 (Quaternionic null space formulation for rigid bodies) *The null space technique, applied to the index-3 system (35) with expansion (41), yields $\nu = \Omega$ and the following special form of (11),*

$$\boxed{\left\{\begin{array}{rcll} \dot{p} &=& \frac{1}{2}p\Omega & \\ \mathfrak{I}\dot{\Omega} &=& \mu - \Omega\times\mathfrak{I}\Omega, & \mu = \frac{1}{2}\Im(\bar{p}\psi^p) + \Omega\times\mathfrak{I}\Omega \\ 0 &=& \frac{1}{2}\big(\|p\|^2 - 1\big) & \end{array}\right.} \quad (42)$$

where $\mathfrak{I}$ as in (16) and ψ^p as in (33).

Proof: Firstly, the tangential vectors $\tau_p^n(p)$ are eigenvectors of $M_p(p)$ with the corresponding eigenvalues $4I_n$ for $n = 1, 2, 3$. Since $\operatorname{null} M_p(p) = \mathbb{R}p$ and $\mathcal{Q}(p) \in \|p\|SO(\mathbb{H})$ — which yields that the system $(p, \tau_p^1(p), \tau_p^2(p), \tau_p^3(p))$ is an orthonormal one on $\mathbb{S}^3$ — we receive $T_p(p)^\top M_p(p) T_p(p) = \mathfrak{I}$. Secondly, the following general identities from quaternionic calculus

$$T_p(p)w = \frac{1}{2}pw, \qquad T_p(p)^\top\pi = \frac{1}{2}\Im(\bar{p}\pi) \qquad \text{for } w \in \Im(\mathbb{H}), \pi \in \mathbb{H}, \quad (43)$$

which can be derived directly from (30), immediately yield $T_p(p)\nu = \frac{1}{2}p\nu$ and $T_p(p)^\top\psi^p = \frac{1}{2}\Im(\bar{p}\psi^p)$. Therefore, especially $\nu = \Omega$ due to Lemma 4.1. Thirdly, since the system is scleronomic, i. e. $\partial g/\partial t \equiv 0$, it follows that $r = \dot{r} \equiv 0$. Finally, from the cyclic relations

$$\frac{\partial\tau_p^1}{\partial p}\tau_p^2(p) = -\tau_p^3(p), \qquad \frac{\partial\tau_p^2}{\partial p}\tau_p^3(p) = -\tau_p^1(p), \qquad \frac{\partial\tau_p^3}{\partial p}\tau_p^1(p) = -\tau_p^2(p)$$

and

$$\frac{\partial\tau_p^n}{\partial p}\tau_p^n(p) = -p, \quad n = 1, 2, 3, \qquad \dot{T}_p = \frac{\partial}{\partial p}\big(\tau_p^1(p)|\tau_p^2(p)|\tau_p^3(p)\big)T_p(p)\nu$$

it follows that the term $T_p(p)^\top M_p(p)\dot{T}_p(p)\nu \equiv 0$ vanishes. This can as well be seen from $\dot{v}_p = \frac{1}{2}p\dot{\nu} - \|v_p\|^2 p$, where the radial part is annihilated by $M_p(p)$. ■

As for the rotation-free case, (42_2) are precisely the classical Newton-Euler equations. But in contrast to (25_2), the reader should observe that the term $\Omega \times \mathfrak{I}\Omega$ is already included as a summand in ψ^p. It corresponds to the mass skew derivative in (33) according to $8T_p(p)^\top \mathcal{Q}(\dot{p})^\top I \mathcal{Q}(\dot{p})p = \Omega \times \mathfrak{I}\Omega$, since $\Omega = 2\bar{p}\dot{p}$, see Lemma 4.1 and [26, 34].

The above lemma yields that the null space technique, applied to the quaternionic rotatory formulation, yields a well known mixed formulation for rigid bodies, which uses the variables (p, Ω) as the primary unknowns [12, 30, 34]. We think, it is an interesting insight that this classical mixed formulation can be embedded into the systematic and general null space coordinate framework.

Let us comment on practical aspects for numerical implementations. The reader should observe that, intrinsically in both the rotation-free and the quaternionic parametrisations of $SO(3)$, there are many skew symmetries. The exploitation of these is one reason, why the right-hand side of the models can be implemented with extremely few elementary arithmetic operations, see Table 1. Another benefit of both parametrisations is that they comprise linear and quadratic — instead of higher algebraic (e. g. roots) or transcendent (e. g. trigonometric) — expressions. So there is no vast blow-up for the Jacobians, Hessians or higher order partial derivatives.

The six benefits (i), ..., (vi) of the preceding sections do as well apply analogously to the quaternionic null space description presented here.

Remark 4.3 (Minimality) It is proven in [41] that any singularity-free parametrisation of the three-dimensional manifold $SO(3)$ necessarily *must be* four-dimensional. Therein, it was as well shown that *no* four-dimensional parametrisation can be one-to-one. (Quaternions yield a two-to-one correspondence, as we have seen.) For a one-to-one correspondence, at least *five* parameters are needed, a funny, but awkward example being given in [41]. In practice, the fact that the quaternionic parametrisation (26) is 'twice onto' is irrelevant. □

Remark 4.4 (Relative coordinates) If one uses relative coordinates to set up a multibody model, where the relative angles between two neighbouring rigid bodies cannot exceed π, it is possible to choose just the three components of the *imaginary* part $\Im(p) = (p_1, p_2, p_3)^\top$ of the relative — quotient — quaternion p as the primary unknowns, simply by letting $p_0 = \sqrt{1 - p_1^2 - p_2^2 - p_3^2}$. In that case, working on the quaternionic 'northern hemisphere' $\{p \in \mathbb{S}^3 : p_0 = \Re(p) > 0\}$ is as minimal as working with relative angles. One receives an ODE instead of a DAE — with the drawback of a full mass matrix. □

Remark 4.5 (Plane rotations) For plane and commutative rotations in $SO(2)$, e. g. for $d^1 = i$ and $\Omega = \Omega_1 i$, the quaternion p simply reduces to a complex number $p = p_0 + p_1 i$ (with $p_2 = p_3 = 0$), subjected to the constraint $\|p\|^2 = p_0^2 + p_1^2 = 1$. Applying the null space technique in the same way as presented before, we have two absolute coordinates $q = (p_0, p_1)$ for the position and one independent quasi-velocity $\nu = \Omega_1$ for the velocity. This is $N_q = 2$, $N_\lambda = 1$ and $N_{\mathrm{DOF}} = 1$.
In the plane case, the null space method does not make sense in practice, as the manifold $SO(2)$ can be parametrised in a singularity-free manner, using just one generalised position coordinate α. Letting, $p_0 = \cos(\alpha/2)$, $p_1 = \sin(\alpha/2)$, we receive $d^2 = (p_0^2 - p_1^2)j + 2p_0p_1k = \cos(\alpha)j + \sin(\alpha)k$, $d^3 = -2p_0p_1j + (p_0^2 - p_1^2)k = -\sin(\alpha)j + \cos(\alpha)k$ and $d^3 = id^2 = -d^2i$. □

Remark 4.6 (Material vs. spatial angular velocity) The reader might ask, why we constrain the columns d_n of $R^\top = (d_1 \,|\, d_2 \,|\, d_3)$ in $g_d(d)$ in (19), not the columns d^n of $R = (d^1 \,|\, d^2 \,|\, d^3)$ itself. If we chose the directors d^n of R, i. e.

$$g_d^\star(d) = \begin{pmatrix} \big((d_1^1)^2 + (d_2^1)^2 + (d_3^1)^2 - 1\big)/2 \\ \big((d_1^2)^2 + (d_2^2)^2 + (d_3^2)^2 - 1\big)/2 \\ \big((d_1^3)^2 + (d_2^3)^2 + (d_3^3)^2 - 1\big)/2 \\ \hline d_1^1 d_1^2 + d_2^1 d_2^2 + d_3^1 d_3^2 \\ d_1^3 d_1^1 + d_2^3 d_2^1 + d_3^3 d_3^1 \\ d_1^2 d_1^3 + d_2^2 d_2^3 + d_3^2 d_3^3 \end{pmatrix} = \begin{pmatrix} \big(\|d^1\|^2 - 1\big)/2 \\ \big(\|d^2\|^2 - 1\big)/2 \\ \big(\|d^3\|^2 - 1\big)/2 \\ \hline \langle d^1, d^2 \rangle \\ \langle d^3, d^1 \rangle \\ \langle d^2, d^3 \rangle \end{pmatrix} \in \mathbb{R}^6 \tag{44}$$

with the gradient

$$G_d^\star(d) = \nabla_d g_d^\star(d) = \left(\begin{array}{ccc|ccc|ccc} d_1^1 & d_2^1 & d_3^1 & & & & & & \\ & & & d_1^2 & d_2^2 & d_3^2 & & & \\ & & & & & & d_1^3 & d_2^3 & d_3^3 \\ \hline d_1^2 & d_2^2 & d_3^2 & d_1^1 & d_2^1 & d_3^1 & & & \\ d_1^3 & d_2^3 & d_3^3 & & & & d_1^1 & d_2^1 & d_3^1 \\ & & & d_1^3 & d_2^3 & d_3^3 & d_1^2 & d_2^2 & d_3^2 \end{array}\right) = \left(\begin{array}{ccc|ccc|ccc} (d^1)^\top & & & & & & & & \\ & & & (d^2)^\top & & & & & \\ & & & & & & & & (d^3)^\top \\ \hline (d^2)^\top & & & (d^1)^\top & & & & & \\ (d^3)^\top & & & & & & & & (d^1)^\top \\ & & & & (d^3)^\top & & & & (d^2)^\top \end{array}\right)$$

the matrix

$$T_d^\star(d) = \left(\begin{array}{ccc|ccc|ccc} & & & d_3^1 & & -d_2^1 & & & \\ -d_3^1 & & & & & d_1^1 & & & \\ d_2^1 & & & -d_1^1 & & & & & \\ \hline & & & d_3^2 & & -d_2^2 & & & \\ -d_3^2 & & & & & d_1^2 & & & \\ d_2^2 & & & -d_1^2 & & & & & \\ \hline & & & d_3^3 & & -d_2^3 & & & \\ -d_3^3 & & & & & d_1^3 & & & \\ d_2^3 & & & -d_1^3 & & & & & \end{array}\right) = \left(\begin{array}{c} -\mathcal{E}(d^1) \\ \hline -\mathcal{E}(d^2) \\ \hline -\mathcal{E}(d^3) \end{array}\right) \in \mathbb{R}^{9\times 3} \tag{45}$$

would serve as a null space matrix, since $\operatorname{null} G_d^\star(d) = \operatorname{im} T_d^\star(d)$, $\operatorname{rk} T_d^\star(d) = 3$. But, similarly as in Lemma 3.1, one sees that we obtain $\nu = \omega$ instead of $\nu = \Omega$. Recall that $\omega = R\Omega = \sum_n \omega_n e^n$ contains the components of the angular velocity w. r. t. the globally fixed basis $(e^1 \,|\, e^2 \,|\, e^3)$. So, choosing the columns does *not* lead to a constant, diagonal mass in (25_2). In fact, we have $\dot{d} = T_d(d)\Omega = T_d^\star(d)\omega = T_d^\star(d)R\Omega$. Therefore, constraining the columns leads to a more expensive right-hand side function, if the material angular velocity Ω is used as the primary unknown in simulations. Likewise, for the quaternionic parametrisation of the rigid body, choosing

$$T_p^\star(p) = \frac{1}{2}\left(\begin{array}{c|c|c} -p_1 & -p_2 & -p_3 \\ \hline p_0 & p_3 & -p_2 \\ -p_3 & p_0 & p_1 \\ p_2 & -p_1 & p_0 \end{array}\right) \in \mathbb{R}^{4\times 3}, \tag{46}$$

which as well satisfies the required property $\operatorname{null} G_p(p) = \operatorname{im} T_p^\star(p)$, leads to $\nu = \omega$ and $\dot{p} = \frac{1}{2}\omega p$ instead of $\dot{p} = \frac{1}{2}p\Omega$ in (42_1). Here as well, it holds that $\dot{p} = T_p(p)\Omega = T_p^\star(p)\omega$, see Lemma 4.1, and the reduced mass matrix $T_p^\star(p)^\top M_p(p) T_p^\star(p)$ is state-dependent. □

There is another important reason, why to choose $T_d(d)$ and not $T_d^\star(d)$ as a null space matrix. Namely, the differential of $\mathcal{R}$ maps the tangential vectors $(\tau_p^1, \tau_p^2, \tau_p^3)$ at p onto the tangential vectors $(\tau_d^1, \tau_d^2, \tau_d^3)$ at $d \sim R(d) = \mathcal{R}(p)$. This is explained now in the coming section.

5 Connection between rotation-free and quaternionic formalisms

In the preceding Sections 3 and 4, we have derived the quaternionic and rotation-free null space formulations for single rigid bodies more or less 'bottom-up'. In this section, we will explain, how to derive the quaternionic null space formulation (42) for the rigid body from the rotation-free formulation (25). The idea is simply to 'pull back' the constraint g_d, its gradient G_d and the corresponding null space matrix T_d. Clearly, the mapping that links both descriptions is the Euler map (26). Pulling back the tangential vectors is done with the Moore-Penrose pseudoinverse of its differential, for which we present a simple analytic expression in closed form.

The pull back procedure is universal and can be applied to any multibody system that is built up of the elementary joints and null space matrices presented in [7]. The quaternionic null space formalism, which is obtained that way, yields an interesting alternative to the state-of-the-art

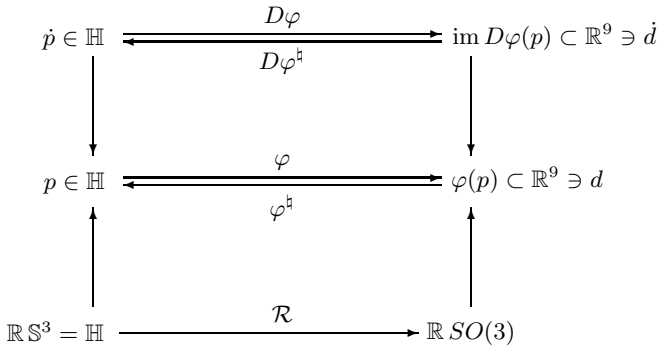

Figure 4: *Mappings between the embeddings of the involved manifolds — and their embedded tangential spaces.*

modeling philosophies in multibody dynamics, which use Euler angles for the parametrisation of $SO(3)$ and absolute coordinates ('ADAMS-like') or relative coordinates in connection with an $O(N)$-multibody formalism ('SIMPACK-like').

First, let us start with a **single rigid body**. We consider the rotation-free system (21) in general, where $g_d(d) \in \mathbb{R}^6$ comprises the six internal constraints of orthonormality in (19). Let $T_d(d) = \mathcal{E}(d) \in \mathbb{R}^{9\times 3}$ denote the null space matrix (24) for the constraint gradient $G_d(d) \in \mathbb{R}^{6\times 9}$ in (20), so that $\dot d = T_d(d)\nu$ with $\nu = \Omega \in \mathbb{R}^3$ and $G_d(d)T_d(d) \equiv 0$. Now, we let

$$d = \begin{pmatrix} \frac{d^1}{d^2} \\ \hline d^3 \end{pmatrix} = \begin{pmatrix} p_0^2+p_1^2-p_2^2-p_3^2 \\ 2(p_1p_2+p_0p_3) \\ \hline 2(p_1p_2-p_0p_3) \\ p_0^2-p_1^2+p_2^2-p_3^2 \\ \hline 2(p_2p_3+p_0p_1) \\ 2(p_1p_3+p_0p_2) \\ \hline 2(p_2p_3-p_0p_1) \\ p_0^2-p_1^2-p_2^2+p_3^2 \end{pmatrix} = \begin{pmatrix} \frac{\varphi^1(p)}{\varphi^2(p)} \\ \hline \varphi^3(p) \end{pmatrix} = \varphi(p) \in \mathbb{R}^9, \tag{47}$$

where $\varphi : \mathbb{H} \to \mathbb{R}^9$ is the vertically concatenated version of the Euler map $\mathcal{R}$, see (27) and (28). The director velocity becomes

$$\dot d = D\varphi(p)\dot p, \qquad D\varphi(p) = \nabla_p \varphi(p) = 2 \left(\begin{array}{c|ccc} p_0 & p_1 & -p_2 & -p_3 \\ p_3 & p_2 & p_1 & p_0 \\ -p_2 & p_3 & -p_0 & p_1 \\ \hline -p_3 & p_2 & p_1 & -p_0 \\ p_0 & -p_1 & p_2 & -p_3 \\ p_1 & p_0 & p_3 & p_2 \\ \hline p_2 & p_3 & p_0 & p_1 \\ -p_1 & -p_0 & p_3 & p_2 \\ p_0 & -p_1 & -p_2 & p_3 \end{array}\right) \in \mathbb{R}^{9\times 4} \tag{48}$$

where $D\varphi(p)$ denotes the differential of the Euler map φ at p. We want to derive an appropriate null space matrix $T_p(p) \in \mathbb{R}^{4\times 3}$ for the quaternion p such that $\dot p = T_p(p)\nu$ with the *same* $\nu = \Omega$ and $G_p^*(p)T_p(p) \equiv 0$ for the gradient $G_p^*(p) = \nabla_p g^*(p) \in \mathbb{R}^{6\times 4}$ of the constraint

$$g_p^*(p) = g_d(\varphi(p)) = \frac{1}{2}\big(\|p\|^2-1\big)\big(\|p\|^2+1\big) \left(\begin{array}{ccc|ccc} 1 & 1 & 1 & 0 & 0 & 0 \end{array}\right)^\top \in \mathbb{R}^6, \tag{49}$$

which is induced by the constraint g_d for the directors d via 'pull back'. Note that the constraints g_p^* are highly redundant: If — and only if — the one unity condition $g_p(p) = 0$ from (34) is

satisfied, the six constraints $g_p^*(p) = 0$ in (49) are fulfilled. That is why we impose an asterisk '$*$' to distinguish from g_p. Now, left-multiplication with $D\varphi(p)^\top$ in $\dot{d} = D\varphi(p)\dot{p} = T_d(\varphi(p))\nu$ yields $D\varphi(p)^\top D\varphi(p)\dot{p} = D\varphi(p)^\top T_d(\varphi(p))\nu$. Since the rank of the 4×4 matrix $D\varphi(p)^\top D\varphi(p)$ is full, except for the degenerate singularity $p = 0$, we can solve this relation for $\dot{p}$ via

$$\dot{p} = D\varphi(p)^\natural \dot{d} \tag{50}$$

yielding $\dot{p} = D\varphi(p)^\natural T_d(\varphi(p))\nu$. Here $D\varphi(p)^\natural = (D\varphi(p)^\top D\varphi(p))^{-1} D\varphi(p)^\top \in \mathbb{R}^{4\times 9}$ denotes the Moore-Penrose inverse [39] of $D\varphi(p)$. The next Lemma gives an explicit algebraic expression for $D\varphi(p)^\natural$. The matrix

$$T_p(p) = \big(D\varphi(p)^\top D\varphi(p)\big)^{-1} D\varphi(p)^\top T_d(\varphi(p)) = D\varphi(p)^\natural T_d(\varphi(p)) \in \mathbb{R}^{4\times 3} \tag{51}$$

is now a good candidate for a quaternionic null space matrix. But we have to convince ourselves that (51) in fact annihilates $G_p^*(p)$. By the chain rule, we find

$$G_p^*(p) = \nabla_p g_p^*(p) = G_d(\varphi(p))D\varphi(p) = 2\|p\|^2 \left(\begin{array}{ccc|ccc} p & p & p & 0 & 0 & 0 \end{array}\right)^\top \in \mathbb{R}^{6\times 4},$$

its rank being $\operatorname{rk} G_p^*(p) = 1$ for $p \neq 0$ by reason of the redundancies, which we have just explained. We have to show that $G_p^*(p)T_p(p) = G_d(\varphi(p))D\varphi(p)D\varphi(p)^\natural T_d(\varphi(p)) \equiv 0$ vanishes. Now if the condition

$$\operatorname{im} T_d(\varphi(p)) \subseteq \operatorname{im} D\varphi(p), \tag{52}$$

holds, this is in fact the case, since the mapping $D\varphi(p)D\varphi(p)^\natural\cdot$, restricted to $\operatorname{im} D\varphi(p)$, is known to be exactly the orthogonal projection onto $\operatorname{im} D\varphi(p)$, see [39]. Here, $D\varphi(p)D\varphi(p)^\natural$ reduces to the identity mapping, this is $D\varphi(p)D\varphi(p)^\natural w = w$ for each $w \in \operatorname{im} D\varphi(p)$.
We have the beautiful property that the quaternionic tangential vectors $\tau_p^n(p)$ are mapped to the corresponding rotation-free ones $\tau_d^n(\varphi(p))$ by the Euler differential and vice versa,

$$D\varphi(p)\tau_p^n(p) = \tau_d^n\big(\varphi(p)\big), \qquad \tau_p^n(p) = D\varphi(p)^\natural \tau_d^n\big(\varphi(p)\big), \qquad n = 1,2,3 \tag{53}$$

The fact that radial stretching of the normal p yields a corresponding radial stretching of the image $d = \varphi(p)$ becomes manifest in

$$D\varphi(p)p = \varphi(p), \qquad p = D\varphi(p)^\natural \varphi(p). \tag{54}$$

The frame $\mathcal{Q}(p) = (p \,\|\, \tau_1^p(p) \,|\, \tau_2^p(p) \,|\, \tau_3^p(p)) \in \mathbb{R}SO(\mathbb{H})$ yields a proper orthonormal basis for $\mathbb{H}$, which is separated into the orthogonal complements $\mathbb{R}p$ and $T_p(p) = (\tau_p^1(p) \,|\, \tau_p^2(p) \,|\, \tau_p^3(p))$, the former spanning the radial normal direction $\mathbb{R}p = G_p(p)^\top \mathbb{R}$, the latter spanning the tangential space $\operatorname{null} G_p(p) = \{\pi \in \mathbb{H} : \langle p, \pi\rangle = 0\}$ of $\|p\|\,\mathbb{S}^3$ at p. The image of $\mathcal{Q}(p)$ under the Euler differential $D\varphi(p)$ is the rotation-free frame $D\varphi(p)\mathcal{Q}(p) = (d \,\|\, \tau_d^1(d) \,|\, \tau_d^2(d) \,|\, \tau_d^3(d))$ with $d = \varphi(p)$. Here in fact, we have the desired property (52), since

$$\operatorname{im} T_d(d) = \big\{\tau_d^1(d), \tau_d^2(d), \tau_d^3(d)\big\} \subset \big\{d, \tau_d^1(d), \tau_d^2(d), \tau_d^3(d)\big\} = \operatorname{im} D\varphi(p), \qquad d = \varphi(p),$$

due to the fundamental relationships (53) and (54). Having all this in mind, it is now straightforward to see that the explained general procedure yields exactly system (42) with $\nu = \Omega$ and $T_p(p)$ as in (41).

Lemma 5.1 (Moore-Penrose inverse of the Euler differential) *The Moore-Penrose pseudoinverse of the differential of the Euler map $D\varphi(p)$ from (48) admits the closed-form expression*

$$D\varphi(p)^\natural = \frac{1}{4\|p\|^2}\left(\frac{1}{2}\mathcal{I} - \frac{1}{6\|p\|^2} p \otimes p\right) D\varphi(p)^\top \tag{55}$$

for $p \neq 0$.

Proof: A straightforward computation yields

$$D\varphi(p)^\top D\varphi(p) = 4\big(2\|p\|^2\mathcal{I} + p\otimes p\big) \tag{56}$$

with rank equal to four, iff $p \neq 0$. The inverse of (56) is precisely the matrix in front of $D\varphi(p)^\top$ in (55). This is not hard to verify with $(p\otimes p)^2 = \|p\|^2 p\otimes p$ for $p\in\mathbb{H}$, which follows from the general identity $(x\otimes y)(u\otimes v) = \langle u,y\rangle(x\otimes v)$ for $u,v,x,y\in\mathbb{R}^N$ from vector/tensor calculus. ■

We are now ready to transform a **general multibody system**, given in rotation-free null space parametrisation. Let us assume that we have such a multibody system, consisting of $L\geq 1$ rigid bodies, each body parametrised by $(x_l, d_l)\in\mathbb{R}^{12}$, this is by three translations $x_l\in\mathbb{R}^3$ and nine 'rotation-free' rotations $d_l\in\mathbb{R}^9$. So the vector of primary unknowns is

$$q_d = \begin{pmatrix} x_1 \\ d_1 \\ \vdots \\ x_L \\ d_L \end{pmatrix} \in \mathbb{R}^{N_q}, \qquad N_{q_d} = (3+9)L = 12L.$$

We denote the translatory masses by m^1, ..., m^L and the principal values of the Euler tensors by (E_1^1, E_2^1, E_3^1), ..., (E_1^L, E_2^L, E_3^L). So, the diagonal and state-independent rotation-free mass matrix becomes

$$\mathcal{M}_d = \begin{pmatrix} m^1\mathcal{I} & & & & \\ & M_d(E_1^1,E_2^1,E_3^1) & & & \\ & & \ddots & & \\ & & & m^L\mathcal{I} & \\ & & & & M_d(E_1^L,E_2^L,E_3^L) \end{pmatrix} \in \mathbb{R}^{12L\times 12L}.$$

The constraints

$$g_d(q_d,t) = \begin{pmatrix} g_d(d_1) \\ \vdots \\ g_d(d_L) \\ \hline g^{\text{ext}}(q_d,t) \end{pmatrix} \in \mathbb{R}^{N_{\lambda_d}} \tag{57}$$

in the system comprise both the $6L$ scleronomic *internal* constraints of orthonormality for each d_l in (19) and $N_\lambda^{\text{ext}}\geq 0$ *external* constraints caused by mechanical *joints* [7]. So, the total number of — internal artificial and external joint — constraints is $N_{\lambda_d} = 6L + N_\lambda^{\text{ext}}$. Consequently, the number of mechanical degrees of freedom in the system is $N_{\text{DOF}} = N_{q_d} - N_{\lambda_d} = 12L - (6L + N_\lambda^{\text{ext}}) = 6L - N_\lambda^{\text{ext}}$. The index-3 system reads

$$\left\{\begin{array}{rcl} \dot q_d &=& v_d \\ \mathcal{M}_d\dot v_d &=& \psi^d(q_d,v_d,t) - \mathcal{G}_d(q_d,t)^\top\lambda_d \\ 0 &=& g_d(q_d,t) \end{array}\right. , \tag{58}$$

where

$$\mathcal{G}_d(q_d,t) = \nabla_{q_d} g(q_d,t) = \begin{pmatrix} 0 & G_d(d_1) & & \\ & & \ddots & \\ & & 0 & G_d(d_L) \\ \hline & & \mathcal{G}_d^{\text{ext}}(q_d,t) & \end{pmatrix} \in \mathbb{R}^{N_{\lambda_d}\times N_{q_d}}$$

If we let $d_l = \varphi(p_l)$ with $p_l\in\mathbb{H}$ for each $l = 1,\ldots,L$, each rigid body is parametrised by quaternions. Simply pulling back the rotation-free constraints leads to redundancies, as we have

seen. Therefore, we pull back only the external joint constraints and replace each of the six constraint functions g_d in (57) by the one constraint function g_p from (34),

$$g_p(q_p,t) = \left(\begin{array}{c} g_p(p_1) \\ \vdots \\ g_p(p_L) \\ \hline g^{\text{ext}}\big(\Phi(p),t\big) \end{array}\right) \in \mathbb{R}^{N_{\lambda_p}}, \qquad N_{\lambda_p} = L + N_\lambda^{\text{ext}}.$$

Clearly, the net number of degrees of freedom $N_{\text{DOF}} = N_{q_p} - N_\lambda = 7L - (L + N_\lambda^{\text{ext}}) = 6L - N_\lambda^{\text{ext}}$ in the system, which is the dimension of the constraint manifold, remains unchanged. This yields a smaller set of primary translatory and rotatory quaternionic unknowns

$$q_p = \left(\begin{array}{c} x_1 \\ p_1 \\ \vdots \\ x_L \\ p_L \end{array}\right) \in \mathbb{R}^{N_p}, \qquad N_{q_p} = (3+4)L = 7L, \quad \text{such that} \quad q_d = \Phi(q_p) = \left(\begin{array}{c} x_1 \\ \varphi(p_1) \\ \vdots \\ x_L \\ \varphi(p_L) \end{array}\right).$$

The absolute translational and rotatory quaternionic velocities transform — component by component — according to the chain rule,

$$\dot q_d = U\dot q_p, \qquad U(p_1,\dots,p_L) = \nabla_{q_p}\Phi(q_p) = \left(\begin{array}{cccc} \mathcal{I} & & & \\ & D\varphi(p_1) & & \\ & & \ddots & \\ & & & \mathcal{I} \\ & & & & D\varphi(p_L) \end{array}\right) \in \mathbb{R}^{12L\times 7L}.$$

Time differentiation yields the accelerations $\ddot q_p = U\ddot q_p + \dot U \dot q_p$, and the system (58) is transformed into the quaternionic index-3 system

$$\left\{\begin{array}{rcl} \dot q_p &=& v_p \\ U(q_p)^\top \mathcal{M}_d U(q_p)\dot v_p &=& U(q_p)^\top\big(\psi^d(q_p,v_p,t) - \mathcal{M}_d\dot U(q_p,v_p,t)v_p\big) - \mathcal{G}_p(q_p,t)^\top\lambda_p \\ 0 &=& g_p(q_p,t) \end{array}\right. \tag{59}$$

where the rotation-free constraint gradient transforms into the quaternionic constraint gradient as well according to the chain rule,

$$\mathcal{G}_p(q_p,t) = \nabla_{q_p} g_p(q_p,t) = \left(\begin{array}{cccc} 0 & G_p(p_1) & & \\ & & \ddots & \\ & & & 0 \quad G_p(p_L) \\ \hline \multicolumn{4}{c}{\mathcal{G}_d^{\text{ext}}\big(\Phi(q_p),t\big)U(p_1,\dots,p_L)} \end{array}\right) \in \mathbb{R}^{N_{\lambda_p}\times N_{q_p}}.$$

Suppose now that we have an appropriate rotation-free null space matrix $\mathcal{T}_d(q_d,t) \in \mathbb{R}^{N_q\times N_{\text{DOF}}}$ for the constraint gradient $\mathcal{G}_d(q_d,t) = \nabla_q g(q_d,t) \in \mathbb{R}^{N_\lambda\times N_{q_d}}$ such that $\dot q_d = \mathcal{T}_d(x_1,d_1,\dots,x_L,d_L,t)\nu$ with some independent quasi-velocities $\nu \in \mathbb{R}^{N_{\text{DOF}}}$, so that the general machinery of section 2 yields the following null space form of (58),

$$\left\{\begin{array}{rcl} \dot q_d &=& \mathcal{T}_d(q_d,t)\nu \\ \mathcal{T}_d(q_d,t)^\top\mathcal{M}_d\mathcal{T}_d(q_d,t)\dot\nu &=& \mathcal{T}_d(q_d,t)^\top\big(\psi^d(q_d,\dot q_d,t) - M_d\dot{\mathcal{T}}_d(q_d,\dot q_d,t)\nu\big) \\ 0 &=& g_d(q_d,t) \end{array}\right. . \tag{60}$$

From $\dot d_l = D\varphi(p_l)\dot p_l$, we have $\dot p_l = D\varphi(p_l)^\natural \dot d_l$ as in (50) for each of the rigid bodies, so $\dot q_p = U^\natural \dot q_d$

Joint	Number external constraints	**Mechanical DOF**	rotation-free ($N_{q_d} = 24$)	quaternionic ($N_{q_p} = 14$)
	N_λ^{ext}	N_{DOF}	N_λ	N_λ
Planar	3	**9**	15	5
Spherical	3	**9**	15	5
Cylindrical	4	**8**	16	6
Prismatic	5	**7**	17	7
Revolute	5	**7**	17	7

Table 2: *Lower kinematic joints/pairs ($L = 2$) from [7].*

with the Moore-Penrose pseudoinverse

$$U^\natural(p_1, \ldots, p_L) = \begin{pmatrix} \mathcal{I} & & & & \\ & D\varphi(p_1)^\natural & & & \\ & & \ddots & & \\ & & & \mathcal{I} & \\ & & & & D\varphi(p_L)^\natural \end{pmatrix} \in \mathbb{R}^{7L \times 12L}$$

of $U(p_1, \ldots, p_L)$. With the same $\nu \in \mathbb{R}^{N_{\text{DOF}}}$, the translatory $\dot{x}_l$ and quaternionic rotatory velocities $\dot{p}_l$ can be expressed as $\dot{q}_p = \mathcal{T}_p(x_1, p_1, \ldots, x_L, p_L, t)\nu$ with the pulled-back quaternionic null space matrix

$$\mathcal{T}_p(x_1, p_1, \ldots, x_L, p_L, t) = U^\natural(p_1, \ldots, p_L)\mathcal{T}_d\big(x_1, \varphi(p_1), \ldots, x_L, \varphi(p_L), t\big).$$

By construction, $\mathcal{T}_p(q_p, t)$ satisfies $\mathcal{G}_p(q_p, t)\mathcal{T}_p(q_p, t) \equiv 0$, as desired. The system (60) is transformed to the much smaller system

$$\left\{ \begin{array}{rcl} \dot{q}_p & = & \mathcal{T}_p(q_p, t)\nu \\ \mathcal{T}_d(q_d, t)^\top \mathcal{M}_d \mathcal{T}_d(q_d, t)\dot{\nu} & = & \mathcal{T}_d(q_d, t)^\top \big(\psi^d(q_d, \dot{q}_d, t) - \mathcal{M}_d \dot{T}_d(q_d, \dot{q}_d, t)\nu\big), \quad q_d = \Phi(q_p) \\ 0 & = & g_p(q_p, t) \end{array} \right. \tag{61}$$

without further ado. Here the independent quasi-velocities ν are precisely the same as in the rotation-free system (60).

Especially for $L = 2$, for the five elementary joints 'revolute pair', 'prismatic pair', 'cylindrical pair', 'spherical pair' and 'planar pair' that are presented in [7] and listed in Table 2 — the so-called 'lower kinematic pairs' — appropriate quaternionic null space matrices can be obtained.
In Example C in Section 7, we test the proposed procedure for the two-body-linkage 'spherical joint' of Figure 5. It works fine. Clearly, the proposed quaternionic null space matrices might not be *optimal* from the algebraic and numerical point of view. The derivation of optimal quaternionic null space matrices deserves to be studied and is therefore the topic of further research.

Remark 5.2 (Material vs. spatial angular velocity) The relationships (53) for the tangential vectors analogously hold for the column vectors of the null space matrices $T_d^\star(d)$ and $T_p^\star(p)$ in (45) and (46). □

Remark 5.3 (The zeroth moment of inertia) The reduced mass $D\varphi(p)^\top M_d D\varphi(p)$ for a single rigid body in (59), equals $M_p(p)$ in (31) with the 'zeroth' moment of inertia equal to $I_0 = \frac{1}{2}(I_1 + I_2 + I_3)$, as it is recommended in [9]. □

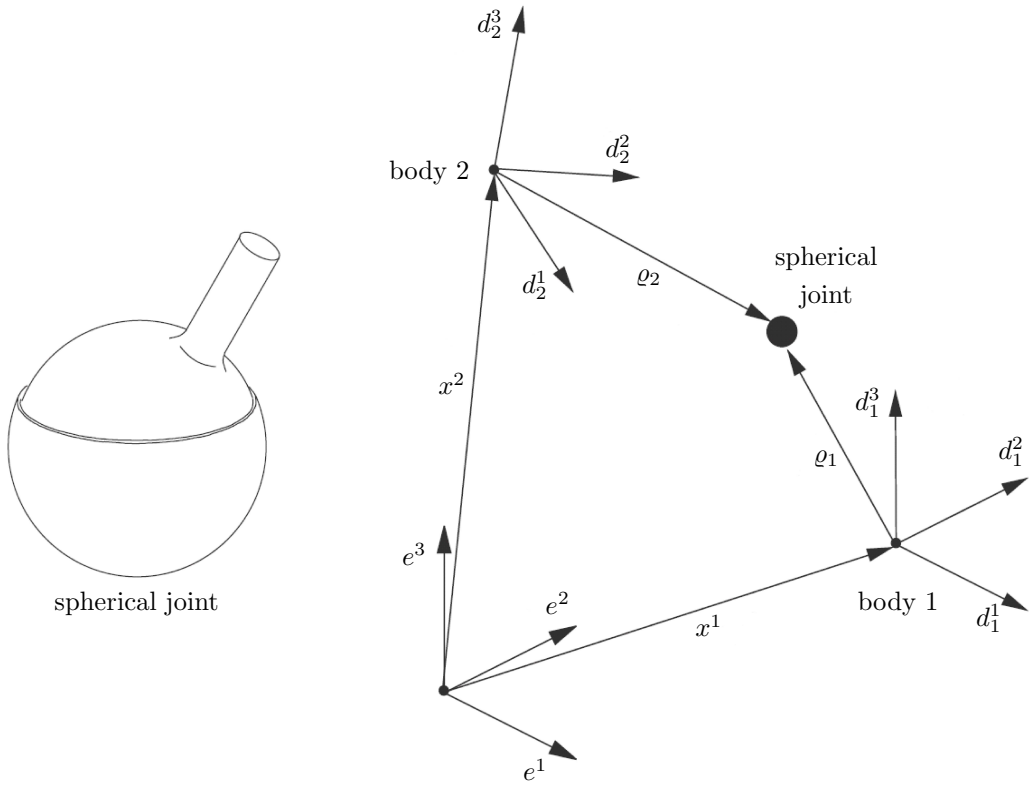

Figure 5: *Two rigid bodies, connected with a spherical joint.*

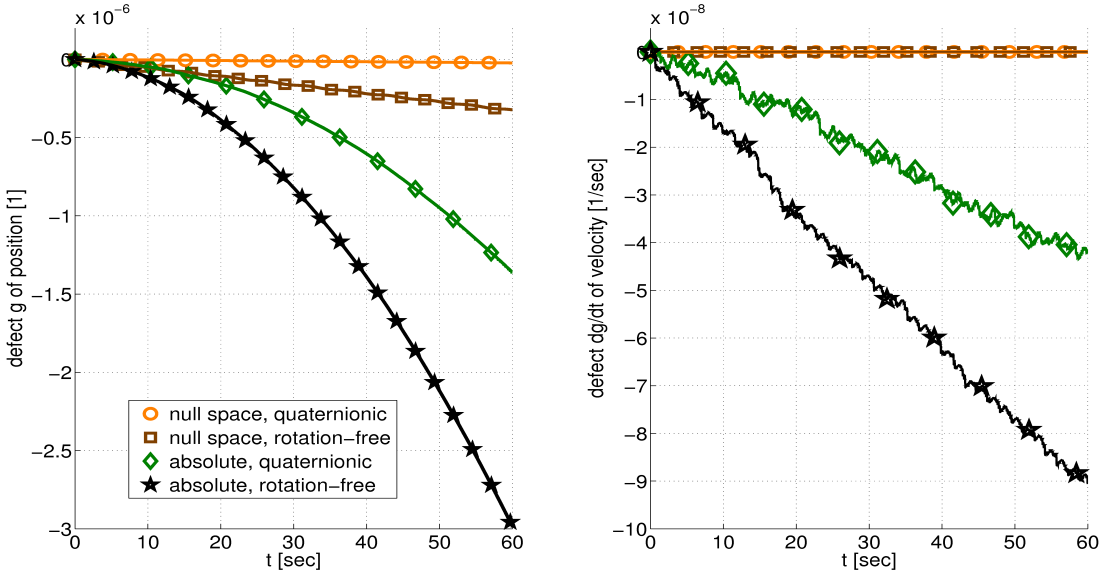

Figure 6: *Drift-off in position g and velocity $\dot{g}$. (For Example A, computed with* RADAU5 *and* ABSTOL $=$ RELTOL $= 1.0e-9$.*)*

6 Stabilisation of the drift-off by projection

Let us inspect in this section, how to avoid the drift-off effect. It is well known that in (4), where the constraint is imposed on *acceleration level*, the position q (resp. the velocity v) drifts quadratically (resp. linearly) from the constraint manifold [2, 4, 12, 19, 27]. In null space coordinate description (11), the drift-off is only linear like it is in index-2 formulation (3). See as well the illustration in Figure 6. In general, subsequent (orthogonal) projection of the position $q^\star$ and (tangential) projection of the velocity $v^\star$ can be applied. In this section, we describe how to do this for the four descriptions (25), (42), (40) and (23). In rotation-free rigid body parametrisation, the standard way to project the position $q^\star = d^\star$ involves the iterative solution of a system of nonlinear equations. Here we present an explicit fast alternative. In quaternionic parametrisation the projection of position $q^\star = p^\star$ is trivial and explicit.
In this section, we do not consider other stabilisation techniques such as the Baumgarte or the Gear-Gupta-Leimkuhler method [4, 12, 19]. (The Baumgarte method usually introduces artificial stiffness into the model. The Gear-Gupta-Leimkuhler method, applied to system (1) leads to an index-2 DAE. In turn, if the null space method is applied to the latter, an index-1 DAE — but no ODE — is obtained.) Note that easy and efficient implementations of the projection method are restricted to one step integration methods. For higher order BDF or NDF methods, non-trivial modifications in the core solver, e. g. DASSL/DASPK of Petzold and Hindmarsh [19, 29] or the MATLAB solver ODE15S of Shampine and Reichelt [35], are necessary [2].

In the **general index-1 formalism** (4) — or in **general index-0 ODE form** ($6_{1,2}$) —, it is common sense to project the drifted-off solution $q^\star$ and $v^\star$ back with respect to the pseudo — or 'semi' — metric $\langle \mathcal{M}(q)\cdot,\cdot\rangle = \cdot^\top \mathcal{M}(q)\cdot$ on $\mathbb{R}^{N_q}$ that is induced by the positive, semi-definite mass matrix $\mathcal{M}(q)$. The requirements of *orthogonality* — i. e. locally minimal distance to the current constraint manifold — resp. *tangentiality* lead to the systems

$$\text{(P)}\ \left\{\begin{array}{rcl} \mathcal{M}(q)(q-q^\star)+\mathcal{G}(q,t)^\top\chi &=& 0\\ g(q,t) &=& 0\end{array}\right. \qquad \text{(V)}\ \left\{\begin{array}{rcl} \mathcal{M}(q)(v-v^\star)+\mathcal{G}(q,t)^\top\eta &=& 0\\ \mathcal{G}(q,t)v+\dfrac{\partial g}{\partial t}(q,t) &=& 0\end{array}\right., \tag{62}$$

where η, $\chi \in \mathbb{R}^{N_\lambda}$ denote additional Lagrange multipliers [19, 28]. These systems must be solved consecutively for (q,χ) and (v,η).
The first system (62, P) is nonlinear and must therefore usually be solved in an iterative fashion. Typically, a few iterations with a Newton or a simplified Newton method are sufficient, if the projection is applied after each accepted time integration step. Here, the Jacobian, which equals the mass-constraint submatrix in (4), for the simplified Newton method is kept constant during iteration. The second system (62, V) is linear and can be solved in one step. Since the **general null space framework** (11) is equivalent to index-2 description (3) with the constraint satisfied on the level of velocity, projection (62, V) is dispensable.

Not that in the same way, at the very beginning of the dynamical simulation for $t = 0$, consistent initial values can be obtained from inconsistent ones.

Let us first have a look at the **quaternionic index-0/1** formulation for the **single rigid body** (40), where $q = p$, $v = v_p = \dot p$. Here, subsequent projection

$$\text{(P)}\quad p = \frac{1}{\|p^\star\|}p^\star, \qquad\qquad \text{(V)}\quad \dot p = \dot p^\star - \langle p, \dot p^\star\rangle p \tag{63}$$

is especially cheap, and no iterative procedure is required. In the next Lemma, we see that (63) is embedded into the general framework (62). Clearly from the the spherical geometry of $\mathbb{S}^3$, $p = p^\star/\|p^\star\|$ yields in fact the point of minimal distance of $p^\star$ to $\mathbb{S}^3$.

Lemma 6.1 (Quaternionic projection) *For $q = p$, $q^\star = p^\star$, $v = v_p = \dot p$, $v^\star = v_p^\star = \dot p^\star$, $\mathcal{M} = M_p(p)$ from (31), $g = g_p(p)$ from (34) and $\mathcal{G} = G_p$ from (36), the solution of (62) is given by p, $\dot p$ in (63) and $\chi = \eta = 0$.*

Proof: Clearly, the constraint equations $g_p(p) = 0$ and $G_p(p)\dot{p} = 0$ in (63) are satisfied. Since $p - p^\star \in \operatorname{null} M_p(p) = \mathbb{R}p$, one sees that $M_p(p)(p - p^\star) = 0$, and (62, P) is satisfied with $\chi = 0$. Since $\dot{p} - \dot{p}^\star$ is in direction of p, we have $M_p(p)(\dot{p} - \dot{p}^\star) = 0$. Thus, (62, V) is satisfied with $\eta = 0$. ■

It is known that stabilisation of *velocity* is much more crucial than stabilisation of position [1, 19]. The projection and the Baumgarte stabilisation methods have in common that they may dissipate energy. Considering the projection technique, it is usually the projection of *velocity* that is the dominant energy consuming process.
We point out that for the quaternionic rigid body and both formulations (40) and (42) the projection of velocity in (63, V) does *not* consume kinetic energy. In formulation (40), we have $(\dot{p}^\star)^\top M_p(p)\dot{p}^\star = \dot{p}^\top M_p(p)\dot{p}$, because of $\operatorname{null} M_p(p) = \mathbb{R}p$. In formulation (63), the velocity $\dot{p} = T_p(p)\Omega$ — by construction — always *is* — up to round-off errors — perfectly tangential to $\mathbb{S}^3$ and there is no need to project it. However, the projection of *position* (63, P) in fact *does* affect the rotatory kinetic energy in both directions. Let $T^\star = \frac{1}{2}(\dot{p}^\star)^\top M(p^\star)\dot{p}^\star$, $T = \frac{1}{2}\dot{p}^\top M_p(p)\dot{p}$ and $\delta T = T - T^\star$ the defect caused by projection. (We have just seen that $2T = (\dot{p}^\star)^\top M_p(p)\dot{p}^\star$.) Now if the quaternion has drifted to the outside of $\mathbb{S}^3$, i. e. $\|p^\star\| > \|p\| = 1$, then $\delta T < 0$. If it has drifted to the inside of $\mathbb{S}^3$, i. e. $\|p^\star\| < \|p\| = 1$, then $\delta T > 0$. Note that the mass is radially sensitive, so that $\|p^\star\|^2 M_p(p) = M(p^\star)$.
Now in null space formulation (42) — and in general — the drift-off in p is only linear — not quadratic — in the long run, see Figure 6. And it is usually much smaller in each time step than in formulation (40). That is one reason, why the null space coordinate formulation enjoys a better energetic behaviour. Figure 10 displays the total energy of the gyro top example, which is Example A in Section 7, along the simulated time interval $[0, T]$, computed with DoPri5. It clearly demonstrates that formulation (42) is superior to (40). In null space coordinates, even for coarse integrator tolerances, sufficiently good energy conservation is obtained in practice.

For the **rotation-free** description (23) for a **rigid body**, (25), where $q = d$, $v = v_d = \dot{d}$, things are more difficult. There are several possibilities to receive an orthonormal frame $d \sim R$ from a drifted-off one $d^\star \sim R^\star$. Using the standard method and solving (62_1) with $\mathcal{M} = M_d$ for (d, χ) is iterative and, consequently, expensive. We propose the following projection algorithm, which is explicit and does not need any iterative procedure. In turn, it relies on the established method of Spurrier and Klumpp, how to extract a quaternion out of a 'direction-cosine' matrix. We give a compact and short exposition below.

Explicit projection algorithm for a rotation-free rigid body

Let $d^\star \sim R(d^\star)$ resp. $\dot{d}^\star \sim \dot{R}(d^\star, \dot{d}^\star)$ denote a given drifted-off rotation-free position resp. velocity. Then the solution $d \sim R(d)$ and $\dot{d} \sim \dot{R}(d, \dot{d})$ of the following algorithm satisfy $g_d(d) = 0$ and $G_d(d)\dot{d} = 0$. That is, $R(d)$ is in $SO(3)$ and $\dot{R}(d, \dot{d})$ is tangential to $SO(3)$ at d. The algorithm reads as follows.

(P) Projection of position.

- (a) Extract a quaternionic position $p^\star$ from $d^\star$ with the Spurrier/Klumpp algorithm $p^\star \in \varphi^\natural(d^\star)$, see below.
- (b) Normalise $p = p^\star/\|p^\star\|$ as in (63).
- (c) Set $d = \varphi(p)$ as in (47).

(V) Projection of velocity.

- (a) Extract a quaternionic velocity $\dot{p}^\star$ from d and $\dot{d}^\star$ via $\dot{p}^\star = D\varphi(p)^\natural \dot{d}^\star$ as in (50).
- (b) Tangentialise $\dot{p} = \dot{p}^\star - \langle p, \dot{p}^\star \rangle p$ as in (63).
- (c) Set $\dot{d} = D\varphi(p)\dot{p}$ as in (48).

Note that the Spurrier-Klumpp algorithm works in a neighbourhood of $SO(3)$. That is, it works as well, if frame $d^\star \sim R^\star$ is just 'almost' orthonormal. Steps (a) in the proposed algorithm correspond to 'pull back' operations, steps (c) correspond to 'push forward' operations in the diagram of Figure 4.

The algorithm of Spurrier and Klumpp

We summarise in short the algorithm of Spurrier and Klumpp, which extracts a quaternion and/or its antipode $p = \pm(p_0 + ip_1 + jp_2 + kp_3) = \pm(p_0\,|\,p_1, p_2, p_3)^\top \in \mathbb{H}$ out of a frame $d \sim R(d) = (d^n_m)_{n,m=1,2,3}$ in a neighbourhood of $SO(3)$. We expose the algorithm as in [37] in a compact fashion. See as well the original articles [24, 38]. The algorithm reads as follows.

Firstly, let $d^0_0 = \mathrm{trace}(R) = d^1_1 + d^2_2 + d^3_3$ for abbreviation. Secondly, choose $n \in \{0, 1, 2, 3\}$ such that $d^n_n = \max\{d^0_0, d^1_1, d^2_2, d^3_3\}$. Thirdly, depending on the value of n, distinguish the following four cases, how to define p from $d \sim R(d)$.

- If $n = 0$, let

$$p_0 = \pm\frac{\sqrt{1 + d^0_0}}{2}, \qquad p_1 = \frac{d^2_3 - d^3_2}{4p_0}, \qquad p_2 = \frac{d^3_1 - d^1_3}{4p_0}, \qquad p_3 = \frac{d^1_2 - d^2_1}{4p_0}.$$

- If $n = 1$, let

$$p_1 = \pm\sqrt{\frac{d^1_1}{2} + \frac{1 - d^0_0}{4}}, \qquad p_0 = \frac{d^2_3 - d^3_2}{4p_1}, \qquad p_2 = \frac{d^1_2 - d^2_1}{4p_1}, \qquad p_3 = \frac{d^1_3 - d^3_1}{4p_1}.$$

- If $n = 2$, let

$$p_2 = \pm\sqrt{\frac{d^2_2}{2} + \frac{1 - d^0_0}{4}}, \qquad p_0 = \frac{d^3_1 - d^1_3}{4p_2}, \qquad p_1 = \frac{d^2_1 - d^1_2}{4p_2}, \qquad p_3 = \frac{d^2_3 - d^3_2}{4p_2}.$$

- If $n = 3$, let

$$p_3 = \pm\sqrt{\frac{d^3_3}{2} + \frac{1 - d^0_0}{4}}, \qquad p_0 = \frac{d^1_2 - d^2_1}{4p_3}, \qquad p_1 = \frac{d^3_1 - d^1_3}{4p_3}, \qquad p_2 = \frac{d^3_2 - d^2_3}{4p_3}.$$

We write $\varphi^\natural(d) = \{\pm p\}$ for the two-valued solution of the algorithm in shorthand. The sign '$\pm$' is not determined uniquely, since the Euler mapping $\mathcal{R} : \mathbb{H} \to \mathbb{R}SO(3)$ is *twice* onto. Note, however, that the sign actually does not affect the result of the proposed projection algorithm.

Lemma 6.2 (Rotation-free projection) *Position $q = d$ and velocity $v = \dot{d}$ of the preceding algorithm solve the two systems in (62) with mass equal to identity. That is*

$$\left\{\begin{array}{rcl} d + G_d(d)^\top\chi &=& d^\star \\ g_d(d) &=& 0 \end{array}\right. \quad \textit{and} \quad \left\{\begin{array}{rcl} \dot{d} + G_d(d)^\top\eta &=& \dot{d}^\star \\ G_d(d)\dot{d} &=& 0 \end{array}\right. , \tag{64}$$

and appropriate χ and η in $\mathbb{R}^6$.

Proof: Firstly, the constraint equations $g_d(d) = 0$ and $G_d(d)\dot{d} = 0$ in (64) are satisfied by construction. Secondly, taking a close look at the Spurrier-Klumpp algorithm, it is seen that $d + G_d(d)^\top\chi = d^\star$ is satisfied with appropriate χ, depending on $d^\star$. Using (P) (a), ..., (c) yields $\chi = G_d(\varphi(p))^\natural(\|p^\star\|^2 d^\star - \varphi(p))$ with the Moore-Penrose pseudoinverse $G_d(d)^\natural = (G_d(d)G_d(d)^\top)^{-1}G_d(d)$

of $G_d(d)$. Note that $\operatorname{null}(G_d(d)G_d(d)^\top) = \operatorname{null} G_d(d)^\top = \{0\}$ for $d \neq 0$. Carrying out the lengthy details with

$$G_d(d)G_d(d)^\top = \left(\begin{array}{ccc|ccc} \|d_1\|^2 & & & \langle d_1,d_2\rangle & \langle d_3,d_1\rangle & \\ & \|d_2\|^2 & & \langle d_1,d_2\rangle & & \langle d_2,d_3\rangle \\ & & \|d_3\|^2 & & \langle d_3,d_1\rangle & \langle d_2,d_3\rangle \\ \hline \langle d_1,d_2\rangle & \langle d_1,d_2\rangle & & \|d_1\|^2+\|d_2\|^2 & \langle d_2,d_3\rangle & \langle d_3,d_1\rangle \\ \langle d_3,d_1\rangle & & \langle d_3,d_1\rangle & \langle d_2,d_3\rangle & \|d_3\|^2+\|d_1\|^2 & \langle d_1,d_2\rangle \\ & \langle d_2,d_3\rangle & \langle d_2,d_3\rangle & \langle d_3,d_1\rangle & \langle d_1,d_2\rangle & \|d_2\|^2+\|d_3\|^2 \end{array}\right)$$

from (20) is left to the reader. Thirdly, letting (V) (a), ..., (c) into $\dot d + G_d(d)^\top\eta = \dot d^\star$ and left-multiplying with $D\varphi(p)^\top$ yields $\langle p,\dot p^\star\rangle D\varphi(p)^\top D\varphi(p)p = D\varphi(p)^\top G_d(\varphi(p))^\top\eta$, which must be fulfilled with a certain η. Now, $D\varphi(p)^\top G_d(\varphi(p))^\top = 2\begin{pmatrix} p & p & p & 0 & 0 & 0\end{pmatrix}$ and $D\varphi(p)^\top D\varphi(p)p = 12p$, which follows from (56) for $\|p\|^2 = 1$. Therefore, η can be chosen proportional to $6\langle p,\dot p^\star\rangle$. ■

The recommended projection method is of purely geometric kind, as we do not weight with the physical mass — i. e. $\mathcal{M} = \mathcal{I}$. The physical moments of inertia do not play any role. It behaves isotropic (or 'fair') in all the three spatial dimensions. Our numerical experiments indicate that it does not deteriorate the numerical accuracy significantly, compared to the case, if we solve (62) with $\mathcal{M} = M_d$. The benefit of the proposed method is that it is explicit and faster.

Before finishing this section, we comment on two alternative projection methods for rotation-free rigid bodies.

Remark 6.3 (Alternative rotation-free projection methods) (a) At first, one might think for example of the *Gram-Schmidt algorithm* or a similar orthonormalisation technique [39] to obtain a $d \sim R$ from $d^\star \sim R^\star$. Unfortunately, this method crucially depend on the order, in which the vectors are orthonormalised sequentially. Thus, it cannot be isotropic in all the spatial dimensions.
(b) Another method would be to use the Lie group structure of $SO(3)$ with Lie algebra $so(3)$. One takes the matrix logarithm $\gamma^\star = \log R^\star$ to receive an 'almost' skew symmetric $\gamma^\star$. Then one skew-symmetrises $\gamma = \frac{1}{2}(\gamma^\star - (\gamma^\star)^\top) \in so(3)$ and sets $d \sim R = e^\gamma \in SO(3)$. The matrix logarithm exists in a neighbourhood of $SO(3)$ and e^γ can be computed with the Euler-Rodriguez formula, which gives a closed form expression for the matrix exponential of a skew symmetric 3×3 matrix,

$$e^\gamma = \sum_{n=0}^{\infty}\frac{1}{n!}\gamma^n = \mathcal{I} + \frac{\sin\|\gamma\|}{\|\gamma\|}\gamma + \frac{1-\cos\|\gamma\|}{\|\gamma\|^2}\gamma^2, \qquad \|\gamma\| = \sqrt{\gamma_1^2+\gamma_2^2+\gamma_3^2}, \qquad \gamma \in so(3),$$

see [10, 32, 40]. However, we do not recommend this method, as the computation of the matrix logarithm is expensive and the overall method is not isotropic. □

7 Numerical examples

In this last section, we compare the four descriptions $(42_{1,2})$, $(25_{1,2})$, $(40_{1,2})$ and $(23_{1,2})$ for single rigid bodies of Sections 3 and 4 at two standard examples, which can be found in literature [7, 9, 23]. In addition to these descriptions, we use as well a parametrisation with classical Euler angles. The examples are chosen such that the solutions keep away from the dangerous gimbal locking configurations. We do not consider other three-parametric possibilities, such as Rodriguez parameters, rotation vectors, Cardan angles [10, 12, 34] or 'vectorial parametrisations' [5]. We test those formulations in connection with the standard time integrators listed in Table 3.
In a third example, we inspect formulations (60), (61) and the index-0 versions of (58), (59) of Section 5 for a simple mechanism with nine degrees of freedom, consisting of two rigid bodies, connected with a spherical joint and attached with a linear translational bushing element.

DoPri5	DoP853	Odex	Radau5	Dassl/Daspk	Seulex
explicit Runge-Kutta method [18]	explicit Runge-Kutta method [18]	explicit extrapolation method [18]	implicit Runge-Kutta method [17, 19, 28]	implicit BDF method [19, 29]	implicit extrapolation method [19]
(Ode45 [35])				(Ode15s [35])	

Table 3: *Collection of explicit and implicit time integrators (with* Matlab *'equivalents').*

In our experiments we measure the achieved absolute accuracy and the numerical costs. We measure the numerical costs in the number of right-hand side function evaluations that the respective solvers need to evaluate. In Examples A and B, each such evaluation needs the number of elementary operations that are listed in Table 1.
The accuracy is measured by the absolute error in the — translational and rotatory — positions and — translational and angular — velocities at the end of the simulation $t = T$ with respect to a numerical benchmark solution that is computed with highly stringent integrator tolerance.
We further investigate typical stepsize histories and the energetic behaviour for each of respective model formulations.

Euler angles Before starting, let us first summarise the use of Euler angles $\theta = (\theta_1, \theta_2, \theta_3)^\top$ for the rigid bodies in Examples A and B. We apply them in the standard convention '$Z - X^* - Z^{**}$' or '3-1-3', see [23, 34]. That is, the rotation

$$R = R(\theta) = \begin{pmatrix} \cos\theta_1 & -\sin\theta_1 & \\ \sin\theta_1 & \cos\theta_1 & \\ & & 1 \end{pmatrix} \begin{pmatrix} 1 & & \\ & \cos\theta_2 & -\sin\theta_2 \\ & \sin\theta_2 & \cos\theta_2 \end{pmatrix} \begin{pmatrix} \cos\theta_3 & -\sin\theta_3 & \\ \sin\theta_3 & \cos\theta_3 & \\ & & 1 \end{pmatrix}$$

is multiplicatively decomposed into an elementary rotation by θ_1 about the 'Z-axis' e^3, an elementary rotation by θ about the new 'X^*-axis' and an elementary rotation by θ_3 about the new 'Z^{**}-axis'. From $\mathcal{E}(\Omega) = R^\top \dot{R}$, we have that

$$\Omega = \begin{pmatrix} \Omega_1 \\ \Omega_2 \\ \Omega_3 \end{pmatrix} = \begin{pmatrix} \sin\theta_3 \sin\theta_2 & \cos\theta_3 & 0 \\ \cos\theta_3 \sin\theta_2 & -\sin\theta_3 & 0 \\ \cos\theta_2 & 0 & 1 \end{pmatrix} \begin{pmatrix} \dot{\theta}_1 \\ \dot{\theta}_2 \\ \dot{\theta}_3 \end{pmatrix} \tag{65}$$

yielding the system

$$\boxed{\begin{cases} \dot{\theta} &= T_\theta(\theta)\Omega \\ \mathfrak{I}\dot{\Omega} &= \mu - \Omega \times \mathfrak{I}\Omega, \quad \mu = T_\theta(\theta)^\top \psi^\theta \end{cases}} \,. \tag{66}$$

Here

$$T_\theta(\theta) = \begin{pmatrix} \dfrac{\sin\theta_3}{\sin\theta_2} & \dfrac{\cos\theta_3}{\sin\theta_2} & 0 \\ \cos\theta_3 & -\sin\theta_3 & 0 \\ -\dfrac{\cos\theta_2 \sin\theta_3}{\sin\theta_2} & -\dfrac{\cos\theta_2 \cos\theta_3}{\sin\theta_2} & 1 \end{pmatrix}$$

is the inverse of the matrix in (65) and can be interpreted as a null space matrix for the gradient of the empty constraint. The moment ψ^θ is obtained from $\psi^\theta = \phi^\theta - \nabla_\theta V(\theta, t)^\top$. In this convention, the gimbal locking singularities are characterised by $\theta_2 = \ldots, -2\pi, -\pi, 0, \pi, 2\pi, \ldots$, where θ_1 and θ_3 are not uniquely undetermined.

Example A In this Example, we study the nutation and precession of a heavy gyro top with $I_1, I_2 \gg I_3 > 0$, similarly to Example 5.2 in [9] or Example 5.1 in [7]. We consider a slightly

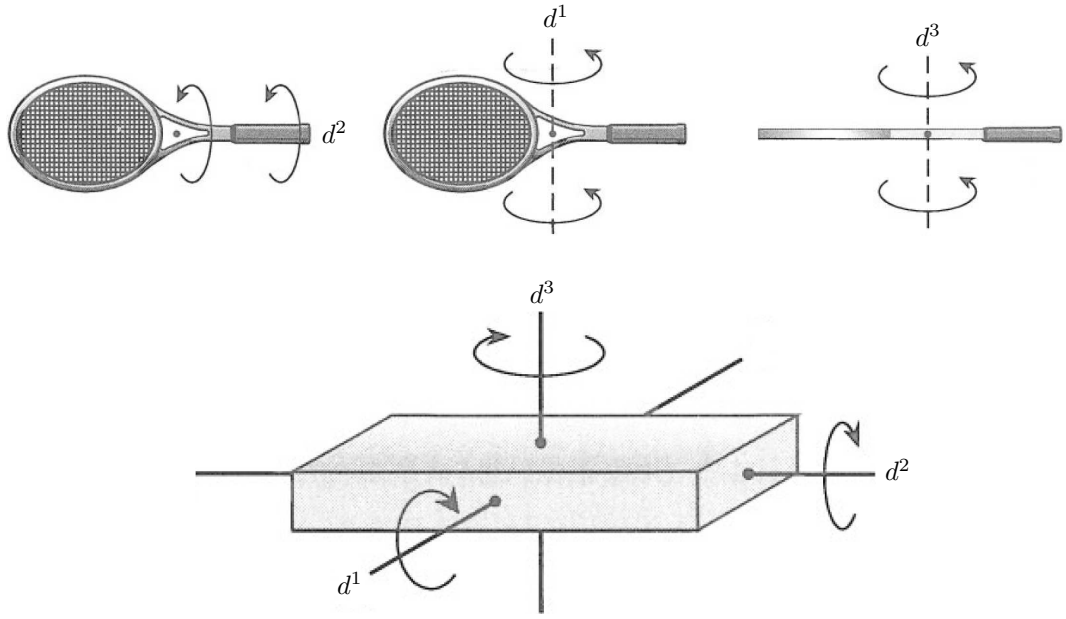

Figure 7: *The tennis racket problem. Free rotations about the axes d^2 and d^3 are stable. Free rotation about axis d^1 is unstable. ($0 < I_2 < I_1 < I_3$.)*

unsymmetrical one, where we set $I_1 = 50.0\,\mathrm{kg\,m^2}$, $I_2 = 42.0\,\mathrm{kg\,m^2}$ and $I_3 = 10.0\,\mathrm{kg\,m^2}$. This corresponds to the principal values $E_1 = 1.0\,\mathrm{kg\,m^2}$, $E_2 = 9.0\,\mathrm{kg\,m^2}$ and $E_3 = 41.0\,\mathrm{kg\,m^2}$ of the Euler tensor due to (18). For the initial positions, we choose $\theta_1(0) = 0$, $\theta_2(0) = \frac{\pi}{3}$ and $\theta_3(0) = 0$ in terms of Euler angles. This corresponds to

$$p(0) = \cos\left(\frac{\theta_2(0)}{2}\right) + \sin\left(\frac{\theta_2(0)}{2}\right) i = \begin{pmatrix} \frac{1}{2}\sqrt{3} \\ \frac{1}{2} \\ 0 \\ 0 \end{pmatrix}, \qquad R(0) = \mathcal{R}(p(0)) = \left(\begin{array}{c|c|c} 1 & 0 & 0 \\ 0 & \frac{1}{2} & -\frac{1}{2}\sqrt{3} \\ 0 & \frac{1}{2}\sqrt{3} & \frac{1}{2} \end{array}\right)$$

in quaternionic and rotation-free description, respectively. As initial angular velocity we choose $\Omega(0) = (0, 0, 20\,\mathrm{s^{-1}})^\top$. The potential energy V for the top and the resulting exterior conservative moments $\psi^{\cdot}$ in (22), (33) can be expressed as [9, 7]

$$V = mgL\langle d^3, e^3\rangle, \qquad \psi^d = -mgLe^3, \qquad \psi^p \sim D\varphi(p)^\top \psi^d = -2mgL \begin{pmatrix} p_0 \\ -p_1 \\ -p_2 \\ p_3 \end{pmatrix}.$$

We set $mL = 11.09\,\mathrm{kg\,m}$ and $g = 9.81\,\mathrm{m\,s^{-2}}$ for the gravitational acceleration. We set $\phi^{\cdot} \equiv 0$ for the exterior moments in (22), (33), especially we exclude any dissipative mechanisms.
Figure 11 displays the solution of the problem, where clearly nutation and precession become visible. Figures 13 resp. 14 display the absolute accuracies of the various solvers against the numerical task they needed. In our testing, we included the implicit solvers RADAU5 and ODE15S, which is the MATLAB BDF-counterpart of DASSL/DASPK, because these methods are standard in nowadays commercial multibody software packages, even though they are not the ideal choice for that scenario here, since it is a non-stiff problem.

Example B This is the tennis racket problem 11–5 in [23], which considers the free rotation of a rigid body around the principal axis d^1, which has the medial moment of inertia I_1, this is $0 < I_2 < I_1 < I_3$. This motion is clearly unstable.

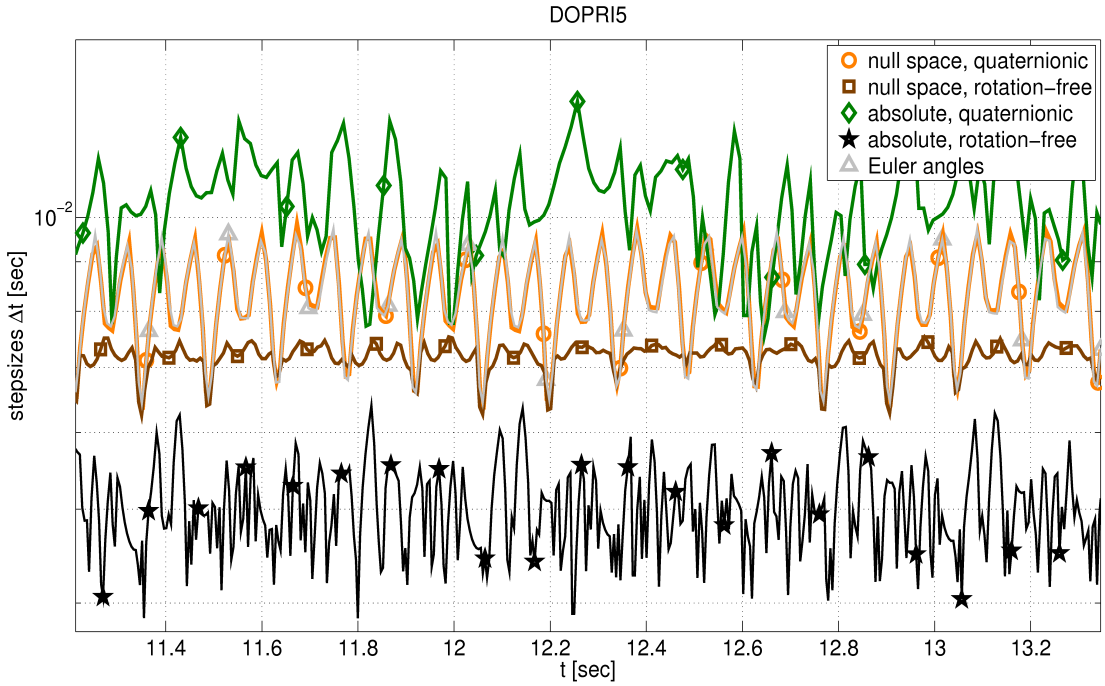

Figure 8: *Typical* DoPri5 *stepsizes for Example A.*

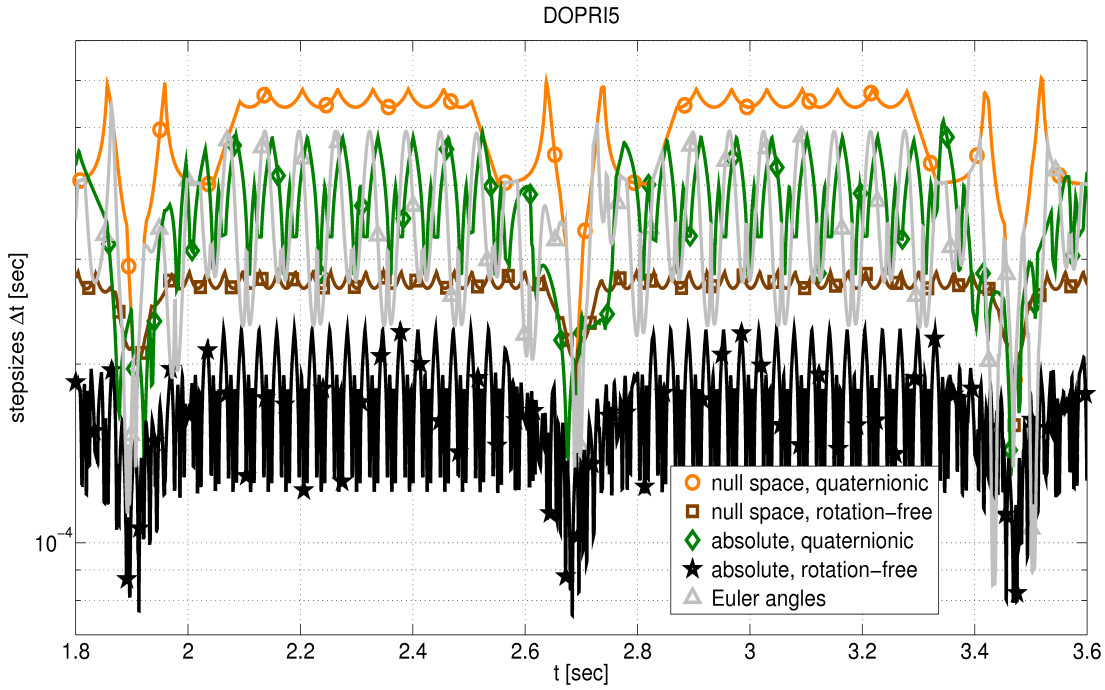

Figure 9: *Typical* DoPri5 *stepsizes for Example B.*

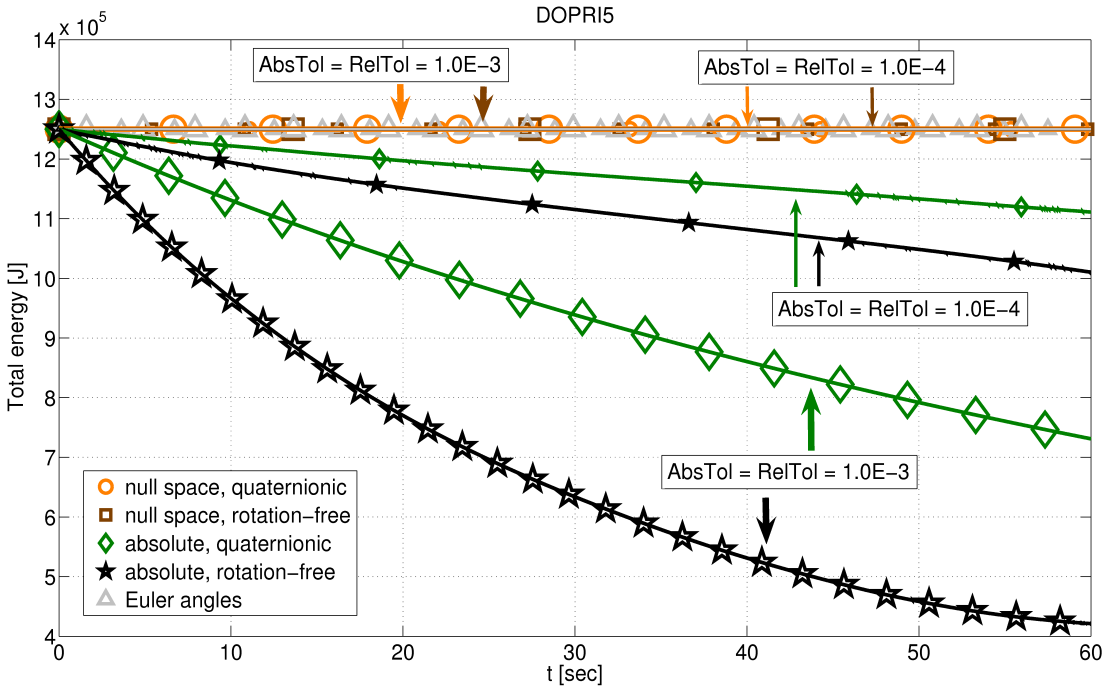

Figure 10: *The numerical solution for the total energy in Example A, computed with* DoPri5 *and* $\Omega(0) = (0, 0, 500\,s^{-1})^\top$.

We choose the same parameters as in [23], $I_1 = 41.6\,\mathrm{kg\,m^2}$, $I_2 = 11.6\,\mathrm{kg\,m^2}$ and $I_3 = 50.0\,\mathrm{kg\,m^2}$, which correspond to $E_1 = 10.0\,\mathrm{kg\,m^2}$, $E_2 = 40.0\,\mathrm{kg\,m^2}$ and $E_3 = 1.6\,\mathrm{kg\,m^2}$. Since we consider free rotations, $V \equiv$ const and $\dot{\phi} \equiv 0$. Note that in this case, the Euler equations (25_2), (42_2) resp. (66_2) resp. decouple from (25_1) (42_1) resp. (66_1), since the exterior moments μ vanish. Therefore, Ω can be integrated without knowledge of the frame position R – and without any parametrisation of the latter.

Note that the initial frame $R(0) = (d^1(0)\,|\,d^2(0)\,|\,d^3(0))$ at $t = 0$ cannot be aligned in parallel to the spatially fixed absolute coordinate system $(e^1\,|\,e^2\,|\,e^3)$, as this corresponds to a singular configuration. But since we are free relative to the absolute space, we may choose $\theta_1(0) = \pi/3$, $\theta_2(0) = \pi/4$, $\theta_3(0) = \pi/2$ as initial positions. That way, it is guaranteed that the solution keeps away from the singularities with a sufficient safety distance.

Figure 12 displays the solution $d(t)$, $\Omega(t)$ for $\Omega_1(0) = 50\,\mathrm{s^{-1}}$ and a small disturbance $\Omega_2(0) = \Omega_3(0) = 1.0\mathrm{E}{-3}\mathrm{s^{-1}}$. So we can see what happens. At first, the free rotation about d^1 seems to be stable and Ω_1 is almost constant. But almost suddenly at about $t = 0.4\,\mathrm{s}$, the body turns over about π, that is, d^1 snaps through to its antipode. Then, again, a period of seemingly stable rotation begins and lasts until at about $t = 1.2\,\mathrm{s}$. Then, another sudden reversal occurs. This turn-over repeats on and on and is almost periodic. (In some respects, this behaviour can be compared to the pole reversal of the earth's magnetic field.) The solution $\Omega(t)$ for the same scenario and $\Omega_1(0) = 50\,\mathrm{s^{-1}}$, $\Omega_2(0) = \Omega_3(0) = 1.0\mathrm{s^{-1}}$ is depicted and discussed in [23].

Figure 15 displays the achieved accuracy vs. the number of right-hand side function evaluations for the explicit embedded Runge-Kutta integrator DoPri5.

Example C In this last example, we fetch up the methodology of Section 5 and consider a simple mechanism $q_d = (x_1, d_1, x_2, d_2) \in \mathbb{R}^{N_{q_d}}$, $N_{q_d} = 24$, with $L = 2$ bodies of masses m_1, m_2 and moments of inertia (I_1^1, I_2^1, I_3^1), (I_1^2, I_2^2, I_3^2), situated at (x_1, d_1), $(x_2, d_2) \in \mathbb{R}^{12}$. They are

connected with a spherical joint

$$g^{\text{ext}}(q_d) = x_1 - x_2 + \varrho_1 - \varrho_2 \in \mathbb{R}^{N_\lambda^{\text{ext}}}, \qquad N_\lambda^{\text{ext}} = 3, \tag{67}$$

which restricts the relative motion to three DOF, see Figure 5. Here the spatial vectors $\varrho_i = \rho_1^i d_i^1 + \rho_2^i d_i^2 + \rho_3^i d_i^3$ for $i = 1, 2$, address the position of the joint relative to the respective centers of mass x_1, x_2. Their material counterparts are $\rho_i = \rho_1^i e^1 + \rho_2^i e^2 + \rho_3^i e^3 = R^{-1}\rho_i$. The system has $N_{\text{DOF}} = 9$ physical degrees of freedom in total, see Table 2. The constraints comprise both 12 internal $g_d(d_i)$ and 3 external joint constraints $g^{\text{ext}}(q_d)$,

$$g(q_d) = \begin{pmatrix} g_d(d_1) \\ g_d(d_2) \\ \hline g^{\text{ext}}(q_d) \end{pmatrix} \in \mathbb{R}^{N_{\lambda_d}}, \qquad N_{\lambda_d} = 15.$$

In the sequel, we append the row and column sizes of the occurring identity resp. zero matrices in the form $\mathcal{I}_{n\times m}$ resp. $0_{n\times m}$. The gradient $\mathcal{G}^{\text{ext}}(q_d) = \nabla_{q_d} g^{\text{ext}}(q_d)$ of the external joint constraint $g^{\text{ext}}(q_d)$ is

$$\mathcal{G}^{\text{ext}} = \begin{pmatrix} -\mathcal{I}_{3\times3} & -\rho_1^1\mathcal{I}_{3\times3} & -\rho_1^2\mathcal{I}_{3\times3} & -\rho_1^3\mathcal{I}_{3\times3} & \mathcal{I}_{3\times3} & \rho_2^1\mathcal{I}_{3\times3} & \rho_2^2\mathcal{I}_{3\times3} & \rho_2^3\mathcal{I}_{3\times3} \end{pmatrix} \in \mathbb{R}^{3\times24}.$$

An appropriate null space matrix for

$$\mathcal{G}_d(q_d) = \nabla_{q_d} g(q_d) = \begin{pmatrix} 0_{6\times3} & G_d(d_1) & 0_{6\times3} & 0_{6\times9} \\ 0_{6\times3} & 0_{6\times9} & 0_{6\times3} & G_d(d_2) \\ \hline \multicolumn{4}{c}{\mathcal{G}^{\text{ext}}(q_d)} \end{pmatrix} \in \mathbb{R}^{15\times24}$$

can be obtained in a multiplicative fashion

$$\mathcal{T}_d(q_d) = \begin{pmatrix} \mathcal{T}_1^{\text{int}}(d_1) & 0_{12\times3} \\ \hline \mathcal{T}_2^{\text{int}}(d_2)\mathcal{T}_2^{\text{ext}}(q_d) & \end{pmatrix} \in \mathbb{R}^{24\times9},$$

where

$$\mathcal{T}_i^{\text{int}} = \begin{pmatrix} \mathcal{I}_{3\times3} & 0_{3\times3} \\ 0_{9\times3} & T_d(d_i) \end{pmatrix} \in \mathbb{R}^{12\times6}, \qquad \mathcal{T}_2^{\text{ext}} = \begin{pmatrix} \mathcal{I}_{3\times3} & -R(d_1)\mathcal{E}(\rho_1) & -R(d_2)\mathcal{E}(\rho_2) \\ 0_{3\times3} & 0_{3\times3} & \mathcal{I}_{3\times3} \end{pmatrix} \in \mathbb{R}^{6\times9}$$

and $T_d(d_i) = \mathcal{E}(d_i) \in \mathbb{R}^{9\times3}$ as in (24). Note that these matrices slightly differ from the ones presented in [7]. This is due to the fact that we constrain the rows of the frame instead of its columns, as explained in Remark 4.6. It is straightforward to see that

$$\nu = \left(\dot{x}_1, \Omega^1, \Omega^2\right)^\top = \left(\dot{x}_1^1, \dot{x}_1^2, \dot{x}_1^3,\, \Omega_1^1, \Omega_2^1, \Omega_3^1,\, \Omega_1^2, \Omega_2^2, \Omega_3^2\right)^\top \in \mathbb{R}^{N_{\text{DOF}}}, \qquad N_{\text{DOF}} = 9. \tag{68}$$

Here $\dot{x}_1 \in \mathbb{R}^3$ contains the components of the translatory velocity $\dot{x}_1 = \dot{x}_1^1 e^1 + \dot{x}_1^2 e^2 + \dot{x}_1^3 e^3$ of the first body w. r. t. the spatially fixed coordinate system $(e^1 \,|\, e^2 \,|\, e^3)$. The material vectors $\Omega^1 = \Omega_1^1 e^1 + \Omega_2^1 e^2 + \Omega_3^1 e^3$ resp. $\Omega^2 = \Omega_1^2 e^1 + \Omega_2^2 e^2 + \Omega_3^2 e^3 \in \mathbb{R}^3$ contain the components of the spatial angular velocities $\omega^1 = \omega_1^1 d_1^1 + \omega_2^1 d_1^2 + \omega_3^1 d_1^3$ resp. $\omega^2 = \omega_1^2 d_2^1 + \Omega_2^2 d_2^2 + \omega_3^2 d_2^3 \in \mathbb{R}^3$ of the first resp. second body w. r. t. the body fixed coordinate systems $(d_1^1 \,|\, d_1^2 \,|\, d_1^3)$ resp. $(d_2^1 \,|\, d_2^2 \,|\, d_2^3)$. Transformation into the quaternionic world as explained in Section 5 yields a smaller system with $q_p = (x_1, p_1, x_2, p_2) \in \mathbb{R}^{N_{q_p}}$, such that $q_d = (x_1, d_1, x_2, d_2)^\top = \Phi(q_p) = (x_1, \varphi(p_1), x_2, \varphi(p_2))^\top$, with $N_{q_p} = 14$ and the algebraic constraints

$$g(q_p) = \begin{pmatrix} g_p(p_1) \\ g_p(p_2) \\ \hline g^{\text{ext}}(\Phi(q_p)) \end{pmatrix} \in N_{\lambda_p}, \qquad N_{\lambda_p} = 5.$$

Here we chose $I_1^1 = I_1^2 = I_1$, $I_2^1 = I_2^2 = I_2$, $I_3^1 = I_3^2 = I_3$ as in Example B, $m_1 = 10\,\text{kg}$, $m_2 = 20\,\text{kg}$, $\rho^1 = (1\,\text{m}, 2\,\text{m}, -3\,\text{m})^\top$, $\rho^2 = (5\,\text{m}, -6\,\text{m}, -7\,\text{m})^\top$. The initial positions were chosen

as $x_1 = (0,0,0)^\top$ and $d_1(0) = d_2(0) \sim R_1(0) = R_2(0)$ as in Example A. For the initial velocities, we chose $\dot{x}_1 = (0,0,0)^\top$, $\Omega^1(0) = (3\,\mathrm{s}^{-1}, 2\,\mathrm{s}^{-1}, 1\,\mathrm{s}^{-1})^\top$, $\Omega^2(0) = (24\,\mathrm{s}^{-1}, 15\,\mathrm{s}^{-1}, 12\,\mathrm{s}^{-1})^\top$. A consistent initial position for x_2 was obtained from $x_2 = x_1 + \varrho_1 - \varrho_2$, according to (67). Consistent initial velocities $\dot{p}_1(0)$, $\dot{p}_2(0)$, $\dot{d}_1(0)$, $\dot{d}_2(0)$, and $\dot{x}_2(0)$ for the absolute formulations were obtained from $\dot{q}_d(0) = \mathcal{T}_d(q_d(0))\nu(0)$, $\dot{q}_p(0) = \mathcal{T}_p(q_p(0))\nu(0)$ with ν as in (68). We attached the mechanism with a translatory linear bushing

$$V(q_d) = \frac{k}{2}\|x_1\|^2, \qquad \psi^d = -\nabla_{q_d} V^\top = -kx_1$$

at the origin, where we choose the stiffness $k = 1.0\mathrm{E}^4\,\mathrm{kg\,m^2\,s^{-2}}$. The solution of the problem is highly nonlinear and almost chaotic, similar to the movement of a double pendulum. Figure 16 displays accuracy vs. right-hand side function evaluations for $T = 4\,\mathrm{s}$.

For each of the three examples and each single simulation, we set the absolute error tolerance of the integrator, AbsTol, equal to the relative one, RelTol. We used the default integration parameters for each solver and did not apply fine tuning. For Examples A and B, in the index-1 descriptions (23) and (40), we discarded the respective Lagrange multipliers during integration. That is, we solved the index-0 subproblems $(23_{1,2})$, $(40_{1,2})$ and computed the Lagrange multipliers in a postprocessing. We did the same in Example C, that is, we solved the index-0 versions of (58) and (59), discarding the Lagrange multipliers. Let us discuss the results of our experimental investigations.

In all examples, the null space descriptions are *superior* to the absolute index-0 descriptions. This is the case, independent of the special time integration method, see Figures 13 and 14 for Example A. The corresponding pictures for Examples B and C and our solver collection of Table 3 look similar. This is, what we expect and obviously by reason of all the benefits (i), ..., (vi) that have been listed and explained in Sections 3 and 4. In Examples A and B, it is seen that both the quaternionic $(42_{1,2})$ and the rotation-free $(25_{1,2})$ null space formalisms are competitive to the (minimal, three-dimensional) Euler parametrisation (66). In Example B — surprisingly — they are even better.
In Example B, for rather large initial disturbances $\Omega_2(0) = \Omega_3(0) = 0.1\,\mathrm{s}^{-1}$, the discrepancy between the methods is small, see Figure 15 (a). For very small initial disturbances $\Omega_2(0) = \Omega_3(0) = 1.0\mathrm{E}^{-5}\,\mathrm{s}^{-1}$, which result in longer 'constant' plateaus in the solution, we can say that the absolute index-0 formalisms *completely fail*, see Figure 15 (b). Even if the tennis racket problem seems to be a very simple scenario, it is a good benchmark to check formalisms and time integration codes.
Even though we do not couple the models with variational integration techniques as in [9, 7], both null space formalisms $(42_{1,2})$, $(25_{1,2})$ display a much better energy conservation than formalisms $(40_{1,2})$, $(23_{1,2})$, as is illustrated in Figure 10 for Example A and the integrator DoPri5. (Of course, the total energy is never conserved exactly in these simulations.) We can give two reasons for this. Firstly, this is due to the better achieved total accuracy in general. Secondly, in the null space formulations, there is no need to project the velocity, which is a crucial step. Here gain, from the energetic point of view, we can say that the absolute index-0 formulations *fail* for coarse integrator tolerances.
In Examples A and B, the quaternionic null space method $(42_{1,2})$ behaves *slightly* better than the rotation-free null space method $(25_{1,2})$. This behaviour is typical and is due to the fact that we have a smaller number of unknowns in the model. The error estimator of the solvers has to control only 7 instead of 12 unknowns. Likewise, the quaternionic absolute index-0 method $(40_{1,2})$ with 8 unknowns behaves better than the rotation-free absolute index-0 method $(23_{1,2})$ with 18 unknowns. The same holds for Example C accordingly with 48, 28, 33 and 23 unknowns in systems (58), (59) and the index-0 versions of (60) and (61), respectively. This is, what one expects a priori. A remedy is to use local reparametrisation techniques [6, 7, 8]. However, changing charts for the manifold is a tedious task in practice [12, 19], since the right-hand side of a model frequently changes.

In Figures 8 resp. 9 for Examples A resp. B, it is seen that the magnitude of selected time steps correlates more or less to the number of unknowns in the model. (Of course, smaller stepsizes do not automatically mean a better accuracy.) This is, the Euler angle (66) and the two quaternionic formalisms $(42_{1,2})$, $(40_{1,2})$ yield larger time steps than the two rotation-free formalisms $(25_{1,2})$, $(23_{1,2})$. And here as well, the null space descriptions $(25_{1,2})$, $(42_{1,2})$ perform much better than the corresponding index-0 descriptions $(23_{1,2})$, $(40_{1,2})$. The reason is that controlling velocities in the error estimators is more crucial than controlling the positions. And on the level of velocity, the null space methods are minimal. There is no physically redundant information contained therein. Stepsize histories for different solvers — and/or Example C — look similar, with different, typical patterns.
We observed that the discrepancies in accuracy and task between the presented formalisms becomes the larger, the larger we choose the magnitude of the initial linear and angular velocities, i. e. the more energy — or dynamics — is contained in the respective systems.

Finishing, we want to remark that the authors have compared formalisms $(42_{1,2})$ and $(40_{1,2})$ at a forth — more complex — example, which is a quaternionic, flexible, geometrically exact Cosserat rod model [25]. The results therein are similar to the ones presented here. They as well confirm the observations of this article that the null space technique definitively ought to be preferred, if $SO(3)$ is parametrised with more than three coordinates.

8 Conclusions

We have studied the rotation-free and quaternionic parametrisation for rigid bodies and revealed analytical interrelations between both descriptions. We supplied appropriate null space matrices, yielding a significant reduction of the numbers of unknowns on the level of velocity. Numerical examples with standard time integration methods demonstrated that the null space coordinate formulations are superior to the index-reduced versions of the standard absolute coordinate descriptions, which are derived from the Euler-Lagrange equations of the first. We further gave a general recipe, how to build up multibody models in quaternionic null space coordinates by the pull back of rotation-free null space matrices with the aid of the Moore-Penrose pseudoinverse of the differential of the Euler map.

Acknowledgements. I want to thank Martin Arnold, Pascal Jung, Sigrid Leyendecker and Joachim Linn for many extensive and fruitful discussions.

References

[1] **Alishenas T., Ólafsson O.** *Modeling and velocity stabilization of constrained mechanical systems.* BIT Numerical Mathematics, Vol. 34, pp. 455–483, 1994.

[2] **Arnold M.** *Numerical methods for simulation in applied mechanics.* In: Simulation techniques for applied mechanics, Eds: Arnold M. and Schiehlen W., Springer, pp. 191–246, 2008.

[3] **Bauchau O. A., Epple A., Bottasso C. L.** *Scaling of constraints and augmented Lagrangian formulations in multibody dynamics simulations.* Journal of computational and nonlinear dynamics, Vol. 4, No. 2, 021007-1–9, 2009.

[4] **Bauchau O. A., Laulusa A.** *Review of contemporary approaches for constraint enforcement in multibody systems.* Journal of computational and nonlinear dynamics, Vol. 3, 011005-1–8, 2008.

[5] **Bauchau O. A., Trainelli L.** *The vectorial parametrization of rotation.* Nonlinear dynamics, Vol. 32, No. 1, pp. 71–92, 2003.

[6] **Betsch P.** *The discrete null space method for the energy consistent integration of constrained mechanical systems. Part I: Holonomic constraints.* International journal for numerical methods in engineering, Vol. 149, pp. 5159–5190, 2005.

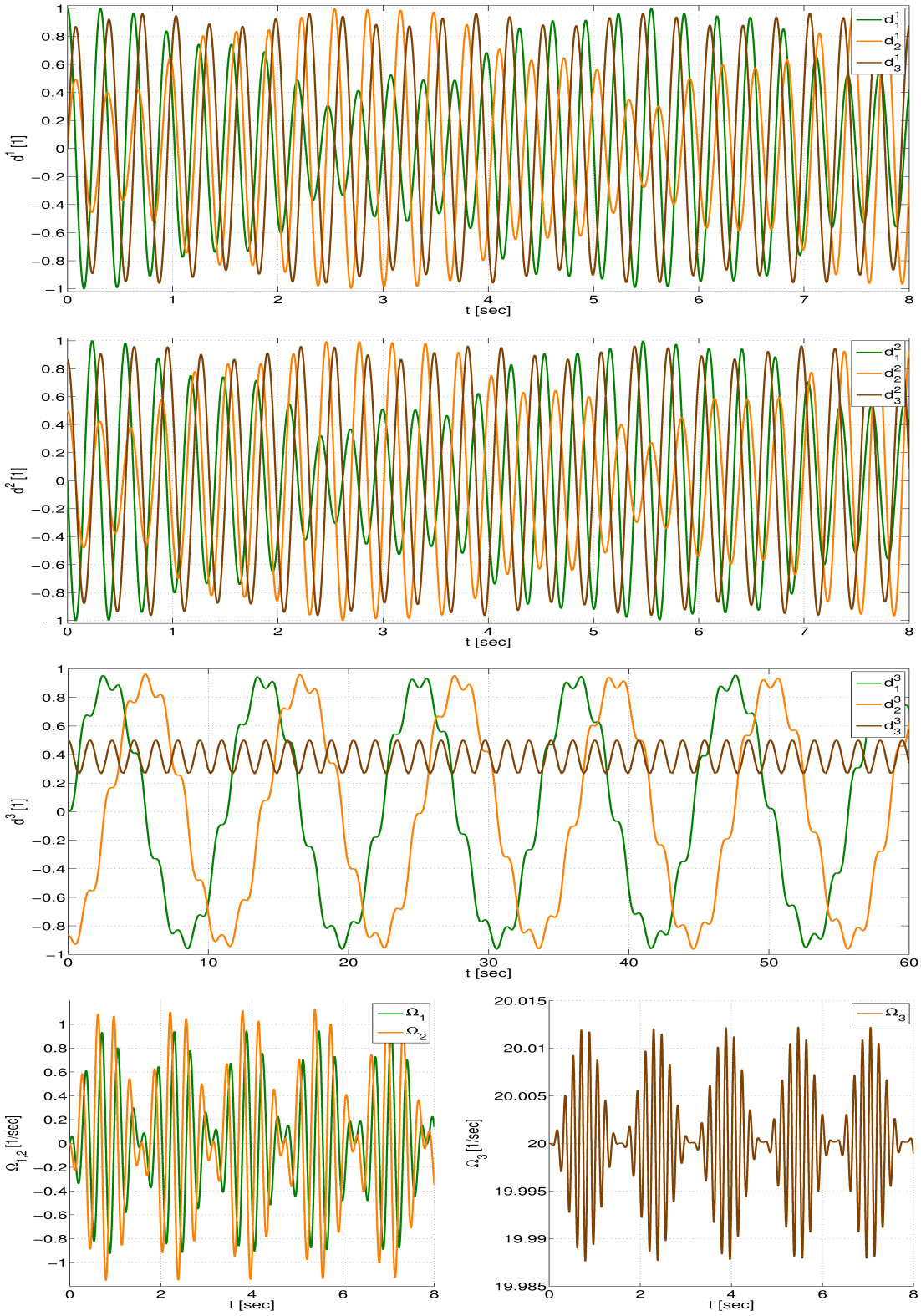

Figure 11: *Solution* $d^1(t)$, $d^2(t)$, $d^3(t)$ *and* $\Omega(t)$ *for Example A.*

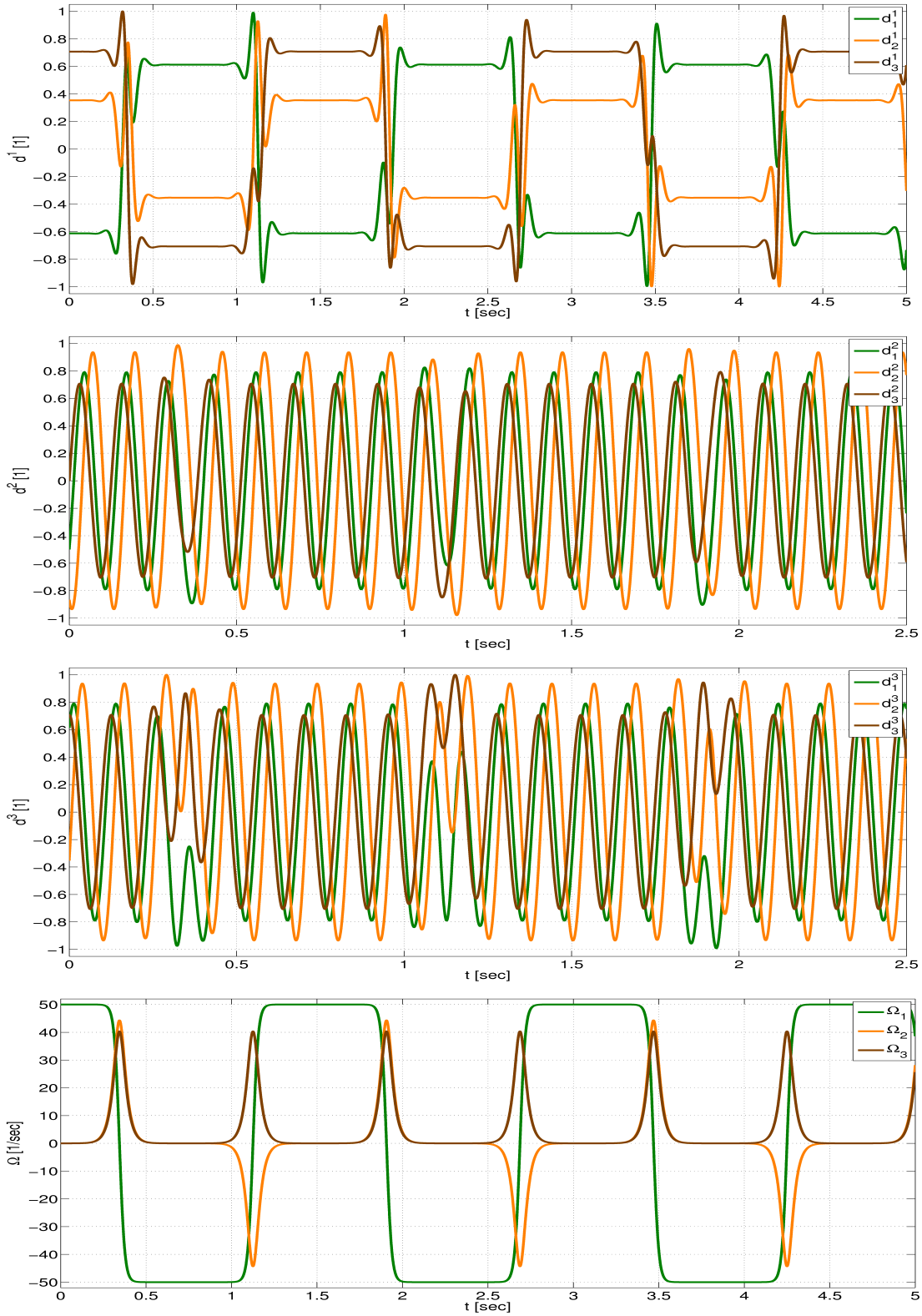

Figure 12: *Solution* $d^1(t)$, $d^2(t)$, $d^3(t)$ *and* $\Omega(t)$ *for Example B.*

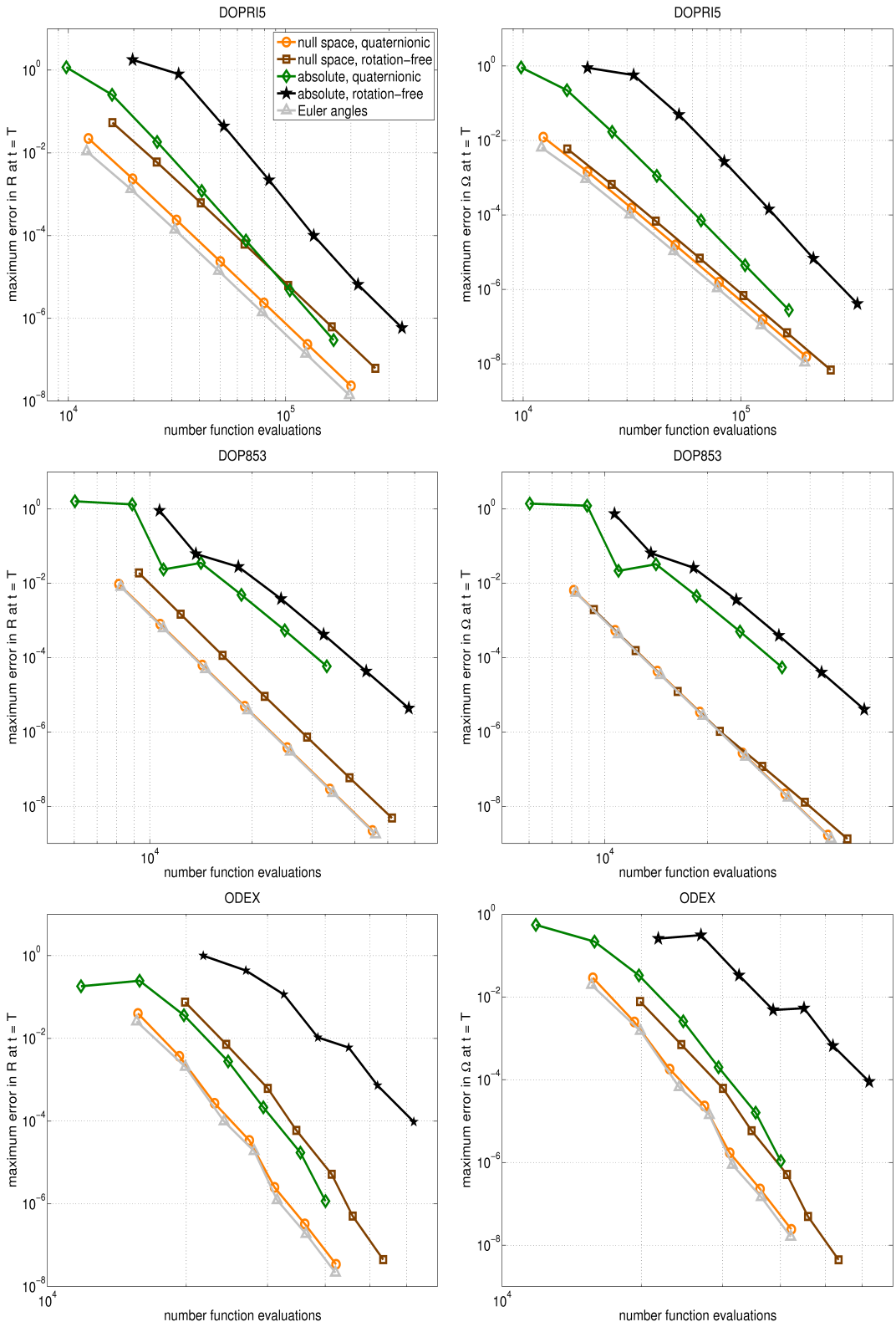

Figure 13: *Accuracy plot for Example A (Explicit solvers, $T = 60\ s$).*

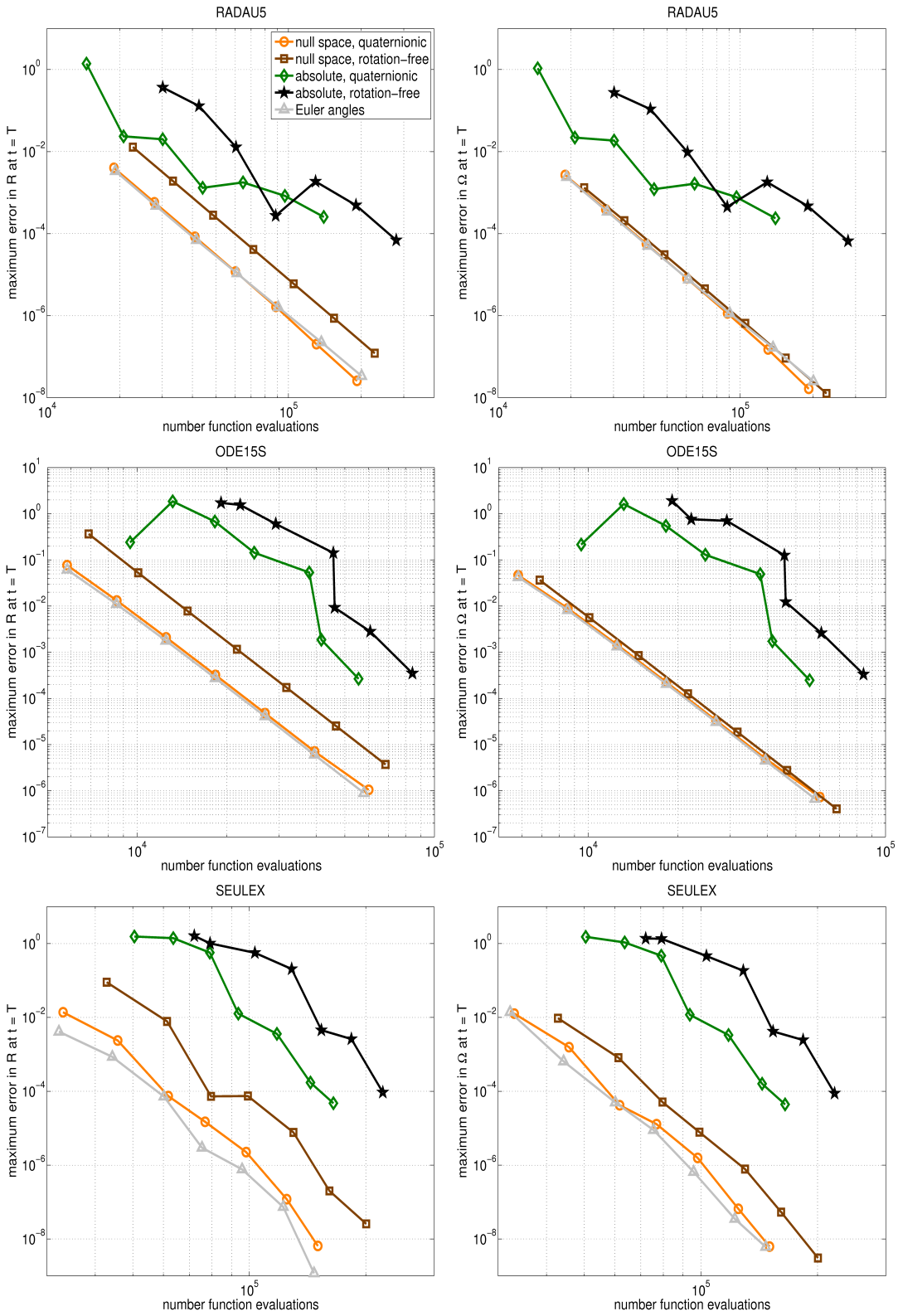

Figure 14: *Accuracy plot for Example A (Implicit solvers, $T = 60\,s$).*

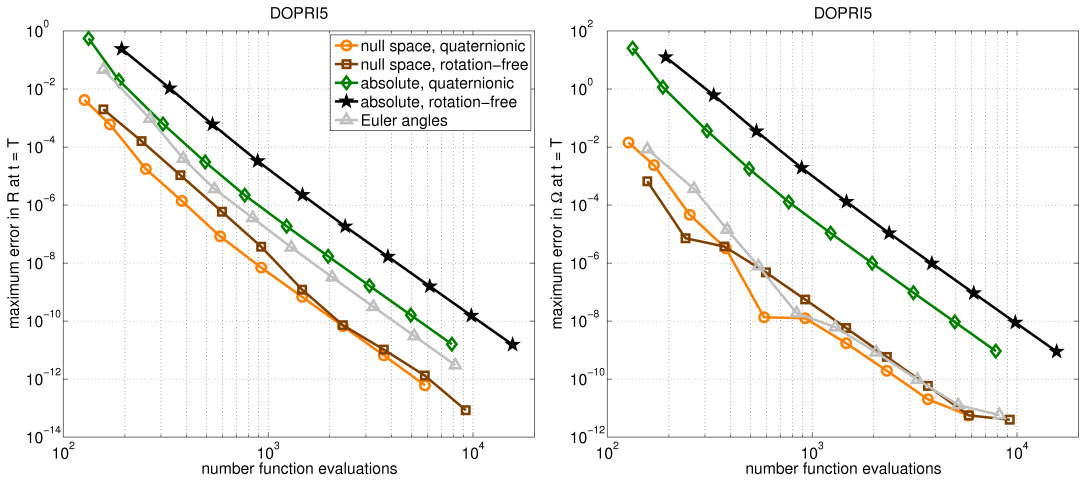

(a) Initial angular velocity $\Omega_1(0) = 50\mathrm{s}^{-1}$, $\Omega_2(0) = \Omega_3(0) = 1.0\mathrm{E}^{-1}\mathrm{s}^{-1}$, Simulation time $T = 0.4\mathrm{s}$

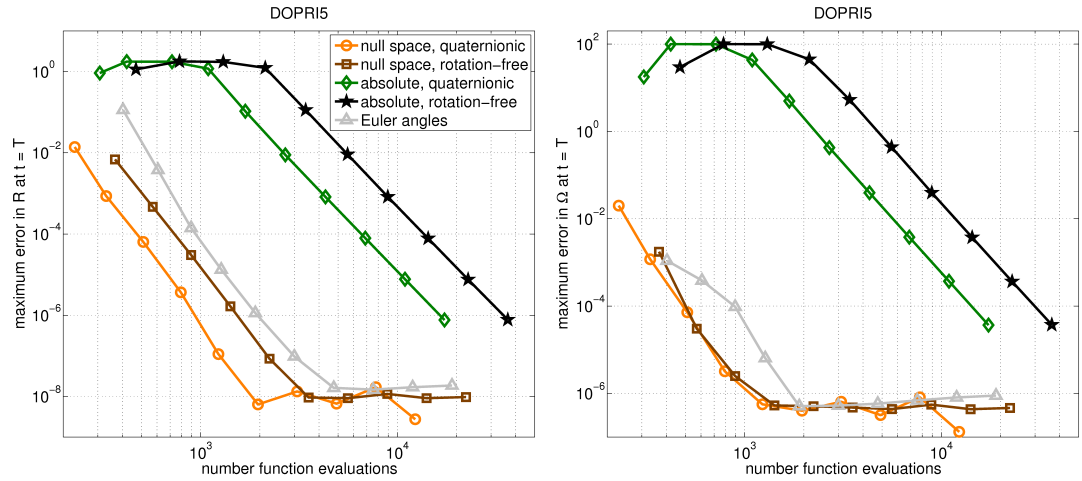

(b) Initial angular velocity $\Omega_1(0) = 50\mathrm{s}^{-1}$, $\Omega_2(0) = \Omega_3(0) = 1.0\mathrm{E}^{-5}\mathrm{s}^{-1}$, Simulation time $T = 1.0\mathrm{s}$

Figure 15: *Accuracy plot for Example B, computed with* DoPri5.

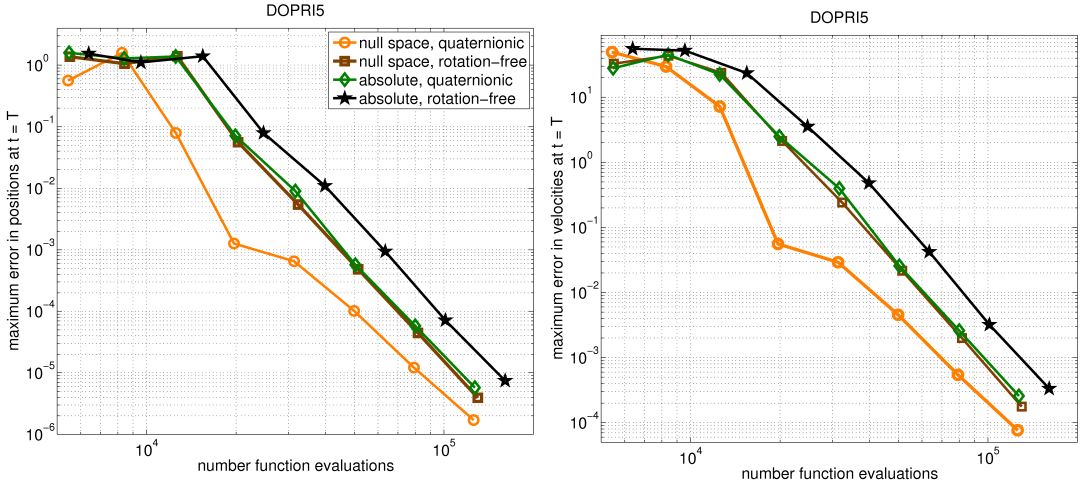

Figure 16: *Accuracy plot for Example C, computed with* DoPri5.

[7] **Betsch P., Leyendecker S.** *The discrete null space method for the energy consistent integration of constrained mechanical systems. Part II: Multibody dynamics.* International journal for numerical methods in engineering, Vol. 67, pp. 499–552, 2006.

[8] **Leyendecker S., Betsch P., Steinmann P.** *The discrete null space method for the energy consistent integration of constrained mechanical systems. Part III: Flexible multibody dynamics.* Multibody system dynamics, Vol. 19, pp. 45–72, 2008.

[9] **Betsch P., Siebert R.** *Rigid body dynamics in terms of quaternions: Hamiltonian formulation and conserving numerical integration.* International journal for numerical methods in engineering, Vol. 79, pp. 444-473, 2009.

[10] **Cardona A., Géradin M.** *Flexible multibody dynamics. A finite element approach.* Wiley, 2001.

[11] **Ebbinghaus H. D. et al.** *Numbers.* Springer, 1992.

[12] **Eich-Soellner E., Führer C.** *Numerical methods in multibody dynamics.* Teubner, 1998.

[13] **Gear C. W.** *Differential-algebraic equations.* Computer aided analysis an optimization of mechanical system dynamics, Ed: Haug E. J., pp. 323–334, 1984.

[14] **Gear C. W.** *Maintaining solution invariants in the numerical solution of ODEs.* SIAM journal on scientific and statistical computing, Vol. 7, pp. 734–743, 1986.

[15] **Golub G., Van Loan C.** *Matrix computations.* Third edition, The John Hopkins university press, 1996.

[16] **Hanson A. J.** *Visualizing quaternions.* Elsevier, 2005.

[17] **Hairer E., Lubich C., Roche M.** *The numerical solutions of differential-algebraic systems by Runge-Kutta methods.* Springer lecture notes in mathematics, Vol. 1409, 1989.

[18] **Hairer E., Noersett S. P., Wanner G.** *Solving ordinary differential equations I.* Springer, 1993.

[19] **Hairer E., Wanner G.** *Solving ordinary differential equations II.* Springer, 1996.

[20] **Hairer E., Lubich C., Wanner G.** *Geometric numerical integration.* Springer, 2002.

[21] **Jung P.** *A discrete mechanics approach to Cosserat rod theory - static equilibria.* Diploma thesis, TU Kaiserslautern, 2009.

[22] **Kuipers J. B.** *Quaternions and rotation sequences.* Princeton university press, 1999.

[23] **Kuypers F.** *Klassische Mechanik.* 5th edition. Wiley-VCH, 1997.

[24] **Klumpp A. R.** *Singularity-free extraction of a quaternion from a direction-cosine matrix.* Journal of spacecraft and rockets, Vol. 13, No. 12, pp. 754-755, 1976.

[25] **Lang H., Arnold M.** *Numerical aspects in the dynamic simulation of geometrically exact rods.* NUMDIFF 12, September 14 – 18, Halle/Saale, Germany, 2009. Available as well as *Report of the Fraunhofer ITWM* Kaiserslautern, Vol. 179, 2009.

[26] **Lang H., Linn J.** *Lagrangian field theory in space-time for geometrically exact Cosserat rods.* Report of the Fraunhofer ITWM Kaiserslautern, Vol. 150, 2009.

[27] **Laulusa A., Bauchau O. A.** *Review of classical approaches for constraint enforcement in multibody systems.* Journal of computational and nonlinear dynamics, Vol. 3, 011004-1–8, 2008.

[28] **Lubich C.** *Integration of stiff mechanical systems by Runge-Kutta methods.* Journal of applied mathematics and physics, Vol. 44, pp. 1022–1053, 1993.

[29] **Petzold L. R.** *A description of DASSL: A differential algebraic system solver.* In: Scientific computing (Ed: Stepleman R. S.) North-Holland, Amsterdam, 1981.

[30] **Rabier P. J., Rheinboldt W. C.** *Non-holonomic motion of rigid mechanical systems from a DAE viewpoint.* SIAM, 2000.

[31] **Romero I.** *The interpolation of rotations and its application to finite-element models of geometrically exact rods.* Computational mechanics, Vol. 34, pp. 121–133, 2004.

[32] **Sander O.** *Geodesic finite elements for Cosserat rods.* Preprint, Freie Universität Berlin, 2009.

[33] **Schiehlen W., Eberhard P.** *Technische Dynamik.* Modelle für Regelung und Simulation. Teubner, 2004.

[34] **Schwab A. L., Meijaard P. J.** *How to draw Euler angles and utilize Euler parameters.* Proceedings of IDETC/CIE, 2008.

[35] **Shampine L. F., Reichelt M. W.:** *The Matlab ODE suite.* SIAM journal on scientific computing, Vol. 18, No. 1, 1997.

[36] **Simeon B.** *Numerical analysis of flexible multibody dynamics.* Multibody system dynamics, Vol. 6, pp. 305–325, 2001.

[37] **Simo J. C., Vu-Quoc L.** *A three dimensional finite strain rod model. Part II.* Computer methods in applied mechanics and engineering, Vol. 58, pp. 79–116, 1986.

[38] **Spurrier R. A.** *Comment on 'Singularity-free extraction of a quaternion from a direction-cosine matrix'.* Journal of spacecraft and rockets, Vol. 15, No. 4, pp. 255, 1978.

[39] **Stoer J., Bulirsch R.** *Introduction to numerical mathematics.* Texts in applied mathematics, Vol. 12, 3rd edition, Springer, 2002.

[40] **Stillwell J.** *Naive Lie theory.* Springer, 2008.

[41] **Stuelpnagel J.** *On the Parametrization of the Three-Dimensional Rotation Group.* SIAM Review, Vol. 6, No. 4, pp. 422–430, 1964.

Published reports of the Fraunhofer ITWM

The PDF-files of the following reports are available under:
www.itwm.fraunhofer.de/de/zentral__berichte/berichte

1. D. Hietel, K. Steiner, J. Struckmeier
A Finite - Volume Particle Method for Compressible Flows
(19 pages, 1998)

2. M. Feldmann, S. Seibold
Damage Diagnosis of Rotors: Application of Hilbert Transform and Multi-Hypothesis Testing
Keywords: Hilbert transform, damage diagnosis, Kalman filtering, non-linear dynamics
(23 pages, 1998)

3. Y. Ben-Haim, S. Seibold
Robust Reliability of Diagnostic Multi-Hypothesis Algorithms: Application to Rotating Machinery
Keywords: Robust reliability, convex models, Kalman filtering, multi-hypothesis diagnosis, rotating machinery, crack diagnosis
(24 pages, 1998)

4. F.-Th. Lentes, N. Siedow
Three-dimensional Radiative Heat Transfer in Glass Cooling Processes
(23 pages, 1998)

5. A. Klar, R. Wegener
A hierarchy of models for multilane vehicular traffic
Part I: Modeling
(23 pages, 1998)

Part II: Numerical and stochastic investigations
(17 pages, 1998)

6. A. Klar, N. Siedow
Boundary Layers and Domain Decomposition for Radiative Heat Transfer and Diffusion Equations: Applications to Glass Manufacturing Processes
(24 pages, 1998)

7. I. Choquet
Heterogeneous catalysis modelling and numerical simulation in rarified gas flows Part I: Coverage locally at equilibrium
(24 pages, 1998)

8. J. Ohser, B. Steinbach, C. Lang
Efficient Texture Analysis of Binary Images
(17 pages, 1998)

9. J. Orlik
Homogenization for viscoelasticity of the integral type with aging and shrinkage
(20 pages, 1998)

10. J. Mohring
Helmholtz Resonators with Large Aperture
(21 pages, 1998)

11. H. W. Hamacher, A. Schöbel
On Center Cycles in Grid Graphs
(15 pages, 1998)

12. H. W. Hamacher, K.-H. Küfer
Inverse radiation therapy planning - a multiple objective optimisation approach
(14 pages, 1999)

13. C. Lang, J. Ohser, R. Hilfer
On the Analysis of Spatial Binary Images
(20 pages, 1999)

14. M. Junk
On the Construction of Discrete Equilibrium Distributions for Kinetic Schemes
(24 pages, 1999)

15. M. Junk, S. V. Raghurame Rao
A new discrete velocity method for Navier-Stokes equations
(20 pages, 1999)

16. H. Neunzert
Mathematics as a Key to Key Technologies
(39 pages (4 PDF-Files), 1999)

17. J. Ohser, K. Sandau
Considerations about the Estimation of the Size Distribution in Wicksell's Corpuscle Problem
(18 pages, 1999)

18. E. Carrizosa, H. W. Hamacher, R. Klein, S. Nickel
Solving nonconvex planar location problems by finite dominating sets
Keywords: Continuous Location, Polyhedral Gauges, Finite Dominating Sets, Approximation, Sandwich Algorithm, Greedy Algorithm
(19 pages, 2000)

19. A. Becker
A Review on Image Distortion Measures
Keywords: Distortion measure, human visual system
(26 pages, 2000)

20. H. W. Hamacher, M. Labbé, S. Nickel, T. Sonneborn
Polyhedral Properties of the Uncapacitated Multiple Allocation Hub Location Problem
Keywords: integer programming, hub location, facility location, valid inequalities, facets, branch and cut
(21 pages, 2000)

21. H. W. Hamacher, A. Schöbel
Design of Zone Tariff Systems in Public Transportation
(30 pages, 2001)

22. D. Hietel, M. Junk, R. Keck, D. Teleaga
The Finite-Volume-Particle Method for Conservation Laws
(16 pages, 2001)

23. T. Bender, H. Hennes, J. Kalcsics, M. T. Melo, S. Nickel
Location Software and Interface with GIS and Supply Chain Management
Keywords: facility location, software development, geographical information systems, supply chain management
(48 pages, 2001)

24. H. W. Hamacher, S. A. Tjandra
Mathematical Modelling of Evacuation Problems: A State of Art
(44 pages, 2001)

25. J. Kuhnert, S. Tiwari
Grid free method for solving the Poisson equation
Keywords: Poisson equation, Least squares method, Grid free method
(19 pages, 2001)

26. T. Götz, H. Rave, D. Reinel-Bitzer, K. Steiner, H. Tiemeier
Simulation of the fiber spinning process
Keywords: Melt spinning, fiber model, Lattice Boltzmann, CFD
(19 pages, 2001)

27. A. Zemitis
On interaction of a liquid film with an obstacle
Keywords: impinging jets, liquid film, models, numerical solution, shape
(22 pages, 2001)

28. I. Ginzburg, K. Steiner
Free surface lattice-Boltzmann method to model the filling of expanding cavities by Bingham Fluids
Keywords: Generalized LBE, free-surface phenomena, interface boundary conditions, filling processes, Bingham viscoplastic model, regularized models
(22 pages, 2001)

29. H. Neunzert
»Denn nichts ist für den Menschen als Menschen etwas wert, was er nicht mit Leidenschaft tun kann«
Vortrag anlässlich der Verleihung des Akademiepreises des Landes Rheinland-Pfalz am 21.11.2001
Keywords: Lehre, Forschung, angewandte Mathematik, Mehrskalenanalyse, Strömungsmechanik
(18 pages, 2001)

30. J. Kuhnert, S. Tiwari
Finite pointset method based on the projection method for simulations of the incompressible Navier-Stokes equations
Keywords: Incompressible Navier-Stokes equations, Meshfree method, Projection method, Particle scheme, Least squares approximation
AMS subject classification: 76D05, 76M28
(25 pages, 2001)

31. R. Korn, M. Krekel
Optimal Portfolios with Fixed Consumption or Income Streams
Keywords: Portfolio optimisation, stochastic control, HJB equation, discretisation of control problems
(23 pages, 2002)

32. M. Krekel
Optimal portfolios with a loan dependent credit spread
Keywords: Portfolio optimisation, stochastic control, HJB equation, credit spread, log utility, power utility, non-linear wealth dynamics
(25 pages, 2002)

33. J. Ohser, W. Nagel, K. Schladitz
The Euler number of discretized sets – on the choice of adjacency in homogeneous lattices
Keywords: image analysis, Euler number, neighborhod relationships, cuboidal lattice
(32 pages, 2002)

34. I. Ginzburg, K. Steiner
Lattice Boltzmann Model for Free-Surface flow and Its Application to Filling Process in Casting
Keywords: Lattice Boltzmann models; free-surface phenomena; interface boundary conditions; filling processes; injection molding; volume of fluid method; interface boundary conditions; advection-schemes; upwind-schemes
(54 pages, 2002)

35. M. Günther, A. Klar, T. Materne, R. Wegener
Multivalued fundamental diagrams and stop and go waves for continuum traffic equations
Keywords: traffic flow, macroscopic equations, kinetic derivation, multivalued fundamental diagram, stop and go waves, phase transitions
(25 pages, 2002)

36. S. Feldmann, P. Lang, D. Prätzel-Wolters
Parameter influence on the zeros of network determinants
Keywords: Networks, Equicofactor matrix polynomials, Realization theory, Matrix perturbation theory
(30 pages, 2002)

37. K. Koch, J. Ohser, K. Schladitz
Spectral theory for random closed sets and estimating the covariance via frequency space
Keywords: Random set, Bartlett spectrum, fast Fourier transform, power spectrum
(28 pages, 2002)

38. D. d'Humières, I. Ginzburg
Multi-reflection boundary conditions for lattice Boltzmann models
Keywords: lattice Boltzmann equation, boudary condistions, bounce-back rule, Navier-Stokes equation
(72 pages, 2002)

39. R. Korn
Elementare Finanzmathematik
Keywords: Finanzmathematik, Aktien, Optionen, Portfolio-Optimierung, Börse, Lehrerweiterbildung, Mathematikunterricht
(98 pages, 2002)

40. J. Kallrath, M. C. Müller, S. Nickel
Batch Presorting Problems: Models and Complexity Results
Keywords: Complexity theory, Integer programming, Assigment, Logistics
(19 pages, 2002)

41. J. Linn
On the frame-invariant description of the phase space of the Folgar-Tucker equation
Key words: fiber orientation, Folgar-Tucker equation, injection molding
(5 pages, 2003)

42. T. Hanne, S. Nickel
A Multi-Objective Evolutionary Algorithm for Scheduling and Inspection Planning in Software Development Projects
Key words: multiple objective programming, project management and scheduling, software development, evolutionary algorithms, efficient set
(29 pages, 2003)

43. T. Bortfeld , K.-H. Küfer, M. Monz, A. Scherrer, C. Thieke, H. Trinkaus
Intensity-Modulated Radiotherapy - A Large Scale Multi-Criteria Programming Problem
Keywords: multiple criteria optimization, representative systems of Pareto solutions, adaptive triangulation, clustering and disaggregation techniques, visualization of Pareto solutions, medical physics, external beam radiotherapy planning, intensity modulated radiotherapy
(31 pages, 2003)

44. T. Halfmann, T. Wichmann
Overview of Symbolic Methods in Industrial Analog Circuit Design
Keywords: CAD, automated analog circuit design, symbolic analysis, computer algebra, behavioral modeling, system simulation, circuit sizing, macro modeling, differential-algebraic equations, index
(17 pages, 2003)

45. S. E. Mikhailov, J. Orlik
Asymptotic Homogenisation in Strength and Fatigue Durability Analysis of Composites
Keywords: multiscale structures, asymptotic homogenization, strength, fatigue, singularity, non-local conditions
(14 pages, 2003)

46. P. Domínguez-Marín, P. Hansen, N. Mladenovi´c , S. Nickel
Heuristic Procedures for Solving the Discrete Ordered Median Problem
Keywords: genetic algorithms, variable neighborhood search, discrete facility location
(31 pages, 2003)

47. N. Boland, P. Domínguez-Marín, S. Nickel, J. Puerto
Exact Procedures for Solving the Discrete Ordered Median Problem
Keywords: discrete location, Integer programming
(41 pages, 2003)

48. S. Feldmann, P. Lang
Padé-like reduction of stable discrete linear systems preserving their stability
Keywords: Discrete linear systems, model reduction, stability, Hankel matrix, Stein equation
(16 pages, 2003)

49. J. Kallrath, S. Nickel
A Polynomial Case of the Batch Presorting Problem
Keywords: batch presorting problem, online optimization, competetive analysis, polynomial algorithms, logistics
(17 pages, 2003)

50. T. Hanne, H. L. Trinkaus
knowCube for MCDM – Visual and Interactive Support for Multicriteria Decision Making
Key words: Multicriteria decision making, knowledge management, decision support systems, visual interfaces, interactive navigation, real-life applications.
(26 pages, 2003)

51. O. Iliev, V. Laptev
On Numerical Simulation of Flow Through Oil Filters
Keywords: oil filters, coupled flow in plain and porous media, Navier-Stokes, Brinkman, numerical simulation
(8 pages, 2003)

52. W. Dörfler, O. Iliev, D. Stoyanov, D. Vassileva
On a Multigrid Adaptive Refinement Solver for Saturated Non-Newtonian Flow in Porous Media
Keywords: Nonlinear multigrid, adaptive refinement, non-Newtonian flow in porous media
(17 pages, 2003)

53. S. Kruse
On the Pricing of Forward Starting Options under Stochastic Volatility
Keywords: Option pricing, forward starting options, Heston model, stochastic volatility, cliquet options
(11 pages, 2003)

54. O. Iliev, D. Stoyanov
Multigrid – adaptive local refinement solver for incompressible flows
Keywords: Navier-Stokes equations, incompressible flow, projection-type splitting, SIMPLE, multigrid methods, adaptive local refinement, lid-driven flow in a cavity
(37 pages, 2003)

55. V. Starikovicius
The multiphase flow and heat transfer in porous media
Keywords: Two-phase flow in porous media, various formulations, global pressure, multiphase mixture model, numerical simulation
(30 pages, 2003)

56. P. Lang, A. Sarishvili, A. Wirsen
Blocked neural networks for knowledge extraction in the software development process
Keywords: Blocked Neural Networks, Nonlinear Regression, Knowledge Extraction, Code Inspection
(21 pages, 2003)

57. H. Knaf, P. Lang, S. Zeiser
Diagnosis aiding in Regulation Thermography using Fuzzy Logic
Keywords: fuzzy logic,knowledge representation, expert system
(22 pages, 2003)

58. M. T. Melo, S. Nickel, F. Saldanha da Gama
Largescale models for dynamic multicommodity capacitated facility location
Keywords: supply chain management, strategic planning, dynamic location, modeling
(40 pages, 2003)

59. J. Orlik
Homogenization for contact problems with periodically rough surfaces
Keywords: asymptotic homogenization, contact problems
(28 pages, 2004)

60. A. Scherrer, K.-H. Küfer, M. Monz, F. Alonso, T. Bortfeld
IMRT planning on adaptive volume structures – a significant advance of computational complexity
Keywords: Intensity-modulated radiation therapy (IMRT), inverse treatment planning, adaptive volume structures, hierarchical clustering, local refinement, adaptive clustering, convex programming, mesh generation, multi-grid methods
(24 pages, 2004)

61. D. Kehrwald
Parallel lattice Boltzmann simulation of complex flows
Keywords: Lattice Boltzmann methods, parallel computing, microstructure simulation, virtual material design, pseudo-plastic fluids, liquid composite moulding
(12 pages, 2004)

62. O. Iliev, J. Linn, M. Moog, D. Niedziela, V. Starikovicius
On the Performance of Certain Iterative Solvers for Coupled Systems Arising in Discretization of Non-Newtonian Flow Equations

Keywords: Performance of iterative solvers, Preconditioners, Non-Newtonian flow
(17 pages, 2004)

63. R. Ciegis, O. Iliev, S. Rief, K. Steiner
On Modelling and Simulation of Different Regimes for Liquid Polymer Moulding
Keywords: Liquid Polymer Moulding, Modelling, Simulation, Infiltration, Front Propagation, non-Newtonian flow in porous media
(43 pages, 2004)

64. T. Hanne, H. Neu
Simulating Human Resources in Software Development Processes
Keywords: Human resource modeling, software process, productivity, human factors, learning curve
(14 pages, 2004)

65. O. Iliev, A. Mikelic, P. Popov
Fluid structure interaction problems in deformable porous media: Toward permeability of deformable porous media
Keywords: fluid-structure interaction, deformable porous media, upscaling, linear elasticity, stokes, finite elements
(28 pages, 2004)

66. F. Gaspar, O. Iliev, F. Lisbona, A. Naumovich, P. Vabishchevich
On numerical solution of 1-D poroelasticity equations in a multilayered domain
Keywords: poroelasticity, multilayered material, finite volume discretization, MAC type grid
(41 pages, 2004)

67. J. Ohser, K. Schladitz, K. Koch, M. Nöthe
Diffraction by image processing and its application in materials science
Keywords: porous microstructure, image analysis, random set, fast Fourier transform, power spectrum, Bartlett spectrum
(13 pages, 2004)

68. H. Neunzert
Mathematics as a Technology: Challenges for the next 10 Years
Keywords: applied mathematics, technology, modelling, simulation, visualization, optimization, glass processing, spinning processes, fiber-fluid interaction, trubulence effects, topological optimization, multicriteria optimization, Uncertainty and Risk, financial mathematics, Malliavin calculus, Monte-Carlo methods, virtual material design, filtration, bio-informatics, system biology
(29 pages, 2004)

69. R. Ewing, O. Iliev, R. Lazarov, A. Naumovich
On convergence of certain finite difference discretizations for 1D poroelasticity interface problems
Keywords: poroelasticity, multilayered material, finite volume discretizations, MAC type grid, error estimates
(26 pages,2004)

70. W. Dörfler, O. Iliev, D. Stoyanov, D. Vassileva
On Efficient Simulation of Non-Newtonian Flow in Saturated Porous Media with a Multigrid Adaptive Refinement Solver
Keywords: Nonlinear multigrid, adaptive renement, non-Newtonian in porous media
(25 pages, 2004)

71. J. Kalcsics, S. Nickel, M. Schröder
Towards a Unified Territory Design Approach – Applications, Algorithms and GIS Integration
Keywords: territory desgin, political districting, sales territory alignment, optimization algorithms, Geographical Information Systems
(40 pages, 2005)

72. K. Schladitz, S. Peters, D. Reinel-Bitzer, A. Wiegmann, J. Ohser
Design of acoustic trim based on geometric modeling and flow simulation for non-woven
Keywords: random system of fibers, Poisson line process, flow resistivity, acoustic absorption, Lattice-Boltzmann method, non-woven
(21 pages, 2005)

73. V. Rutka, A. Wiegmann
Explicit Jump Immersed Interface Method for virtual material design of the effective elastic moduli of composite materials
Keywords: virtual material design, explicit jump immersed interface method, effective elastic moduli, composite materials
(22 pages, 2005)

74. T. Hanne
Eine Übersicht zum Scheduling von Baustellen
Keywords: Projektplanung, Scheduling, Bauplanung, Bauindustrie
(32 pages, 2005)

75. J. Linn
The Folgar-Tucker Model as a Differetial Algebraic System for Fiber Orientation Calculation
Keywords: fiber orientation, Folgar–Tucker model, invariants, algebraic constraints, phase space, trace stability
(15 pages, 2005)

76. M. Speckert, K. Dreßler, H. Mauch, A. Lion, G. J. Wierda
Simulation eines neuartigen Prüfsystems für Achserprobungen durch MKS-Modellierung einschließlich Regelung
Keywords: virtual test rig, suspension testing, multibody simulation, modeling hexapod test rig, optimization of test rig configuration
(20 pages, 2005)

77. K.-H. Küfer, M. Monz, A. Scherrer, P. Süss, F. Alonso, A. S. A. Sultan, Th. Bortfeld, D. Craft, Chr. Thieke
Multicriteria optimization in intensity modulated radiotherapy planning
Keywords: multicriteria optimization, extreme solutions, real-time decision making, adaptive approximation schemes, clustering methods, IMRT planning, reverse engineering
(51 pages, 2005)

78. S. Amstutz, H. Andrä
A new algorithm for topology optimization using a level-set method
Keywords: shape optimization, topology optimization, topological sensitivity, level-set
(22 pages, 2005)

79. N. Ettrich
Generation of surface elevation models for urban drainage simulation
Keywords: Flooding, simulation, urban elevation models, laser scanning
(22 pages, 2005)

80. H. Andrä, J. Linn, I. Matei, I. Shklyar, K. Steiner, E. Teichmann
OPTCAST – Entwicklung adäquater Strukturoptimierungsverfahren für Gießereien Technischer Bericht (KURZFASSUNG)
Keywords: Topologieoptimierung, Level-Set-Methode, Gießprozesssimulation, Gießtechnische Restriktionen, CAE-Kette zur Strukturoptimierung
(77 pages, 2005)

81. N. Marheineke, R. Wegener
Fiber Dynamics in Turbulent Flows Part I: General Modeling Framework
Keywords: fiber-fluid interaction; Cosserat rod; turbulence modeling; Kolmogorov's energy spectrum; double-velocity correlations; differentiable Gaussian fields
(20 pages, 2005)

Part II: Specific Taylor Drag
Keywords: flexible fibers; k-ε turbulence model; fiber-turbulence interaction scales; air drag; random Gaussian aerodynamic force; white noise; stochastic differential equations; ARMA process
(18 pages, 2005)

82. C. H. Lampert, O. Wirjadi
An Optimal Non-Orthogonal Separation of the Anisotropic Gaussian Convolution Filter
Keywords: Anisotropic Gaussian filter, linear filtering, orientation space, nD image processing, separable filters
(25 pages, 2005)

83. H. Andrä, D. Stoyanov
Error indicators in the parallel finite element solver for linear elasticity DDFEM
Keywords: linear elasticity, finite element method, hierarchical shape functions, domain decom-position, parallel implementation, a posteriori error estimates
(21 pages, 2006)

84. M. Schröder, I. Solchenbach
Optimization of Transfer Quality in Regional Public Transit
Keywords: public transit, transfer quality, quadratic assignment problem
(16 pages, 2006)

85. A. Naumovich, F. J. Gaspar
On a multigrid solver for the three-dimensional Biot poroelasticity system in multilayered domains
Keywords: poroelasticity, interface problem, multigrid, operator-dependent prolongation
(11 pages, 2006)

86. S. Panda, R. Wegener, N. Marheineke
Slender Body Theory for the Dynamics of Curved Viscous Fibers
Keywords: curved viscous fibers; fluid dynamics; Navier-Stokes equations; free boundary value problem; asymptotic expansions; slender body theory
(14 pages, 2006)

87. E. Ivanov, H. Andrä, A. Kudryavtsev
Domain Decomposition Approach for Automatic Parallel Generation of Tetrahedral Grids
Key words: Grid Generation, Unstructured Grid, Delaunay Triangulation, Parallel Programming, Domain Decomposition, Load Balancing
(18 pages, 2006)

88. S. Tiwari, S. Antonov, D. Hietel, J. Kuhnert, R. Wegener
A Meshfree Method for Simulations of Interactions between Fluids and Flexible Structures
Key words: Meshfree Method, FPM, Fluid Structure Interaction, Sheet of Paper, Dynamical Coupling
(16 pages, 2006)

89. R. Ciegis , O. Iliev, V. Starikovicius, K. Steiner
Numerical Algorithms for Solving Problems of Multiphase Flows in Porous Media
Keywords: nonlinear algorithms, finite-volume method, software tools, porous media, flows
(16 pages, 2006)

90. D. Niedziela, O. Iliev, A. Latz
On 3D Numerical Simulations of Viscoelastic Fluids
Keywords: non-Newtonian fluids, anisotropic viscosity, integral constitutive equation
(18 pages, 2006)

91. A. Winterfeld
Application of general semi-infinite Programming to Lapidary Cutting Problems
Keywords: large scale optimization, nonlinear programming, general semi-infinite optimization, design centering, clustering
(26 pages, 2006)

92. J. Orlik, A. Ostrovska
Space-Time Finite Element Approximation and Numerical Solution of Hereditary Linear Viscoelasticity Problems
Keywords: hereditary viscoelasticity; kern approximation by interpolation; space-time finite element approximation, stability and a priori estimate
(24 pages, 2006)

93. V. Rutka, A. Wiegmann, H. Andrä
EJIIM for Calculation of effective Elastic Moduli in 3D Linear Elasticity
Keywords: Elliptic PDE, linear elasticity, irregular domain, finite differences, fast solvers, effective elastic moduli
(24 pages, 2006)

94. A. Wiegmann, A. Zemitis
EJ-HEAT: A Fast Explicit Jump Harmonic Averaging Solver for the Effective Heat Conductivity of Composite Materials
Keywords: Stationary heat equation, effective thermal conductivity, explicit jump, discontinuous coefficients, virtual material design, microstructure simulation, EJ-HEAT
(21 pages, 2006)

95. A. Naumovich
On a finite volume discretization of the three-dimensional Biot poroelasticity system in multilayered domains
Keywords: Biot poroelasticity system, interface problems, finite volume discretization, finite difference method
(21 pages, 2006)

96. M. Krekel, J. Wenzel
A unified approach to Credit Default Swaption and Constant Maturity Credit Default Swap valuation
Keywords: LIBOR market model, credit risk, Credit Default Swaption, Constant Maturity Credit Default Swap-method
(43 pages, 2006)

97. A. Dreyer
Interval Methods for Analog Circiuts
Keywords: interval arithmetic, analog circuits, tolerance analysis, parametric linear systems, frequency response, symbolic analysis, CAD, computer algebra
(36 pages, 2006)

98. N. Weigel, S. Weihe, G. Bitsch, K. Dreßler
Usage of Simulation for Design and Optimization of Testing
Keywords: Vehicle test rigs, MBS, control, hydraulics, testing philosophy
(14 pages, 2006)

99. H. Lang, G. Bitsch, K. Dreßler, M. Speckert
Comparison of the solutions of the elastic and elastoplastic boundary value problems
Keywords: Elastic BVP, elastoplastic BVP, variational inequalities, rate-independency, hysteresis, linear kinematic hardening, stop- and play-operator
(21 pages, 2006)

100. M. Speckert, K. Dreßler, H. Mauch
MBS Simulation of a hexapod based suspension test rig
Keywords: Test rig, MBS simulation, suspension, hydraulics, controlling, design optimization
(12 pages, 2006)

101. S. Azizi Sultan, K.-H. Küfer
A dynamic algorithm for beam orientations in multicriteria IMRT planning
Keywords: radiotherapy planning, beam orientation optimization, dynamic approach, evolutionary algorithm, global optimization
(14 pages, 2006)

102. T. Götz, A. Klar, N. Marheineke, R. Wegener
A Stochastic Model for the Fiber Lay-down Process in the Nonwoven Production
Keywords: fiber dynamics, stochastic Hamiltonian system, stochastic averaging
(17 pages, 2006)

103. Ph. Süss, K.-H. Küfer
Balancing control and simplicity: a variable aggregation method in intensity modulated radiation therapy planning
Keywords: IMRT planning, variable aggregation, clustering methods
(22 pages, 2006)

104. A. Beaudry, G. Laporte, T. Melo, S. Nickel
Dynamic transportation of patients in hospitals
Keywords: in-house hospital transportation, dial-a-ride, dynamic mode, tabu search
(37 pages, 2006)

105. Th. Hanne
Applying multiobjective evolutionary algorithms in industrial projects
Keywords: multiobjective evolutionary algorithms, discrete optimization, continuous optimization, electronic circuit design, semi-infinite programming, scheduling
(18 pages, 2006)

106. J. Franke, S. Halim
Wild bootstrap tests for comparing signals and images
Keywords: wild bootstrap test, texture classification, textile quality control, defect detection, kernel estimate, nonparametric regression
(13 pages, 2007)

107. Z. Drezner, S. Nickel
Solving the ordered one-median problem in the plane
Keywords: planar location, global optimization, ordered median, big triangle small triangle method, bounds, numerical experiments
(21 pages, 2007)

108. Th. Götz, A. Klar, A. Unterreiter, R. Wegener
Numerical evidance for the non-existing of solutions of the equations desribing rotational fiber spinning
Keywords: rotational fiber spinning, viscous fibers, boundary value problem, existence of solutions
(11 pages, 2007)

109. Ph. Süss, K.-H. Küfer
Smooth intensity maps and the Bortfeld-Boyer sequencer
Keywords: probabilistic analysis, intensity modulated radiotherapy treatment (IMRT), IMRT plan application, step-and-shoot sequencing
(8 pages, 2007)

110. E. Ivanov, O. Gluchshenko, H. Andrä, A. Kudryavtsev
Parallel software tool for decomposing and meshing of 3d structures
Keywords: a-priori domain decomposition, unstructured grid, Delaunay mesh generation
(14 pages, 2007)

111. O. Iliev, R. Lazarov, J. Willems
Numerical study of two-grid preconditioners for 1d elliptic problems with highly oscillating discontinuous coefficients
Keywords: two-grid algorithm, oscillating coefficients, preconditioner
(20 pages, 2007)

112. L. Bonilla, T. Götz, A. Klar, N. Marheineke, R. Wegener
Hydrodynamic limit of the Fokker-Planck-equation describing fiber lay-down processes
Keywords: stochastic dierential equations, Fokker-Planck equation, asymptotic expansion, Ornstein-Uhlenbeck process
(17 pages, 2007)

113. S. Rief
Modeling and simulation of the pressing section of a paper machine
Keywords: paper machine, computational fluid dynamics, porous media
(41 pages, 2007)

114. R. Ciegis, O. Iliev, Z. Lakdawala
On parallel numerical algorithms for simulating industrial filtration problems
Keywords: Navier-Stokes-Brinkmann equations, finite volume discretization method, SIMPLE, parallel computing, data decomposition method
(24 pages, 2007)

115. N. Marheineke, R. Wegener
Dynamics of curved viscous fibers with surface tension
Keywords: Slender body theory, curved viscous bers with surface tension, free boundary value problem
(25 pages, 2007)

116. S. Feth, J. Franke, M. Speckert
Resampling-Methoden zur mse-Korrektur und Anwendungen in der Betriebsfestigkeit
Keywords: Weibull, Bootstrap, Maximum-Likelihood, Betriebsfestigkeit
(16 pages, 2007)

117. H. Knaf
Kernel Fisher discriminant functions – a concise and rigorous introduction
Keywords: wild bootstrap test, texture classification, textile quality control, defect detection, kernel estimate, nonparametric regression
(30 pages, 2007)

118. O. Iliev, I. Rybak
On numerical upscaling for flows in heterogeneous porous media

Keywords: numerical upscaling, heterogeneous porous media, single phase flow, Darcy's law, multiscale problem, effective permeability, multipoint flux approximation, anisotropy
(17 pages, 2007)

119. O. Iliev, I. Rybak
On approximation property of multipoint flux approximation method
Keywords: Multipoint flux approximation, finite volume method, elliptic equation, discontinuous tensor coefficients, anisotropy
(15 pages, 2007)

120. O. Iliev, I. Rybak, J. Willems
On upscaling heat conductivity for a class of industrial problems
Keywords: Multiscale problems, effective heat conductivity, numerical upscaling, domain decomposition
(21 pages, 2007)

121. R. Ewing, O. Iliev, R. Lazarov, I. Rybak
On two-level preconditioners for flow in porous media
Keywords: Multiscale problem, Darcy's law, single phase flow, anisotropic heterogeneous porous media, numerical upscaling, multigrid, domain decomposition, efficient preconditioner
(18 pages, 2007)

122. M. Brickenstein, A. Dreyer
POLYBORI: A Gröbner basis framework for Boolean polynomials
Keywords: Gröbner basis, formal verification, Boolean polynomials, algebraic cryptoanalysis, satisfiability
(23 pages, 2007)

123. O. Wirjadi
Survey of 3d image segmentation methods
Keywords: image processing, 3d, image segmentation, binarization
(20 pages, 2007)

124. S. Zeytun, A. Gupta
A Comparative Study of the Vasicek and the CIR Model of the Short Rate
Keywords: interest rates, Vasicek model, CIR-model, calibration, parameter estimation
(17 pages, 2007)

125. G. Hanselmann, A. Sarishvili
Heterogeneous redundancy in software quality prediction using a hybrid Bayesian approach
Keywords: reliability prediction, fault prediction, non-homogeneous poisson process, Bayesian model averaging
(17 pages, 2007)

126. V. Maag, M. Berger, A. Winterfeld, K.-H. Küfer
A novel non-linear approach to minimal area rectangular packing
Keywords: rectangular packing, non-overlapping constraints, non-linear optimization, regularization, relaxation
(18 pages, 2007)

127. M. Monz, K.-H. Küfer, T. Bortfeld, C. Thieke
Pareto navigation – systematic multi-criteria-based IMRT treatment plan determination
Keywords: convex, interactive multi-objective optimization, intensity modulated radiotherapy planning
(15 pages, 2007)

128. M. Krause, A. Scherrer
On the role of modeling parameters in IMRT plan optimization
Keywords: intensity-modulated radiotherapy (IMRT), inverse IMRT planning, convex optimization, sensitivity analysis, elasticity, modeling parameters, equivalent uniform dose (EUD)
(18 pages, 2007)

129. A. Wiegmann
Computation of the permeability of porous materials from their microstructure by FFF-Stokes
Keywords: permeability, numerical homogenization, fast Stokes solver
(24 pages, 2007)

130. T. Melo, S. Nickel, F. Saldanha da Gama
Facility Location and Supply Chain Management – A comprehensive review
Keywords: facility location, supply chain management, network design
(54 pages, 2007)

131. T. Hanne, T. Melo, S. Nickel
Bringing robustness to patient flow management through optimized patient transports in hospitals
Keywords: Dial-a-Ride problem, online problem, case study, tabu search, hospital logistics
(23 pages, 2007)

132. R. Ewing, O. Iliev, R. Lazarov, I. Rybak, J. Willems
An efficient approach for upscaling properties of composite materials with high contrast of coefficients
Keywords: effective heat conductivity, permeability of fractured porous media, numerical upscaling, fibrous insulation materials, metal foams
(16 pages, 2008)

133. S. Gelareh, S. Nickel
New approaches to hub location problems in public transport planning
Keywords: integer programming, hub location, transportation, decomposition, heuristic
(25 pages, 2008)

134. G. Thömmes, J. Becker, M. Junk, A. K. Vaikuntam, D. Kehrwald, A. Klar, K. Steiner, A. Wiegmann
A Lattice Boltzmann Method for immiscible multiphase flow simulations using the Level Set Method
Keywords: Lattice Boltzmann method, Level Set method, free surface, multiphase flow
(28 pages, 2008)

135. J. Orlik
Homogenization in elasto-plasticity
Keywords: multiscale structures, asymptotic homogenization, nonlinear energy
(40 pages, 2008)

136. J. Almquist, H. Schmidt, P. Lang, J. Deitmer, M. Jirstrand, D. Prätzel-Wolters, H. Becker
Determination of interaction between MCT1 and CAII via a mathematical and physiological approach
Keywords: mathematical modeling; model reduction; electrophysiology; pH-sensitive microelectrodes; proton antenna
(20 pages, 2008)

137. E. Savenkov, H. Andrä, O. Iliev
An analysis of one regularization approach for solution of pure Neumann problem
Keywords: pure Neumann problem, elasticity, regularization, finite element method, condition number
(27 pages, 2008)

138. O. Berman, J. Kalcsics, D. Krass, S. Nickel
The ordered gradual covering location problem on a network
Keywords: gradual covering, ordered median function, network location
(32 pages, 2008)

139. S. Gelareh, S. Nickel
Multi-period public transport design: A novel model and solution approaches
Keywords: Integer programming, hub location, public transport, multi-period planning, heuristics
(31 pages, 2008)

140. T. Melo, S. Nickel, F. Saldanha-da-Gama
Network design decisions in supply chain planning
Keywords: supply chain design, integer programming models, location models, heuristics
(20 pages, 2008)

141. C. Lautensack, A. Särkkä, J. Freitag, K. Schladitz
Anisotropy analysis of pressed point processes
Keywords: estimation of compression, isotropy test, nearest neighbour distance, orientation analysis, polar ice, Ripley's K function
(35 pages, 2008)

142. O. Iliev, R. Lazarov, J. Willems
A Graph-Laplacian approach for calculating the effective thermal conductivity of complicated fiber geometries
Keywords: graph laplacian, effective heat conductivity, numerical upscaling, fibrous materials
(14 pages, 2008)

143. J. Linn, T. Stephan, J. Carlsson, R. Bohlin
Fast simulation of quasistatic rod deformations for VR applications
Keywords: quasistatic deformations, geometrically exact rod models, variational formulation, energy minimization, finite differences, nonlinear conjugate gradients
(7 pages, 2008)

144. J. Linn, T. Stephan
Simulation of quasistatic deformations using discrete rod models
Keywords: quasistatic deformations, geometrically exact rod models, variational formulation, energy minimization, finite differences, nonlinear conjugate gradients
(9 pages, 2008)

145. J. Marburger, N. Marheineke, R. Pinnau
Adjoint based optimal control using mesh-less discretizations
Keywords: Mesh-less methods, particle methods, Eulerian-Lagrangian formulation, optimization strategies, adjoint method, hyperbolic equations
(14 pages, 2008

146. S. Desmettre, J. Gould, A. Szimayer
Own-company stockholding and work effort preferences of an unconstrained executive
Keywords: optimal portfolio choice, executive compensation
(33 pages, 2008)

147. M. Berger, M. Schröder, K.-H. Küfer
A constraint programming approach for the two-dimensional rectangular packing problem with orthogonal orientations
Keywords: rectangular packing, orthogonal orientations non-overlapping constraints, constraint propagation
(13 pages, 2008)

148. K. Schladitz, C. Redenbach, T. Sych, M. Godehardt
Microstructural characterisation of open foams using 3d images
Keywords: virtual material design, image analysis, open foams
(30 pages, 2008)

149. E. Fernández, J. Kalcsics, S. Nickel, R. Ríos-Mercado
A novel territory design model arising in the implementation of the WEEE-Directive
Keywords: heuristics, optimization, logistics, recycling
(28 pages, 2008)

150. H. Lang, J. Linn
Lagrangian field theory in space-time for geometrically exact Cosserat rods
Keywords: Cosserat rods, geometrically exact rods, small strain, large deformation, deformable bodies, Lagrangian field theory, variational calculus
(19 pages, 2009)

151. K. Dreßler, M. Speckert, R. Müller, Ch. Weber
Customer loads correlation in truck engineering
Keywords: Customer distribution, safety critical components, quantile estimation, Monte-Carlo methods
(11 pages, 2009)

152. H. Lang, K. Dreßler
An improved multiaxial stress-strain correction model for elastic FE postprocessing
Keywords: Jiang's model of elastoplasticity, stress-strain correction, parameter identification, automatic differentiation, least-squares optimization, Coleman-Li algorithm
(6 pages, 2009)

153. J. Kalcsics, S. Nickel, M. Schröder
A generic geometric approach to territory design and districting
Keywords: Territory design, districting, combinatorial optimization, heuristics, computational geometry
(32 pages, 2009)

154. Th. Fütterer, A. Klar, R. Wegener
An energy conserving numerical scheme for the dynamics of hyperelastic rods
Keywords: Cosserat rod, hyperealstic, energy conservation, finite differences
(16 pages, 2009)

155. A. Wiegmann, L. Cheng, E. Glatt, O. Iliev, S. Rief
Design of pleated filters by computer simulations
Keywords: Solid-gas separation, solid-liquid separation, pleated filter, design, simulation
(21 pages, 2009)

156. A. Klar, N. Marheineke, R. Wegener
Hierarchy of mathematical models for production processes of technical textiles
Keywords: Fiber-fluid interaction, slender-body theory, turbulence modeling, model reduction, stochastic differential equations, Fokker-Planck equation, asymptotic expansions, parameter identification
(21 pages, 2009)

157. E. Glatt, S. Rief, A. Wiegmann, M. Knefel, E. Wegenke
Structure and pressure drop of real and virtual metal wire meshes
Keywords: metal wire mesh, structure simulation, model calibration, CFD simulation, pressure loss
(7 pages, 2009)

158. S. Kruse, M. Müller
Pricing American call options under the assumption of stochastic dividends – An application of the Korn-Rogers model
Keywords: option pricing, American options, dividends, dividend discount model, Black-Scholes model
(22 pages, 2009)

159. H. Lang, J. Linn, M. Arnold
Multibody dynamics simulation of geometrically exact Cosserat rods
Keywords: flexible multibody dynamics, large deformations, finite rotations, constrained mechanical systems, structural dynamics
(20 pages, 2009)

160. P. Jung, S. Leyendecker, J. Linn, M. Ortiz
Discrete Lagrangian mechanics and geometrically exact Cosserat rods
Keywords: special Cosserat rods, Lagrangian mechanics, Noether's theorem, discrete mechanics, frame-indifference, holonomic constraints
(14 pages, 2009)

161. M. Burger, K. Dreßler, A. Marquardt, M. Speckert
Calculating invariant loads for system simulation in vehicle engineering
Keywords: iterative learning control, optimal control theory, differential algebraic equations(DAEs)
(18 pages, 2009)

162. M. Speckert, N. Ruf, K. Dreßler
Undesired drift of multibody models excited by measured accelerations or forces
Keywords: multibody simulation, full vehicle model, force-based simulation, drift due to noise
(19 pages, 2009)

163. A. Streit, K. Dreßler, M. Speckert, J. Lichter, T. Zenner, P. Bach
Anwendung statistischer Methoden zur Erstellung von Nutzungsprofilen für die Auslegung von Mobilbaggern
Keywords: Nutzungsvielfalt, Kundenbeanspruchung, Bemessungsgrundlagen
(13 pages, 2009)

164. I. Correia, S. Nickel, F. Saldanha-da-Gama
Anwendung statistischer Methoden zur Erstellung von Nutzungsprofilen für die Auslegung von Mobilbaggern
Keywords: Capacitated Hub Location, MIP formulations
(10 pages, 2009)

165. F. Yaneva, T. Grebe, A. Scherrer
An alternative view on global radiotherapy optimization problems
Keywords: radiotherapy planning, path-connected sublevelsets, modified gradient projection method, improving and feasible directions
(14 pages, 2009)

166. J. I. Serna, M. Monz, K.-H. Küfer, C. Thieke
Trade-off bounds and their effect in multi-criteria IMRT planning
Keywords: trade-off bounds, multi-criteria optimization, IMRT, Pareto surface
(15 pages, 2009)

167. W. Arne, N. Marheineke, A. Meister, R. Wegener
Numerical analysis of Cosserat rod and string models for viscous jets in rotational spinning processes
Keywords: Rotational spinning process, curved viscous fibers, asymptotic Cosserat models, boundary value problem, existence of numerical solutions
(18 pages, 2009)

168. T. Melo, S. Nickel, F. Saldanha-da-Gama
An LP-rounding heuristic to solve a multi-period facility relocation problem
Keywords: supply chain design, heuristic, linear programming, rounding
(37 pages, 2009)

169. I. Correia, S. Nickel, F. Saldanha-da-Gama
Single-allocation hub location problems with capacity choices
Keywords: hub location, capacity decisions, MILP formulations
(27 pages, 2009)

170. S. Acar, K. Natcheva-Acar
A guide on the implementation of the Heath-Jarrow-Morton Two-Factor Gaussian Short Rate Model (HJM-G2++)
Keywords: short rate model, two factor Gaussian, G2++, option pricing, calibration
(30 pages, 2009)

171. A. Szimayer, G. Dimitroff, S. Lorenz
A parsimonious multi-asset Heston model: calibration and derivative pricing
Keywords: Heston model, multi-asset, option pricing, calibration, correlation
(28 pages, 2009)

172. N. Marheineke, R. Wegener
Modeling and validation of a stochastic drag for fibers in turbulent flows
Keywords: fiber-fluid interactions, long slender fibers, turbulence modelling, aerodynamic drag, dimensional analysis, data interpolation, stochastic partial differential algebraic equation, numerical simulations, experimental validations
(19 pages, 2009)

173. S. Nickel, M. Schröder, J. Steeg
Planning for home health care services
Keywords: home health care, route planning, metaheuristics, constraint programming
(23 pages, 2009)

174. G. Dimitroff, A. Szimayer, A. Wagner
Quanto option pricing in the parsimonious Heston model
Keywords: Heston model, multi asset, quanto options, option pricing
(14 pages, 2009) 174. G. Dimitroff, A. Szimayer, A. Wagner

175. S. Herkt, K. Dreßler, R. Pinnau
Model reduction of nonlinear problems in structural mechanics
Keywords: flexible bodies, FEM, nonlinear model reduction, POD
(13 pages, 2009)

176. M. K. Ahmad, S. Didas, J. Iqbal
Using the Sharp Operator for edge detection and nonlinear diffusion
Keywords: maximal function, sharp function,image processing, edge detection, nonlinear diffusion
(17 pages, 2009)

177. M. Speckert, N. Ruf, K. Dreßler, R. Müller, C. Weber, S. Weihe
Ein neuer Ansatz zur Ermittlung von Erprobungslasten für sicherheitsrelevante Bauteile
Keywords: sicherheitsrelevante Bauteile, Kundenbeanspruchung, Festigkeitsverteilung, Ausfallwahrscheinlichkeit, Konfidenz, statistische Unsicherheit, Sicherheitsfaktoren
(16 pages, 2009)

178. J. Jegorovs
Wave based method: new applicability areas
Keywords: Elliptic boundary value problems, inhomogeneous Helmholtz type differential equations in bounded domains, numerical methods, wave based method, uniform B-splines
(10 pages, 2009)

179. H. Lang, M. Arnold
Numerical aspects in the dynamic simulation of geometrically exact rods
Keywords: Kirchhoff and Cosserat rods, geometrically exact rods, deformable bodies, multibody dynamics,artial differential algebraic equations, method of lines, time integration
(21 pages, 2009)

180. H. Lang
Comparison of quaternionic and rotation-free null space formalisms for multibody dynamics
Keywords: Parametrisation of rotations, differential-algebraic equations, multibody dynamics, constrained mechanical systems, Lagrangian mechanics.
(40 pages, 2010)

Status quo: February 2010